Scuola di Dottorato
PhD in Neuroscience

**UNIVERSITY OF TURIN**

**DOCTORAL SCHOOL IN LIFE AND HEALTH SCIENCES**

**PhD PROGRAM IN NEUROSCIENCE - CYCLE: XXXIV**

**DOCTORAL THESIS**

# "Perspective of transorbital sonography for detecting and monitoring intracranial hypertension"

Thesis' Author: Dr. Andrea Naldi, M.D.

Supervisor: Prof. Mauro Bergui, M.D., Ph.D.

Prof. Alessandro Vercelli, M.D., Ph.D.

Ph.D. Program Coordinator: Prof. Andrea Calvo, M.D., Ph.D.

ACADEMIC YEARS 2018-2022

MED/26

UNIVERSITÀ
DI TORINO

**CONTENT**

## ABSTRACT

### State of the art and purpose

The optic nerve sheath diameter (ONSD) assessment by transorbital sonography (TOS) is a promising method for the non-invasive detection of intracranial hypertension (IH). Methodological discrepancies are limiting its use in clinical practice. We focused on some unsolved questions in this field, proposing solutions for favoring the standardization of the technique.

### Methods

1. An observational study recruited patients with intracerebral hemorrhage (ICH) for evaluating the accuracy of ONSD assessment in detecting IH in acute ICH and establishing the role of ONSD monitoring over time.
2. A retrospective study of patients with and without IH for establishing the presence of ONSD asymmetry between the eyes, and evaluating the role of the maximum ONSD value in detecting IH.
3. A completely automated algorithm was used for measuring the ONSD and compared to manual assessment.
4. A review of current clinical application of TOS in estimating intracranial pressure.

### Results

The ONSD assessment by TOS was accurate for detecting IH in patients with ICH. A second ONSD evaluation was useful for confirming IH. An interocular asymmetry was present in 52.5% of patients, being more consistent in those with IH than healthy subjects (0.45 vs 0.23mm, p=0.007). The maximum value of ONSD between the eyes was accurate for detecting IH. Automatic measurements did not significantly differ from the manual ones and the agreement between operators and the algorithm was good.

**Additions to the current state of the art**

These findings may reduce the methodological discrepancies of the ONSD assessment, favoring a standardization of the technique. Future approaches should consider automated systems for the ONSD measurement.

## LIST OF PUBLICATIONS

### Scientific articles published during Ph.D. program

1. Gambino A, Ravetti E, **Naldi A**, Russo R, Molinaro S, Mistretta F, Jorfida M, Castagno D, De Ferrari GM, Cerrato P, Bosco G, D'Agata F, Cicerale A, Bergui M. Embolic Stroke of Undetermined Source: Role of Implantable Loop recorder in secondary prevention. Can J Neurol Sci. 2022 Jun 3:1-17. doi: 10.1017/cjn.2022.66. Epub ahead of print. PMID: 35656581.

2. Mirandola L, Arena G, Pagliaro M, Boghi A, **Naldi A**, Castellano D, Vaccarino A, Silengo D, Aprà F, Cavallo R, Livigni S. Massive cerebral venous sinus thrombosis in vaccine-induced immune thrombotic thrombocytopenia after ChAdOx1 nCoV-19 serum: case report of a successful multidisciplinary approach. Neurol Sci. 2022 Mar;43(3):1499-1502. doi: 10.1007/s10072-021-05805-y. PMID: 35001190.

3. Bragazzi NL, Kolahi AA, Nejadghaderi SA, Lochner P, Brigo F, **Naldi A**, Lanteri P, Garbarino S, Sullman MJM, Dai H, Wu J, Kong JD, Jahrami H, Sohrabi MR, Safiri S. Global, regional, and national burden of Guillain-Barré syndrome and its underlying causes from 1990 to 2019. J Neuroinflammation. 2021 Nov 11;18(1):264. doi: 10.1186/s12974-021-02319-4.

4. Kämpfer NA, **Naldi A**, Bragazzi NL, Fassbender K, Lesmeister M, Lochner P. Reorganizing stroke and neurological intensive care during the COVID-19 pandemic in Germany. Acta Biomed. 2021 Nov 3;92(5):e2021266. doi: 10.23750/abm.v92i5.10418.

5. Knodel S, Roemer SN, Moslemani K, Wykrota A, Käsmann-Kellner B, Seitz B, Wagenpfeil G, Fassbender K, **Naldi A**, Kalampokini S, Lochner P. Sonographic and ophthalmic assessment of optic nerve in patients with

idiopathic intracranial hypertension: A longitudinal study. J Neurol Sci. 2021 Nov 15;430:118069. doi: 10.1016/j.jns.2021.118069.

6. **Naldi A,** Mirandola L, Di Liberto A, Cavallo R, Boghi A. Asynchronous bithalamic infarction in presence of artery of Percheron. Neurol Sci. 2021 Oct;42(10):4353-4356. doi: 10.1007/s10072-021-05454-1.

7. Franzoi IG, Granieri A, Sauta MD, Agnesone M, Gonella M, Cavallo R, Lochner P, Bragazzi NL, **Naldi A**. Anxiety, Post-Traumatic Stress, and Burnout in Health Professionals during the COVID-19 Pandemic: Comparing Mental Health Professionals and Other Healthcare Workers. Healthcare (Basel). 2021 May 27;9(6):635. doi: 10.3390/healthcare9060635.

8. Bonacina S, Grassi M, Zedde M, Zini A, Bersano A, Gandolfo C, Silvestrelli G, Baracchini C, Cerrato P, Lodigiani C, Marcheselli S, Paciaroni M, Rasura M, Cappellari M, Del Sette M, Cavallini A, Morotti A, Micieli G, Lotti EM, DeLodovici ML, Gentile M, Magoni M, Azzini C, Calloni MV, Giorli E, Braga M, La Spina P, Melis F, Tassi R, Terruso V, Calabrò RS, Piras V, Giossi A, Locatelli M, Mazzoleni V, Pezzini D, Sanguigni S, Zanferrari C, Mannino M, Colombo I, Dallocchio C, Nencini P, Bignamini V, Adami A, Magni E, Bella R, Padovani A, Pezzini A; IPSYS CeAD Research Group*. Among collaborators: **Naldi A**. Clinical Features of Patients With Cervical Artery Dissection and Fibromuscular Dysplasia. Stroke. 2021 Mar;52(3):821-829. doi: 10.1161/STROKEAHA.120.031579.

9. **Naldi A,** Vallelonga F, Di Liberto A, Cavallo R, Agnesone M, Gonella M, Sauta MD, Lochner P, Tondo G, Bragazzi NL, Botto R, Leombruni P. COVID-19 pandemic-related anxiety, distress and burnout: prevalence and associated factors in healthcare workers of North-West Italy. BJPsych Open. 2021 Jan 7;7(1):e27. doi: 10.1192/bjo.2020.161.

10. Sallustio F, Saia V, Marrama F, Pracucci G, Gandini R, Koch G, Mascolo AP, D'Agostino F, Rocco A, Argiro' R, Nezzo M, Morosetti D, Wlderk A,

Da Ros V, Diomedi M, Renieri L, Nencini P, Vallone S, Zini A, Bigliardi G, Caragliano A, Francalanza I, Bracco S, Tassi R, Bergui M, **Naldi A**, Saletti A, De Vito A, Gasparotti R, Magoni M, Cirillo L, Commodaro C, Biguzzi S, Castellan L, Malfatto L, Menozzi R, Grisendi I, Cosottini M, Orlandi G, Comai A, Franchini E, D'Argento F, Frisullo G, Puglielli E, Casalena A, Causin F, Baracchini C, Boghi A, Chianale G, Augelli R, Cappellari M, Chiumarulo L, Petruzzellis M, Sgreccia A, Tosi P, Cavasin N, Critelli A, Semeraro V, Boero G, Vizzari F, Cariddi LP, Di Benedetto O, Pugliese P, Iacobucci M, De Michele M, Fusaro F, Moller J, Allegretti L, Tassinari T, Nuzzi NP, Marcheselli S, Sacco S, Pavia M, Invernizzi P, Gallesio I, Ruiz L, Zedda S, Rossi R, Amistà P, Russo M, Pintus F, Sanna A, Craparo G, Mannino M, Inzitari D, Mangiafico S, Toni D; Italian Registry of Endovascular Treatment in Acute Stroke (IRETAS) Collaborators. Mechanical Thrombectomy for Acute Intracranial Carotid Occlusion with Patent Intracranial Arteries : The Italian Registry of Endovascular Treatment in Acute Stroke. Clin Neuroradiol. 2021 Mar;31(1):21-29. doi: 10.1007/s00062-020-00980-5.

11. Salsano G, Pracucci G, Mavilio N, Saia V, Bandettini di Poggio M, Malfatto L, Sallustio F, Wlderk A, Limbucci N, Nencini P, Vallone S, Zini A, Bigliardi G, Velo M, Francalanza I, Gennari P, Tassi R, Bergui M, Cerrato P, Carità G, Azzini C, Gasparotti R, Magoni M, Isceri S, Commodaro C, Cordici F, Menozzi R, Latte L, Cosottini M, Mancuso M, Comai A, Franchini E, Alexandre A, Marca GD, Puglielli E, Casalena A, Causin F, Baracchini C, Di Maggio L, **Naldi A**, Grazioli A, Forlivesi S, Chiumarulo L, Petruzzellis M, Sanfilippo G, Toscano G, Cavasin N, Adriana C, Ganimede MP, Prontera MP, Andrea G, Mauri M, Auteri W, Petrone A, Cirelli C, Falcou A, Corraine S, Piras V, Ganci G, Tassinari T, Nuzzi NP, Corato M, Sacco S, Squassina G, Invernizzi P, Gallesio I, Ferrandi D, Dui G, Deiana G, Amistà P, Russo M, Pintus F, Baule A, Craparo G, Mannino M, Castellan L, Toni D, Mangiafico S. Complications of mechanical thrombectomy for acute ischemic stroke: Incidence, risk factors, and clinical relevance in the Italian Registry of Endovascular Treatment in acute stroke. Int J Stroke. 2021 Oct;16(7):818-827. doi: 10.1177/1747493020976681.

12. **Naldi A**, Di Liberto A, Duc E, Rapellino A, Vaudano GP, Cavallo R, Boghi A. Perfusion-computed tomography for simultaneous bilateral middle cerebral artery occlusion. Neurol Sci. 2021 Apr;42(4):1541-1544. doi: 10.1007/s10072-020-04918-0.

13. Sacco S, Ricci S, Ornello R, Eusebi P, Petraglia L, Toni D; Italian Stroke Organization. Among collaborators: **Naldi A**. Reduced Admissions for Cerebrovascular Events During COVID-19 Outbreak in Italy. Stroke. 2020 Dec;51(12):3746-3750. doi: 10.1161/STROKEAHA.120.031293.

14. Lochner P, Lesmeister M, Nardone R, Orioli A, Siniscalchi A, **Naldi A**. Posterior reversible encephalopathy syndrome: role of transorbital ultrasound. Neurol Sci. 2021 Mar;42(3):1171-1174. doi: 10.1007/s10072-020-04719-5.

15. Cappellari M, Pracucci G, Forlivesi S, Saia V, Limbucci N, Nencini P, Inzitari D, Da Ros V, Sallustio F, Vallone S, Bigliardi G, Zini A, Vinci SL, Dell'Aera C, Bracco S, Cioni S, Tassi R, Bergui M, **Naldi A**, Carità G, Azzini C, Casetta I, Gasparotti R, Magoni M, Castellan L, Finocchi C, Menozzi R, Scoditti U, Causin F, Viaro F, Puglielli E, Casalena A, Ruggiero M, Biguzzi S, Castellano D, Cavallo R, Lazzarotti GA, Orlandi G, Sgreccia A, Denaro MF, Cavasin N, Critelli A, Ciceri EFM, Bonetti B, Chiumarulo L, Petruzzelli M, Pellegrino C, Carimati F, Burdi N, Prontera MP, Auteri W, Petrone A, Guidetti G, Nicolini E, Ganci G, Sugo A, Filauri P, Sacco S, Squassina G, Invernizzi P, Nuzzi NP, Corato M, Amistà P, Gentile M, Barbero S, Schirru F, Craparo G, Mannino M, Simonetti L, Mangiafico S, Toni D. Direct thrombectomy for stroke in the presence of absolute exclusion criteria for thrombolysis. J Neurol. 2020 Dec;267(12):3731-3740. doi: 10.1007/s00415-020-10098-w.

16. Casetta I, Fainardi E, Saia V, Pracucci G, Padroni M, Renieri L, Nencini P, Inzitari D, Morosetti D, Sallustio F, Vallone S, Bigliardi G, Zini A, Longo M, Francalanza I, Bracco S, Vallone IM, Tassi R, Bergui M, **Naldi A**, Saletti

A, De Vito A, Gasparotti R, Magoni M, Castellan L, Serrati C, Menozzi R, Scoditti U, Causin F, Pieroni A, Puglielli E, Casalena A, Sanna A, Ruggiero M, Cordici F, Di Maggio L, Duc E, Cosottini M, Giannini N, Sanfilippo G, Zappoli F, Cavallini A, Cavasin N, Critelli A, Ciceri E, Plebani M, Cappellari M, Chiumarulo L, Petruzzellis M, Terrana A, Cariddi LP, Burdi N, Tinelli A, Auteri W, Silvagni U, Biraschi F, Nicolini E, Padolecchia R, Tassinari T, Filauri P, Sacco S, Pavia M, Invernizzi P, Nuzzi NP, Marcheselli S, Amistà P, Russo M, Gallesio I, Craparo G, Mannino M, Mangiafico S, Toni D; Italian Registry of Endovascular Treatment in Acute Stroke. Endovascular Thrombectomy for Acute Ischemic Stroke Beyond 6 Hours From Onset: A Real-World Experience. Stroke. 2020 Jul;51(7):2051-2057. doi: 10.1161/STROKEAHA.119.027974.

17. Meiburger KM, **Naldi A**, Michielli N, Coppo L, Fassbender K, Molinari F, Lochner P. Automatic Optic Nerve Measurement: A New Tool to Standardize Optic Nerve Assessment in Ultrasound B-Mode Images. Ultrasound Med Biol. 2020 Jun;46(6):1533-1544. doi: 10.1016/j.ultrasmedbio.2020.01.034.

18. **Naldi A**, Provero P, Vercelli A, Bergui M, Mazzeo AT, Cantello R, Tondo G, Lochner P. Optic nerve sheath diameter asymmetry in healthy subjects and patients with intracranial hypertension. Neurol Sci. 2020 Feb;41(2):329-333. doi: 10.1007/s10072-019-04076-y.

19. Lochner P, Czosnyka M, **Naldi A**, Lyros E, Pelosi P, Mathur S, Fassbender K, Robba C. Optic nerve sheath diameter: present and future perspectives for neurologists and critical care physicians. Neurol Sci. 2019 Dec;40(12):2447-2457. doi: 10.1007/s10072-019-04015-x.

20. Cappellari M, Mangiafico S, Saia V, Pracucci G, Nappini S, Nencini P, Konda D, Sallustio F, Vallone S, Zini A, Bracco S, Tassi R, Bergui M, Cerrato P, Pitrone A, Grillo F, Saletti A, De Vito A, Gasparotti R, Magoni M, Puglielli E, Casalena A, Causin F, Baracchini C, Castellan L, Malfatto L, Menozzi R, Scoditti U, Comelli C, Duc E, Comai A, Franchini E,

Cosottini M, Mancuso M, Peschillo S, De Michele M, Giorgianni A, Delodovici ML, Lafe E, Denaro MF, Burdi N, Internò S, Cavasin N, Critelli A, Chiumarulo L, Petruzzellis M, Doddi M, Carolei A, Auteri W, Petrone A, Padolecchia R, Tassinari T, Pavia M, Invernizzi P, Turcato G, Forlivesi S, Ciceri EFM, Bonetti B, Inzitari D, Toni D; Among collaborators: **Naldi A**. IER-SICH Nomogram to Predict Symptomatic Intracerebral Hemorrhage After Thrombectomy for Stroke. Stroke. 2019 Apr;50(4):909-916. doi: 10.1161/STROKEAHA.118.023316. Epub 2019 Mar 14. Erratum in: Stroke. 2019 Nov;50(11):e341. PMID: 31233386.

21. **Naldi A**, Pivetta E, Coppo L, Cantello R, Comi C, Stecco A, Cerrato P, Lesmeister M, Lochner P. Ultrasonography Monitoring of Optic Nerve Sheath Diameter and Retinal Vessels in Patients with Cerebral Hemorrhage. J Neuroimaging. 2019 May;29(3):394-399. doi: 10.1111/jon.12604.

22. **Naldi A**, Lochner P, Canu P, Settembre R, Alessi S, Sanguigni S. Transcranial Color-Coded Sonography for Monitoring Idiopathic Intracranial Hypertension. Ultraschall Med. 2019 Aug;40(4):473-475. English. doi: 10.1055/a-0783-2541.

**Book Chapters published during the Ph.D. program:**

1. Lochner P, Canu P, Coppo L, **Naldi A**. (2022). Sonografia Transorbitale. In: Sanguigni S, Ultrasonografia in Neurologia, Poletto Editore, pp. 165-173.

2. Lochner, P., Siniscalchi, A., **Naldi A**. (2022). Transcranial Color-Coded Duplex Sonography (TCCS): Importance of Angle Correction. In: Neurosonology in Critical Care. Springer, Cham. htpps://doi.org/10.1007/978-3-030-81419-9_15

3. Lochner, P., **Naldi, A.** (2021). Brain US in the Neurological Settings. In: Robba, C., Citerio, G. (eds) Echography and Doppler of the Brain. Springer, Cham. https://doi.org/10.1007/978-3-030-48202-2_17

**Publications included in the Doctoral thesis**

1. Meiburger KM, **Naldi A**, Michielli N, Coppo L, Fassbender K, Molinari F, Lochner P. Automatic Optic Nerve Measurement: A New Tool to Standardize Optic Nerve Assessment in Ultrasound B-Mode Images. Ultrasound Med Biol. 2020 Jun;46(6):1533-1544. doi: 10.1016/j.ultrasmedbio.2020.01.034.

2. **Naldi A**, Provero P, Vercelli A, Bergui M, Mazzeo AT, Cantello R, Tondo G, Lochner P. Optic nerve sheath diameter asymmetry in healthy subjects and patients with intracranial hypertension. Neurol Sci. 2020 Feb;41(2):329-333. doi: 10.1007/s10072-019-04076-y.

3. Lochner P, Czosnyka M, **Naldi A**, Lyros E, Pelosi P, Mathur S, Fassbender K, Robba C. Optic nerve sheath diameter: present and future perspectives for neurologists and critical care physicians. Neurol Sci. 2019 Dec;40(12):2447-2457. doi: 10.1007/s10072-019-04015-x.

4. **Naldi A**, Pivetta E, Coppo L, Cantello R, Comi C, Stecco A, Cerrato P, Lesmeister M, Lochner P. Ultrasonography Monitoring of Optic Nerve Sheath Diameter and Retinal Vessels in Patients with Cerebral Hemorrhage. J Neuroimaging. 2019 May;29(3):394-399. doi: 10.1111/jon.12604.

# INTRODUCTION

## Intracranial pressure assessment

Intracranial hypertension (IH) is a severe condition that may follow various neurological disorders. It is defined as a sustained elevation of the intracranial pressure (ICP) of more than 20 mmHg [Rangel Castilla, 2008]. IH occurs when the three elements of the cranial cavity (brain, blood, and cerebrospinal fluid [CSF]) become unable to compensate for volume variation within the skull after cerebral damage. Clinical manifestations of IH include headache, nausea and vomiting, disorder of consciousness (from drowsiness to coma), cranial nerves deficit, papilledema, pupillary alterations, and irregular ventilatory patterns. If not promptly treated, IH is associated with a poor prognosis, including death due to herniation of cerebral structures. Many neurological diseases may determine IH such as traumatic brain injury, cerebral hemorrhage, major ischemic strokes, cerebral venous sinus thrombosis, hydrocephalus, meningitis or encephalitis, brain tumors, idiopathic intracranial hypertension. Therefore, the recognition of raised intracranial pressure (ICP) is mandatory for saving brain tissue by ensuring an adequate treatment, which may include both medical and surgical strategies. To date, the most accurate technique for measuring the ICP is the invasive positioning of an intraventricular or parenchymal catheter [Evensen, 2020]. This approach is considered the gold standard and allows the direct measurement and continuous monitoring of ICP, also offering therapeutic options such as aspiration of CSF and drug administration. However, the invasive placement of a cerebral catheter requires third-level hospitals with intensive care and neurosurgery units and may itself determine brain damage due to the risk of infections and local hemorrhages. Furthermore, the technique is contraindicated in case of concurrent use of anticoagulants, brain abscess, scalp infection, or bleeding disorders.

A second, invasive way of measuring ICP is a lumbar puncture, which as well may be contraindicated in many cases, it is not without risks and does not allow continuous monitoring of ICP.

Since measurements of intracranial pressure are invasive and present inherent risk of complications, non-invasive methods for detecting and monitoring ICP have been proposed over years [Robba, 2016]. Computed tomography (CT) and

magnetic resonance imaging (MRI) are widely used for detecting signs of elevated ICP and are considered the reference among the non-invasive methods. Typical radiological findings of IH are compression of cisterns, collapsed third ventricle, midline shift ≥3mm, effacement of sulci with evidence of substantial edema, and hydrocephalus [Eisenberg, 1990]. However, patients require to be moved to the radiology suite to perform the exams, which may not be simple considering the complexity of these patients, especially when multiple evaluations are needed. In addition, CT exposes the patients to radiation while MRI is not available in many centers and can be contraindicated in various medical conditions.

Conversely, fundoscopy with the detection of papilledema may be considered a valid and non-invasive alternative to conventional imaging. However, an experienced examiner is required and the performer has to be aware that changes in the fundus usually occur later and after a prolonged raised ICP so that the evaluation can be falsely negative in the early phase.

Among the non-invasive method for estimating ICP, Transcranial Doppler for the evaluation of flow pattern and indexes of the intracranial arteries and veins have been proposed, with various – never definitive – results [Cardim, 2016; Moraes, 2021].

On this basis, other non-invasive methods have been proposed and transorbital sonography (TOS) is considered one of the most promising [Robba, 2018; Robba, 2019; Geeraerts, 2008; Tayal, 2007].

**Transorbital sonography for detecting intracranial pressure**

The orbital and ocular structures can be visualized with ultrasonography, providing various information regarding the parenchymal and vascular status [Ertl, 2014]. The estimation of ICP by TOS is based on the variations that may occur in the optic nerve (ON) and its meningeal sheath. The ON origins in the posterior part of the eyeball and runs from the retrobulbar region to the optic chiasm through the optic canal. The ON consists of nerve fibers surrounded by a meningeal sheath. From inside to outside, the sheath is composed of the pia mater, the subarachnoid space (containing CSF), and the dura mater. The meningeal sheath follows the nerve from the intraorbital part to the intracranial one, where it opens at the levels of the perichiasmatic cisterns. Therefore, due to this anatomical contiguity, the CSF in the

subarachnoid spaces is free to circulate from the intracranial regions to the retro-orbital ones. This specific connection is the reason why the ICP can be indirectly and non-invasively measured by TOS. In fact, with the increase of the ICP determined by a pathological cerebral condition, the CSF of the intracranial spaces may be pushed into the optic canals, reaching the orbital structures inside the subarachnoid space that surrounds the ON. The passage of CSF toward the orbital region determines distension of the subarachnoid space, with an enlargement of the optic nerve sheath. Within a specific threshold, the greater the ICP, the greater will be the optic nerve sheath (ONS) distension [Hansen, 2011; Bäuerle, 2016]. Moreover, it has been proven that the ONS reacts in real-time to variation of ICP after lumbar puncture [Chen, 2018]. Thus, measurement of the diameter of the optic nerve sheath (ONSD, optic nerve sheath diameter) may be used as a surrogate marker of the ICP changes.

TOS allows the visualization of the optic nerve and its sheath. Measurement of the diameter of the optic nerve is defined as optic nerve diameter (OND), while measurement of the optic nerve and its sheath is defined as optic nerve sheath diameter (ONSD), which includes pia mater and the subarachnoid space containing CSF.

## Optic nerve assessment by transorbital sonography: execution technique

*Machine settings*

TOS has to be performed following the ALARA (As Low As Reasonably Achievable) principles [Toms, 2006]. The mechanical index should be ≤0.23 to reduce the potential damage to the eye structures caused by the mechanical and thermal effects of ultrasound [Shankar, 2011; Shah, 2009]. Linear array probes with conventional 3-11 MHz and a lateral resolution of at least 0.4 mm allow adequate visualization of the ON and its sheath; 10 MHz has been proposed to achieve a good balance between resolution and ultrasound penetration [Aspide, 2020; Lin, 2020].

*Patients and probe positioning*

TOS is usually performed with the patient lying supine, with a head elevation of about 15-30°. The examiner should sit behind the patient, and the probe should be

gently laid on the upper closed eyelid. Any pressure of the probe on the eyeball should be avoided during the examination because possibly causes deformed and not reliable images. The probe should be transversally placed on the temporal part of the upper eyelid, which has to be closed and covered by a thick layer of ultrasound gel. This position of the probe allows the US beam to be perpendicularly directed to the orbital' structures, thus ensuring a proper view of the ON. The patient is asked to keep the eyes in a neutral position looking straight ahead.

*Optic nerve diameter and sheath diameter assessment*

The ON appears behind the retina as a hypoechogenic structure surrounded by a hyperechogenic area, the subarachnoid space. Figure 1 shows the typical appearance of ON structures visualizable by TOS.

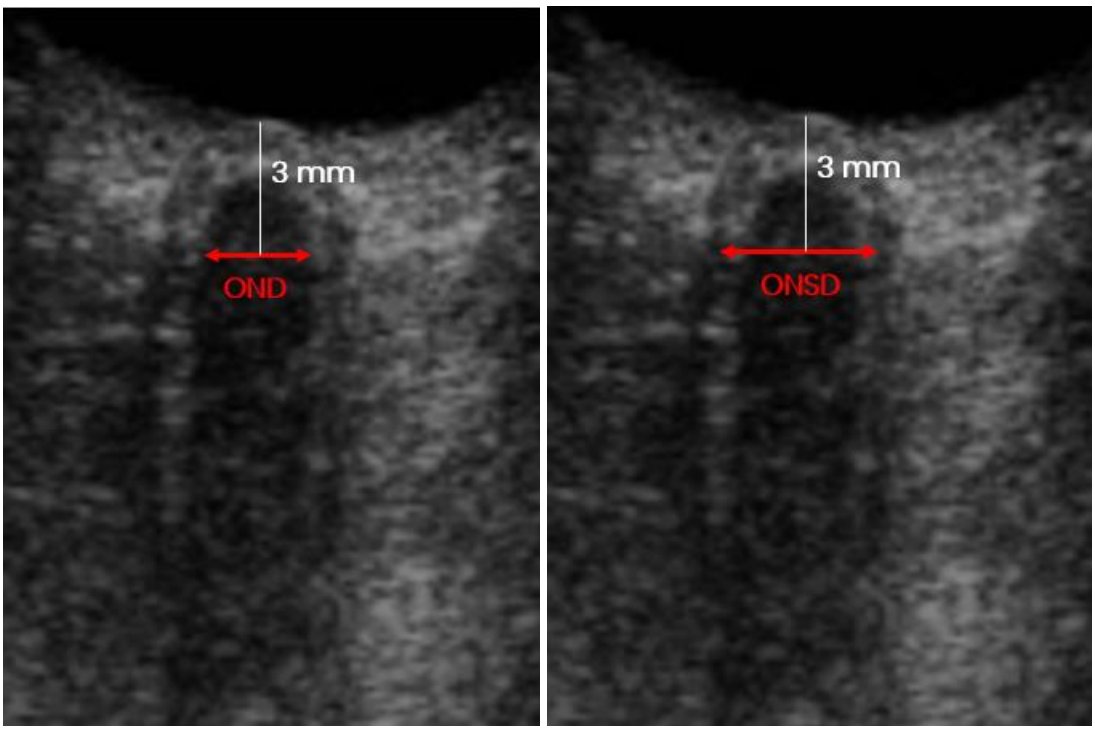


***Figure 1.*** Appearance of optic nerve structures by transorbital sonography

The OND corresponds to the distance between the internal borders of the hyperechogenic area surrounding the optic nerve, while the ONSD to the distance between the external borders of the hyperechogenic area surrounding the optic nerve [Ertl, 2014; Stevens, 2021].

Conventionally, the OND and ONSD are measured perpendicularly at a depth of 3mm behind the optic disc, as this point corresponds - for anatomical reasons - to the site of maximum dilation of the optic sheath after exposure to elevated ICP [Helmke, 1996; Hansen, 1997].

Most of the studies in this field consider adequate the measurements obtained on the axial plane, which means that the probe is placed transversally on the upper eyelid. Commonly, three measurements of the ONSD and OND are taken per eye. The average of measurements for each eye and then between the eyes provides the mean binocular value of ONSD and OND.

## Advantages, limitations, and unsolved questions of transorbital sonography

*Generality*

The ultrasonographic assessment of the ON structures may represent a valid option for estimating intracranial pressure, particularly when the other referring methods are not available and/or contraindicated. Advantages of the sonographic evaluation include the non-invasiveness (no ionizing radiation), the low cost compared to the other techniques, and the wide availability. Only the ultrasound machine and a trained operator are required, thus being applicable in different wards and, potentially, also in the first territorial aid by using portable devices. Furthermore, the ultrasound assessment is bedside and easily repeatable, appearing particularly useful in critically ill and unstable patients who usually require multiple evaluations and transportation to the radiology suite [Wang, 2018].

The technique is feasible and several studies demonstrated a low intra and interobserver variability [Lochner, 2014; Bäuerle, 2010; Ballantyne, 2002; Zeiler, 2014]. Measurements of ONSD made by ultrasound showed good reproducibility and accuracy compared to both CT and MRI [Bäuerle, 2013; Kim, 2021]. These characteristics make TOS particularly suitable both for suggesting the diagnosis of elevated ICP and monitoring the course of the diseases.

However, the acquisition of images may be challenging. Patients may be unconscious or not collaborative, making it difficult to obtain high-quality images. The eye movements may reduce the image's resolution, which may be a limit because an adequate assessment of the ONSD requires the millimetric evaluation

of the ON structures. Low-quality images can lead to errors or inaccurate measurements and may increase the proportion of artifacts [Copetti, 2009].
Despite these limits, the learning curve for the ONSD assessment is estimated in approximately 10-25 scans, depending on previous ultrasound experience [Tayal, 2007].
To date, the spreading of the technique is limited by some doubts and "unsolved questions" that have reduced its routinary use in clinical practice. Some of these uncertainties are listed below and the object of this Ph.D. research project.

*ONSD normative and cut-off values for intracranial hypertension*

The cut-off value of ONSD for the diagnosis of IH is not established. In 2011, two independent metanalyses identified values for elevated ICP ranging from 5.2 to 5.9 mm (Dubourg, 2011; Moretti, 2011). More recently, Schroeder placed the ONSD normality as 4.78 mm, while Montorfano set the value for intracranial hypertension over 5.82mm [Schroeder, 2020; Montorfano, 2021].
However, these values are still debated because several technical and anatomical factors may have influenced the results of these analyses. In adults, elements such as age, sex, and ethnicity initially did not seem to affect ONSD values, but more recent evidence did not confirm this data [Ertl, 2020; Cardim, 2020].
Thus, further studies for large samples are required to establish the range of normality and optimal cut-off point of ONSD for IH, as well as its variability in pathological situations. Overall, the detection of ONSD values > 6 mm, jointly with a clinical condition consistent with IH can be reasonably considered pathological.

*Which role for transorbital sonography?*

The initial studies on TOS in this field were focused on the confirmation of the enlargement of ONSD during IH. This was made by comparing the ONSD values obtained by TOS with those detected with invasive methods such as intraventricular probes [Rajajee, 2011; Kimberly, 2008; Moretti, 2009; Geeraerts, 20080]. Even if concrete, this evidence was limited to a small sample size due to the difficulties to obtain data in these complex patients and intensive care unit settings. Thereafter, ONSD values have been compared to non-invasive methods able to detect raised

ICP such as CT and MRI, paving the way to studies with much larger samples. As a result, many works have demonstrated the accuracy of the method in the detection of IH and a recent metanalysis of 16 studies showed a pooled sensitivity of 0.9 (confidence intervals 95%: 0.85-0.94) and specificity of 0.85 (confidence interval 95%: 0.8-0.89) [Aletreby, 2022]. Thus, TOS resulted in a valid tool for the diagnosis of IH or as a screening test to detect it.

However, the lack of a unique cut-off value of ONSD for IH has limited its applicability. As a consequence, the research has successively focused on a potential different role of the technique, namely the monitoring of raised ICP. Rather than its determination on a single assessment, repeated and serial ONSD measurements perfectly fit with the advantages of ultrasonography, particularly when multiple evaluations are needed. Therefore, studies on the feasibility of ONSD in the serial monitoring of elevated ICP arose, demonstrating its usefulness in predicting the outcomes of patients with a progressive increase of the ONSD values over time. Thus, the method seemed to have a role in the decision-making in specific clinical conditions such as malignant cerebral artery stroke, brain death, traumatic brain injury, and diabetic ketoacidosis [Hansen, 2016; Thotakura, 2017; Toscano, 2017; Albert, 2017; Lochner, 2020].

However, data on serial ONSD monitoring is available only for a few pathologies, and evidence is currently missing for many severe conditions such as cerebral hemorrhage.

*The binocular ONSD assessment and the interocular asymmetry*

Commonly, the ONSD assessment is made by evaluating both eyes, and the final ONSD value is determined by averaging the interocular measurements (the so-called “binocular” ONSD value). This approach implies that the ONSDs should enlarge similarly between the eyes and that the final ONSD value should not be influenced by the averaging process.

However, many factors can be involved in the orbital response to ICP, and asymmetrical dilation of the ONSDs has been described [Bidot, 2015, Hayrey, 2016; Swinkin, 2022]. This is probably due to anatomical differences in the optic canals’ conformation, which may determine a different CSF transmission between the eyes [Hayreh, 1984; Killer, 2003; Bidot, 2016; Mitchell, 2021]. In addition, very few

data are available about individual interocular differences of ONSD both in healthy and pathological conditions. In the case of asymmetry, the averaging process may lead to a false value of ONDS, thus limiting its diagnostic role. However, the effects of the ONSD asymmetry between eyes have never been studied, leaving doubts regarding the validity of the binocular assessment.

*Standardization of the technique and automatic ONSD measurements*

As previously reported, the ONSD assessment is considered reliable, with good inter and intra-operator variability. However, to date, there are no definitive guidelines or clear recommendations about how to assess it. Several protocols have been proposed, but they have never been validated for large samples and they have never been widely approved [Ertl, 2014; Aspide, 2020]. The consequence is a wide heterogeneity among the studies regarding the ONSD assessment, which is limiting the interpretation of the results [Schroeder, 2020]. Specifically, the following are some critical points of the ONSD evaluation that are still debated:

- Measurements are usually taken on the axial plane. However, some studies also reported the use of measures obtained on the vertical plane, but it is uncertain whether they are as reproducible as the axial ones [Blehar, 2008; Amini, 2015; Agrawal, 2019]. In addition, the exact number of measurements that have to be taken per eye is not clear, being usually – but not universally – three. Because measurements of axial and vertical planes do not completely overlap, the absence of a unique model for ONSD assessment may lead to inter-operator variability and heterogeneity across the studies.

- As previously mentioned, the use of the binocular value of ONSD does not take into account the possibility of an interocular asymmetry. On the other hand, the use of the maximum ONSD value between the eyes could be reasonably more accurate than the averaging process, but data are missing to confirm this hypothesis.

- From a technical point of view, methodological aspects have to be considered. The quality of images depends on the kind of ultrasound machine, settings, and probes used for the assessment. To increase the reproducibility of the studies, these equipment requirements should be standardized. Methodological dissimilarities have been described, leading to a difficult interpretation of the results [Schroeder, 2020; Stevens, 2021]. Therefore, a unique, widely shared, and approved model of the ONSD assessment is mandatory [Bloria, 2019]. In this context, the use of automatic measurements of ONSD may contribute to reducing the variability of results across the studies and cover the absence of a standardized protocol. Preliminary evidence is encouraging, but very few data are still available [Gerber, 2017; Meiburger, 2020; Stevens, 2021; Rajajee, 2021].

## AIMS OF THE STUDY

This research project sought to clarify some critical points regarding the application of TOS in clinical practice. In the following section, three original studies and a review are presented. Here, the aims of each research are summarized.

***Study #1**. Ultrasonography monitoring of optic nerve sheath diameter and retinal vessels in patients with cerebral hemorrhage (Naldi et al., 2019)*

This study was designed for evaluating the applicability of TOS for the detection of IH in patients with intracerebral hemorrhage (ICH), comparing its diagnostic accuracy with a different non-invasive technique such as the Doppler indexes of retinal vessels. In addition, the study evaluated the usefulness of a second assessment of the ONSD after the hyper-acute phase of ICH to establish its role in monitoring the evolution of the disease. Finally, we looked for a correlation between the ONSD findings and radiological data, including the cerebral hematoma volume and midline shift.

***Study #2**. Optic nerve sheath diameter asymmetry in healthy subjects and patients with intracranial hypertension (Naldi et al., 2019)*

This work aimed to investigate the existence of an asymmetry of the ONSD (measured by TOS) between the eyes, both in healthy subjects and patients with IH. Because the asymmetry could potentially impact the averaging process during the binocular assessment, we also evaluated if the maximum ONSD value between the eyes could be as useful as the commonly applied binocular assessment for the detection of elevated ICP.

***Study #3**. Automatic optic nerve measurement: a new tool to standardize optic nerve assessment in ultrasound B-mode images (Meiburger et al., 2020)*

This study aimed to evaluate the role of automatic measurements of ONSD to reduce the variability of the manual ONSD assessment, favoring a standardization of the technique. For this purpose, jointly with the PoliToBIOMed Laboratory of Turin (Politecnico di Torino), a completely automatic algorithm for the ON assessment was realized ("AUTomatic Optic Nerve MeAsurement - AUTONoMA"). Thus, this study aimed to investigate the reliability of computerized measurements of OND and ONSD compared to manual ones. The performances of AUTONoMA were evaluated, as well as the agreement between human operators and the automated system.

***Study #4***. *Optic nerve sheath diameter: present and future perspectives for neurologists and critical care physicians (Lochner et al., 2019)*

In this work we reviewed the current clinical applications of the ONSD assessment by TOS in estimating ICP. Limitations and future perspective of the technique are discussed.

# STUDY #1

"**Ultrasonography monitoring of optic nerve sheath diameter and retinal vessels in patients with cerebral hemorrhage**"


## ABSTRACT

**Background and Purpose:** Evaluation of the diagnostic accuracy of optic nerve sheath diameter (ONSD) and Doppler indices of central retinal arteries and veins for the detection of increased intracranial pressure (ICP) in intracerebral hemorrhage (ICH) and of the usefulness of a second assessment of these variables in the monitoring of ICH.

**Methods:** A total of 46 acute ICH patients with (group 1, n=25) and without (group 2, n=21) clinical and radiological CT signs of raised ICP and 40 healthy controls were recruited. The median binocular ONSD and Doppler indices of retinal vessels including resistive index (RI) and retinal venous pulsation (RVP) were compared among groups, both at admission and later during ICH monitoring.

**Results:** Median binocular ONSD showed higher accuracy for the detection of increased ICP (sensitivity and specificity 100%), while Doppler indices were less accurate (sensitivity 48% and specificity 95% for RI; 80% and 62% for RVP). In ICH patients, ONSD was significantly elevated in group 1 both at admission (6.40 mm [IQR 0.70] vs 4.70 [0.40]) and at control time (6.00 [0.55] vs 4.55 [0.40]; $p<0.01$), as well as RI (0.79 [0.11] vs 0.77 [0.03] and 0.80 [0.06] vs 0.75 [0.35]; $p=0.01$). RVP was significantly increased in group 1 only at admission (3.20 cm/s [1.05] vs 2.00 [1.55], $p = 0.02$).

**Conclusions:** Median binocular ONSD evaluation showed a higher accuracy for the estimation of elevated ICP compared with Doppler indices of retinal vessels. The ONSD enlargement detected in the early phase of ICH persists at control time.


## INTRODUCTION

The mortality of patients with intracerebral hemorrhage (ICH) is about 30-40% worldwide and it is mostly due to the occurrence of increased intracranial hypertension (ICP) that may lead to dislocation of midline structures and cerebral herniation.[1,2] Therefore, the availability of diagnostic and monitoring tools for the estimation of ICP may improve the management of these vulnerable patients. Ultrasonography of the optic nerve sheath diameter (ONSD) is a promising simple, non-invasive, repeatable, and bedside technique for the detection of increased ICP and, thus, particularly suitable in an intensive care or stroke-unit setting.[3-5] Recently, two studies demonstrated the reliability of ultrasonography of ONSD to identify raised ICP in ICH patients, but only one case series assessed the possible role of serial measurements of ONSD beyond the acute phase of ICH.[6-8]

The central retinal artery and vein run closely inside the dura mater of the optic nerve and they are accessible to ultrasound through the identical transorbital acoustic window used for ONSD evaluation.[9] Considering their path, we speculated that ONSD enlargement during raised ICP could be transmitted into the intra-axial structures of the meningeal sheaths and therefore determine flow variations of Doppler parameters of retinal vessels. In this context, very few data are available concerning possible hemodynamic flow alterations of orbital vessels in conditions of elevated ICP, especially for central retinal artery and vein.[10,11]

Thus, the primary aim of our study was to evaluate the diagnostic accuracy of ONSD values compared with Doppler parameters of retinal vessels for the detection of elevated ICP in acute ICH. The secondary aim was to establish the usefulness of a second assessment of ONSD and Doppler variables of retinal vessels in monitoring ICH and to look for correlations between sonographic and radiological data.

## METHODS

### *Study design and participants*

This observational study was performed from January to December 2017 at the "Maggiore della Carità University Hospital" of Novara, Italy. All first-ever spontaneous supratentorial ICH patients admitted to the Neurology and Stroke Unit Department were consecutively enrolled.

Inclusion criteria were: age ≥ 18 years old and primary ICH on cerebral CT scan (treated with medical therapies); exclusion criteria were: age < 18 years old, ocular trauma or other conditions that contraindicate ultrasound examination (e.g. glaucoma, orbital tumors), other concomitant causes of intracranial hypertension (e.g. subarachnoid hemorrhage), presence of cardiac arrhythmias that could alter Doppler findings (e.g. atrial fibrillation).

All ICH patients underwent a cerebral CT scan at admission and later during their hospital stay, depending on clinical conditions. Based on first cerebral CT findings and clinical conditions, patients with ICH were assigned to the increased ICP group (group 1 [G1], n = 25) and the not increased ICP group (group 2 [G2], n = 21). A control group (n = 40) consisted of healthy subjects of similar age and vascular risk factors, who underwent a general medical, ophthalmological, and neurological examination to exclude concomitant pathologies.

The study was approved by the local ethics committee (Novara No. CE 95/17). All procedures were in accordance with the ethical standards of the responsible committee on human experimentation (institutional and national) and with the Helsinki Declaration of 1975, as revised in 2013. Written informed consent was obtained from each participant or legal guardian.

***Radiological evaluation***

Cerebral CT scans were performed on a Philips, Brillance with 16 rows of detectors, 3 mm of thickness. According to previous studies, radiological indicators of raised ICP were defined as follows: midline shift ≥ 3 mm, compression of cisterns, effacement of sulci with evidence of substantial edema, collapsed 3$^{rd}$ ventricle, hydrocephalus.[12] Radiological parameters were contextually recorded. Hemorrhage volume was calculated with the ABC/2 score if of rounded or ellipsoid shape, while the ABC/3 score was applied if irregular or multinodular.[13,14] Midline shift was measured as the perpendicular distance between the septum pellucidum and the falx cerebri. An expert neuroradiologist (A.S.), who was unaware about the patients' clinical conditions, independently evaluated the images.

Patients were allocated in Group 1 in presence of at least one clinical and radiological sign of elevated ICP (clinical features for elevated ICP were the follows: alteration of consciousness, headache, vomiting, bradycardia and pupillary abnormalities).

***Transorbital sonography***

Transorbital sonography was executed immediately after both cerebral CT scans for ICH patients, while healthy subjects underwent a single evaluation.

The ultrasonographic studies of ONSD and Doppler indices of retinal vessels were performed with a Toshiba Medical System Aplio 300 (Nasu, Japan) using a high resolution 7.5-11 MHz linear probe with a lateral resolution of < 0.4 mm; mechanical index was reduced to < 0.2 following ALARA principle.[15] ONSD examinations were made according to a previously described protocol. In order to perform the ocular ultrasound examination the patients lay in supine position with head elevated to 30°; a large amount of water soluble gel was carefully applied on both the closed upper eyelid and the probe, which was placed on the temporal region of the eye and the optic nerve was detected posterior the globe. The ONSD was identified by measuring the distance between the external borders of the hyperechogenic area surrounding the optic nerve, corresponding to the periorbital subarachnoid space (Figure 1).[16] Because a different method for the ONSD evaluation is described in literature (that includes the external hypoechogenic borders of the ONSD - the so called $ONSD_E$, corresponding to dura mater and periorbital fat), for descriptive and comparative scopes we also measured this diameter.[17] Once recognized, 3 measurements (taken 3 mm behind the globe) of the ONSD on the transverse plane were recorded for each eye. By averaging these values, the binocular median ONSD values were obtained for each eye.

**Figure 1**. Main ocular sonographic and neuroimaging findings (cerebral CT scan) in ICH patients with (left) and without (right) raised ICP.

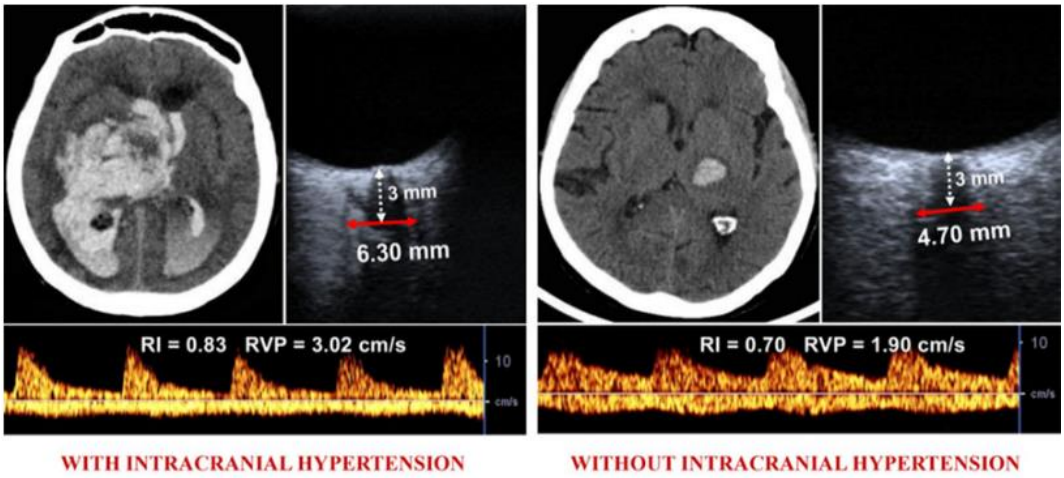


Legend. ICH – Intracerebral hemorrhage; ICP – Intracranial pressure; RI – Resistive index; RVP – Retinal venous pulsation.

The central retinal artery and vein were identified in combination inside the optic nerve using color Doppler sonography with a low pulse repetition frequency. Angle flow correction was applied, varying between 0 and 45°; gate size was 1.5 mm.[18] At least three complete Doppler waveforms were registered to decrease the effects of physiologic variation and measurements were made approximately at 3 mm behind the globe.[19] From central retinal artery, binocular values of peak systolic velocity (PSV), end diastolic velocity (EDV), and resistive index (RI) were recorded, while maximum and minimum velocity (v-max, v-min) as well as retinal venous pulsation (RVP) were registered from central retinal vein. The averaging of these measurements between the eyes determined the binocular median values of RI and RVP (Figure 1).

Ultrasonographic evaluations were executed by a skilled accredited examiner (A.N.), who was not blinded to the clinical condition of patients, while all measurements were calculated off-line by a second expert neurosonologist (P.L.), blinded to clinical and radiological findings. Agreement between the two operators had been preliminary assessed for ONSD and optic nerve diameter by using the same device in 9 healthy subjects in a previous study.[20]

***Statistical analysis***

Descriptive data are shown as median with interquartile range (IQR) for continuous variables and as numbers and percentages for categorical variables. Differences among three groups were tested using the Kruskal-Wallis test. Radiological and sonographic data between couples of groups were tested using the Wilcoxon-Mann-Whitney test. Diagnostic accuracy in detecting elevated ICP was evaluated using area under the receiver operating characteristic (ROC) curve. Correlation between variables was assessed using the Spearman's coefficient. Statistical analyses were conducted using Stata 13.0/SE (Stata Corp, College Station, TX, USA).

## RESULTS

Of the 55 patients who presented with ICH, 9 did not meet the study criteria and were excluded from further analysis (1 glaucoma, 3 missing consent, 2 atrial fibrillation, 3 subarachnoid hemorrhage).

Demographic and clinical data are shown in Table 1. Forty-six acute primary ICH patients were recruited, 25 with radiological signs of raised ICP (G1) and 21 without (G2); 40 healthy subjects composed the control group. The three groups differed significantly for the median age (lower in G2) and smoking habits (higher in G2); no dissimilarities were present for other vascular risk factors. Predictably, patients with increased ICP had a higher median NIHSS score (28, IQR 18) at stroke onset than those without (8, IQR 7).

The main differences in radiological findings and median values of binocular ONSD and Doppler indices among the groups are presented in Table 2. Because of the severity of cerebral hemorrhage within G1, the radiological control in patients with raised ICP was available for 13 patients (10 died, while 2 were lost at follow-up). As expected, the median hemorrhage volume at admission was higher in G1 with 47.70 $cm^3$ (IQR 47.40) compared to G2 with 2.20 $cm^3$ (IQR 0.90) as well as the median midline shift in G1 with 10.10 mm (IQR 9.60) compared with G2 with 0.00 mm (IQR 0.00). No significant dissimilarities in ONSD, RI and RVP were observed between patients in G2 and healthy controls. Median binocular ONSD values in patients with increased ICP were significantly higher from those without at both times of study.

Within G1, ONSD did not discriminate early mortality risk between patients who died and those who survived (6.58 mm [IQR 0.55] vs 6.15 [IQR 0.55]; p = 0.14). Median binocular RI and RVP were significantly higher in patients with raised ICP at both times of assessment, excepting for RVP at control time.

The diagnostic accuracy of sonographic variables in the acute phase of ICH with relative cut-off values for the detection of elevated ICP are reported in Table 3. ONSD shows the higher accuracy, followed by RI and RVP (ROC curves are compared in Figure 2).

Spearman coefficient analyses between radiological and sonographic variables at onset time was statistically significant for ONSD and hemorrhage volume (r = 0.734 p < 0.001). No significant correlations were found at control time.

Table 1. Demographic and Clinical Data

| | Cerebral hemorrhage | | | |
|---|---|---|---|---|
| | With increased ICP (G1) (n = 25) | Without increased ICP (G2) (n = 21) | Healthy controls (n = 40) | *P* |
| Age (years) (median, IQR) | 80 (14) | 72 (13) | 77 (12) | .01 |
| Male sex (n, %) | 11 (44) | 14 (67) | 21 (53) | NS |
| Arterial hypertension (n, %) | 21 (84) | 16 (76) | 30 (75) | NS |
| Diabetes (n, %) | 5 (20) | 9 (43) | 6 (15) | NS |
| Dyslipidemia (n, %) | 12 (48) | 11 (52) | 22 (55) | NS |
| History of heart disease (n, %) | 6 (24) | 4 (19) | 6 (15) | NS |
| Smoke (n, %) | 4 (16) | 9 (43) | 6 (15) | .05 |
| NIHSS at onset (median, IQR) | 28 (18) | 8 (7) | – | <.001 |
| Hemorrhage characteristics | | | | |
| Typical (n, %) | 9 (36) | 11 (52) | – | NS |
| Atypical (n, %) | 16 (64) | 10 (48) | – | NS |
| Intraventricular (n, %) | 12 (48) | 0 (0) | – | <.01 |

*P* < .05 was considered statistically significant.
G1 = group 1; G2 = group 2; ICP = intracranial pressure; IQR= interquartile range; n = number of subjects; NIHSS = National Institutes of Health Stroke Scale.

Table 2. Radiological and Sonographic Data in Patients with Cerebral Hemorrhage and Controls

| Variable | Cerebral hemorrhage | | | | |
|---|---|---|---|---|---|
| At admission | With increased ICP (G1) (*n* = 25) | P G1/G2 | Without increased ICP (G2) (*n* = 21) | P G2/controls | Healthy controls *n* = 40 |
| ONSD (mm) | 6.40 (.70) | <.01 | 4.70 (.40) | NS | 4.50 (.25) |
| $ONSD_E$ (mm) | 7.50 (.65) | <.01 | 5.85 (.70) | NS | 5.60 (.75) |
| RI | .79 (.11) | .01 | .77 (.03) | NS | .75 (.07) |
| RVP (cm/s) | 3.20 (1.05) | .02 | 2.00 (1.55) | NS | 2.30 (.68) |
| Hemorrhage volume ($cm^3$) | 47.70 (47.40) | <.01 | 2.20 (.90) | – | – |
| Midline shift (mm) | 10.10 (9.60) | <.01 | .00 (.00) | – | – |
| **At control time** | **(*n* = 13)** | | **(*n* = 21)** | | |
| ONSD (mm) | 6.00 (.55) | <.01 | 4.55 (.40) | – | – |
| RI | .80 (.06) | .01 | .75 (.35) | – | – |
| RVP (cm/s) | 2.80 (1.25) | NS | 2.40 (1.40) | – | – |
| Hemorrhage volume ($cm^3$) | 45.00 (38.70) | <.01 | 2.00 (1.60) | – | – |
| Midline shift (mm) | 8.80 (6.10) | <.01 | .00 (.00) | – | – |
| Time of CT control (days) | 3 (2) | NS | 5 (5) | – | – |

Sonographic data are intended as binocular values; all data are expressed as median (interquartile range, IQR).
*P* < .05 was considered statistically significant.
G1 = group 1; G2 = group 2; ONSD = optic nerve sheath diameter; $ONSD_E$= optic nerve sheath diameter external; RI = resistive index; RVP = retinal venous pulsation; NS = not significant.

Table 3. Diagnostic Accuracy and Relative Cut-Off Values of the Single Variables for the Detection of Raised Intracranial Pressure

| Parameter | AUC | 95% CI | Cut-off value | Sensitivity (%) | Specificity (%) |
|---|---|---|---|---|---|
| ONSD | 1.00 | 1.00 -1.00 | 5.60 | 100 | 100 |
| RI | .72 | .58 -.87 | .80 | 48 | 95 |
| RVP | .70 | .54 -.86 | 2.73 | 80 | 62 |

AUC = area under the curve; CI = confidence interval; ONSD = optic nerve sheath diameter; RI = resistivity index; RVP = retinal venous pulsation.

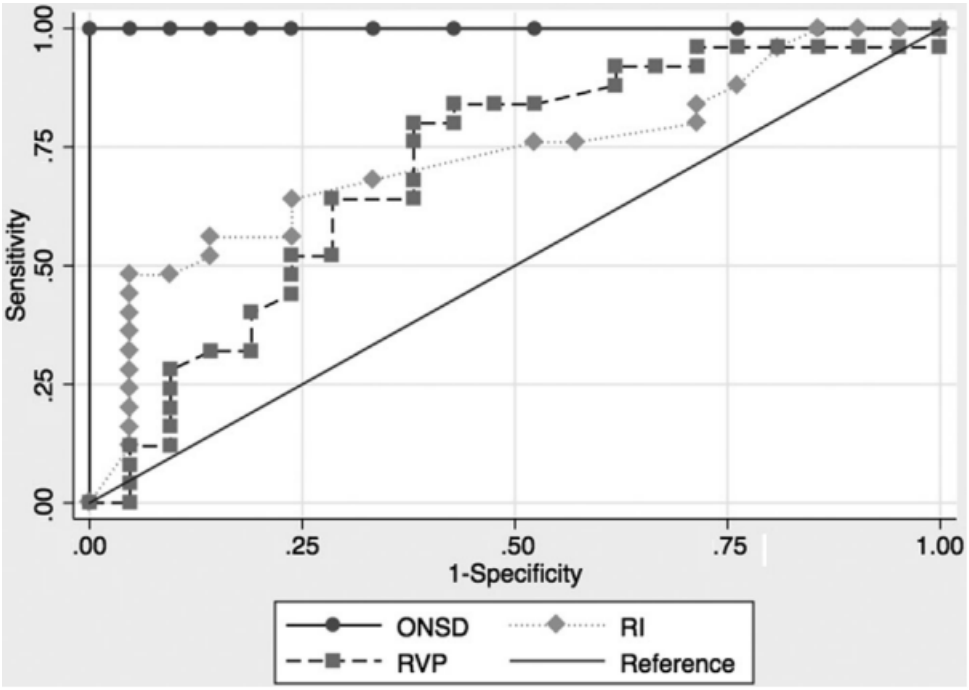


**Fig 2.** Comparison of ROC curves for the identification of elevated ICP among the variables.
ICP = intracranial pressure; ONSD = nerve sheath diameter; RI = resistive index; ROC = receiver operator characteristic; RVP = retinal venous pulsation.

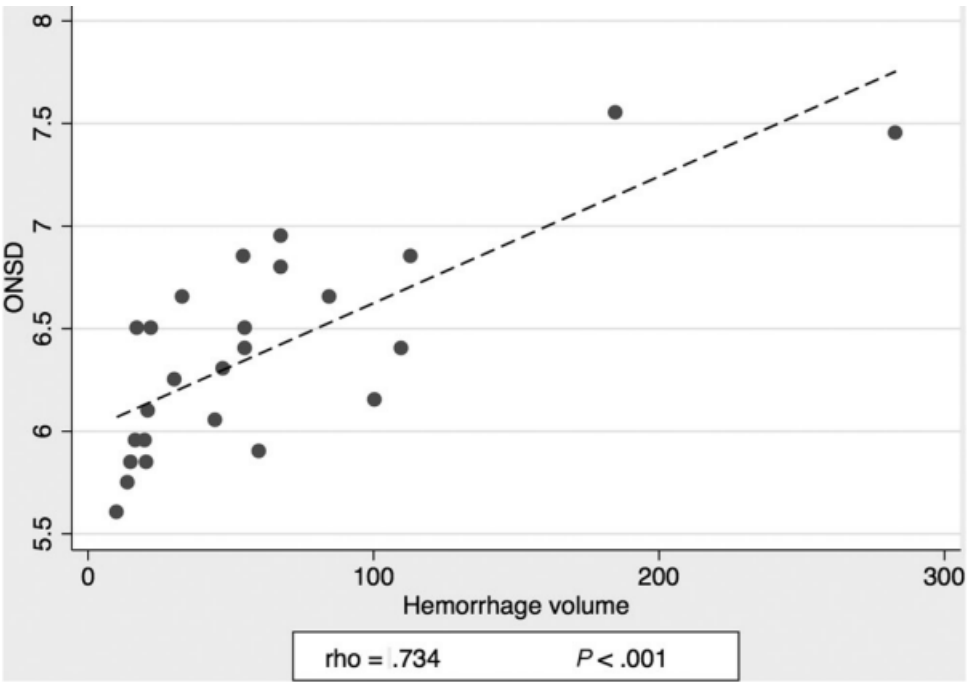


**Fig 3.** Spearman correlation between median binocular ONSD (mm) and hemorrhage volume ($cm^3$) in patients with elevated ICP at admission.
ICP = intracranial pressure; ONSD = optic nerve sheath diameter.

## DISCUSSION

To the best of our knowledge, this work provides for the first time information about ocular ultrasound findings of ONSD and Doppler indices of retinal vessels during the acute phase and monitoring of ICH. Our study includes the largest series of ICH patients in this topic and confirms that the ONSD is enlarged in the subgroup of ICH patients with elevated ICP.[6,7]

The main finding of our study is that ONSD shows the highest diagnostic accuracy compared to Doppler indices of central retinal artery and vein for the identification of elevated ICP.

Furthermore, the ONSD behavior in course of elevated ICP is not well established and this is particularly true for ICH patients where only a small case series has been evaluated for this purpose.[8] In this regard, our data show that the widening of ONSD seems to persist over time, leading to the hypothesis that ICP remains elevated.

Previous studies showed a positive correlation between ONSD and hemorrhage volume or midline shift.[7,8,10] In patients with ICH and elevated ICP, our work

confirmed a good correlation between ONSD and hemorrhage volume at admission, but missed to find an association with midline shift. A possible explanation may be attributed to the elevated age of patients and the relative brain atrophy that could have prevented the early development of cerebral shift; moreover, midline shift may appear later because of edema growth. In this regard, our analysis observed a possible positive trend towards a significant correlation between ONSD and shift values ($r = 0.40$, $p = 0.18$) at control time. Even if speculative, we remark that in G1 CT scan and sonographic evaluation were not repeated in 10 subjects because they died. In these patients, an increment of midline shift was conceivable and may have altered the result of a possible significant correlation.

ONSD was not related to hemorrhage volume anymore at the time of second CT scan: the reasons may include the initial adsorption of parenchymal blood with no correspondent changes of the ONSD and the drop-out of deceased patients. The ONSD thickening seems to follow the variations of raised ICP in chronic conditions like primary intracranial hypertension, where the dilatation or contraction of the sheath proceeds slowly.[21] At contrary (if not promptly treated), an acute distension may not be followed by a shrink during ICH, where rapid changes of ICP occur, as observed in subarachnoid hemorrhage.[22] Overall, the edema growth may maintain an elevated ICP despite the reduction of hemorrhage, resulting in a persistent enlargement of ONSD.

The combination of these findings may suggest that variations of ICP could be predicted by serial ONSD evaluations and, thus, provide further data when compared to radiological signs of elevated ICP. Therefore, ultrasound monitoring may give the opportunity to detect and track changes of ICP, providing useful information to optimize treatments in ICH patients.[23]

In this context, the attention is currently moving to the possible role of this method in monitoring raised ICP during acute conditions, where still little is known. Toscano et al. recently demonstrated the efficacy of the technique for the early identification of malignant increased ICP and brain death in neurocritical patients with daily ONSD monitoring, in order to detect potential candidates for organ donation.[24] In head injury patients, the trend observed in ONSD values obtained by serial measurements provided useful information on decision making, more than the single evaluation.[25]

In addition to ONSD ultrasonography, transcranial Doppler sonography has been proposed as another alternative non-invasive tool for raised ICP detection.[26] Whether those techniques are promising, data on diagnostic accuracy are variable and no consensus has been reached.[27-29] Recently, the diagnostic performance of Doppler indices of ophthalmic arteries has been compared to ONSD, resulting in lower ability in the detection of elevated ICP.[10] The central retinal artery and vein are accessible to ultrasound in their terminal portion through the transorbital window but they have never been studied for this purpose during acute raised ICP. In our hypothesis, the demonstrated maximum enlargement of the ONSD (approximately 3 mm behind the globe) could be transferred to the inward structures and, thus, cause variations on Doppler indices of these vessels. Our findings confirmed this assumption, but results are still limited because of inferiority if compared to the accuracy of ONSD measurements. These results agree with those achieved by Tarzamni, suggesting that the study of the orbital vessels appears to be not accurate enough for the evaluation of ICP because many factors including arterial pressure, diseases affecting the small vessels, age of patients, local autoregulation, cerebral perfusion pressure, and inter-individual variability may influence the local flow.[10]

Finally, despite the increasing number of works in this field, there is still no consensus on a unique ONSD cut-off value for the identification of elevated ICP, placed between 4.5 and 6.3 mm.[3,5,25] These discrepancies may depend on various factors, including the execution technique, the subject selection, the underlying pathology and ethnicity, limiting the validation of the method for a more extensive use. Our optimal cut-off point for detection of raised ICP was 5.6 mm, being in line with cited previous reports and more recent findings.[30,31]

This study presents some limitations like the small study population and that we presumed that ICP was normal in control subjects without performing a CSF opening pressure evaluation. Additionally, we are aware of the limited predictive value of abnormal CT findings in the assessment of ICP.[32] Finally, the date of the second CT scan was depending on clinical conditions instead of being performed on a given day.

Altogether, the results of this study suggest a higher accuracy of the median binocular ONSD compared to the retinal vessels' Doppler indices in detecting raised ICP. In ICH patients, a second assessment of ONSD measurements may

provide other indirect information on persistency of elevated ICP and variations of radiological parameters, but more extensive data are required to confirm this scenario.

**References Study #1**


1. Chen S, Zhao B, Wang W, Shi L, Reis C, Zhang J. Predictors of hematoma expansion predictors after intracerebral hemorrhage. Oncotarget 2017;8:89348-63.
2. Al-Mufti F, Thabet AM, Singh T, El-Ghanem M, Amuluru K, Gandhi CD. Clinical and radiographic predictors of intracerebral hemorrhage outcome. Interv Neurol 2018;7:118-36.
3. Messerer M, Berhouma M, Messerer R, Dubourg J. Interest of optic nerve sheath diameter ultrasonography in detecting non-invasively raised intracranial pressure. Neurochirurgie 2013;59:55-9.
4. Ohle R, McIsaac SM, Woo MY, Perry JJ. Sonography of the optic nerve sheath diameter for detection of raised intracranial pressure compared to computer tomography: a systematic review and meta-analysis. J Ultrasound Med 2015;34:1285-94.
5. Dubourg J, Javouhey E, Geeraerts T, Messerer M, Kassai B. Ultrasonography of optic nerve sheath diameter for detection of raised intracranial pressure: a systematic review and meta-analysis. Intensive Care Med 2011;37:1059-68.
6. Moretti R, Pizzi B, Cassini F, Vivaldi N. Reliability of optic nerve ultrasound for the evaluation of patients with spontaneous intracranial hemorrhage. Neurocrit Care 2009;11:406-10.
7. Školoudík D, Herzig R, Fadrná T et al. Distal enlargement of the optic nerve sheath in the hyperacute stage of intracerebral haemorrhage. Br J Ophthalmol 2011;95:217-21.
8. Lochner P, Mader C, Nardone R et al. Sonography of the optic nerve sheath beyond the hyperacute stage of intracerebral hemorrhage. J Ultrasound 2014;17:225-8.
9. Bird B, Stawicki SP. Anatomy, Head, Face, Eye, Arteries, Ophthalmic. Dec 29, 2017. StatPearls [Internet]. Treasure Island (FL): StatPearls Publishing; 2018 Jan-. http://www.ncbi.nlm.nih.gov/books/NBK482317/. Accessed July 18, 2018.
10. Tarzamni MK, Derakhshan B, Meshkini A et al. The diagnostic performance of ultrasonographic optic nerve sheath diameter and color Doppler indices of the ophthalmic arteries in detecting elevated intracranial pressure. Clin Neurol Neurosurg 2016;141:82-8.

11. Querfurth HW, Lagrèze WD Hedges TR 3rd, Heggerick PA. Flow velocity and pulsatility of the ocular circulation in chronic intracranial hypertension. Acta Neurol Scand 2002:105:431-40.
12. Eisenberg HM, Gary HE Jr, Aldrich EF et al. Initial CT findings in 753 patients with severe head injury. A report from the NIH Traumatic Coma Data Bank. J Neurosurg 1990;73:688-98.
13. Kothari RU, Brott T, Broderick JP et al. The ABCs of measuring intracerebral hemorrhage volumes. Stroke 1996;27:1304-5.
14. Huttner HB, Steiner T, Hartmann M et al. Comparison of ABC/2 estimation technique to computer-assisted planimetric analysis in warfarin-related intracerebral parenchymal hemorrhage. Stroke 2006;37:404-8.
15. Ertl M, Gamulescu MA, Schlachetzki F. Application of orbital sonography in neurology; in Thoirs K (ed): Sonography. DOI: 10.5772/31181, InTech, 2012. http://www.intechopen.com/books/sonography/application-of-orbital-sonography-in-neurology. Accessed July 18, 2018.
16. Ertl M, Barinka F, Torka E et al. Ocular color-coded sonography – a promising tool for neurologists and intensive care physicians. Ultraschall Med 2014;35:422-31.
17. Topcuoglu MA, Arsava EM, Bas DF, Kozak HH. Transorbital Ultrasonographic Measurement of Optic Nerve Sheath Diameter in Brain Death. J Neuroimaging 2015 Nov-Dec;25(6):906-9
18. Baxter GM, Williamson TH. Color Doppler imaging of the eye: normal ranges, reproducibility, and observer variation. J Ultrasound Med 1995;14:91-6.
19. Williamson TH, Harris A. Color Doppler ultrasound imaging of the eye and orbit. Surv Ophthalmol 1996;40:255-67.
20. Lochner P, Cantello R, Brigo F et al. Transorbital sonography in acute optic neuritis: a case-control study. AJNR Am J Neuroradiol 2014;35:2371-5.
21. Lochner P, Fassbender K, Lesmeister M et al. Ocular ultrasound for monitoring pseudotumor cerebri syndrome. J Neurol 2018;265:356-61.
22. Bäuerle J, Niesen WD, Egger K, Buttler KJ, Reinhard M. Enlarged optic nerve sheath in aneurysmal subarachnoid hemorrhage despite normal intracranial pressure. J Neuroimaging 2016;26:194-6.

23. Robba C, Bacigaluppi S, Cardim D, Donnelly J, Bertuccio A, Czosnyka M. Non-invasive assessment of intracranial pressure. Acta Neurol Scand 2016;134:4-21.
24. Toscano M, Spadetta G, Pulitano P et al. Optic nerve sheath diameter ultrasound evaluation in intensive care unit: possible role and clinical aspects in neurological critical patients' daily monitoring. Biomed Res Int 2017;2017:1621428.
25. Thotakura AK, Marabathina NR, Danaboyina AR, Mareddy RR. Role of serial ultrasonic optic nerve sheath diameter monitoring in head injury. Neurochirurgie 2017;63:444-8.
26. Hassler W, Steinmetz H, Gawlowski J. Transcranial Doppler ultrasonography in raised intracranial pressure and in intracranial circulatory arrest. J Neurosurg 1988;68:745-51.
27. Nair S. Clinical review of non-invasive intracranial pressure measurement in medical cases. J Neuroanaesthesiol Crit Care 2016;3:9-14.
28. Morgalla MH, Magunia H. Noninvasive measurement of intracranial pressure via the pulsatility index on transcranial Doppler sonography: Is improvement possible? J Clin Ultrasound 2016;44:40-5.
29. Cardim D, Robba C, Bohdanowicz M et al. Non-invasive monitoring of intracranial pressure using transcranial Doppler ultrasonography: Is it possible? Neurocrit Care 2016;25:473-1.
30. Lee SU, Jeon JP, Lee H et al. Optic nerve sheath diameter threshold by ocular ultrasonography for detection of increased intracranial pressure in Korean adult patients with brain lesions. Medicine (Baltimore) 2016;95:e5061.
31. Amini A, Kariman H, Arhami Dolatabadi A et al. Use of the sonographic diameter of optic nerve sheath to estimate intracranial pressure. Am J Emerg Med 2013;31:236-9.
32. Rosenberg JB, Shiloh AL, Savel RH, Eisen LA. Non-invasive methods of estimating intracranial pressure. Neurocrit Care 2011;15:599.

# STUDY #2

## "Optic nerve sheath diameter asymmetry in healthy subjects and patients with intracranial hypertension"


## ABSTRACT

**Background.** Ultrasonography of the optic nerve sheath diameter (ONSD) is used for the non-invasive assessment of increased intracranial pressure (ICP). ONSD values are usually obtained by averaging the measurements of the two eyes, but asymmetric ONSD dilation is possible, leading to potentially inaccurate ICP estimation when using binocular averaging. In addition, few data are available about the asymmetry of the ONSD and the use of the maximum ONSD value between eyes for raised ICP detection. The aim of the study was to evaluate the interocular ONSD asymmetry in healthy subjects and patients with intracranial hypertension (IH) by ultrasonography, and to investigate whether the maximum ONSD could be as useful as the binocular assessment.

**Methods.** Forty healthy subjects and 40 patients with IH (20 with idiopathic intracranial hypertension and 20 with intracerebral hemorrhage) who underwent transorbital sonography were retrospectively enrolled. The prevalence and degree of ONSD asymmetry were compared among groups; ONSD median binocular and maximum values were compared.

**Results.** Forty-two out of 80 subjects (52.5%) showed significant ONSD asymmetry, without significant differences in prevalence among groups ($p$=0.28). The median asymmetry was higher in patients than in healthy subjects (0.45 mm vs 0.23 mm; $p$=0.007), without significant differences between the two pathologies ($p$=0.58). Both binocular and maximum ONSD measurements were significantly higher in patients with IH than in controls ($p$<0.001).

**Conclusions.** Interocular ONSD asymmetry occurs both in healthy subjects and, more consistently, in patients with IH. Both binocular and maximum ONSD may be useful markers for increased ICP detection.

## INTRODUCTION

Elevated intracranial pressure (ICP) may be indirectly evaluated the measuring the optic nerve sheath diameter (ONSD) [1]. The rationale resides in the anatomical continuity between the subarachnoid space of the optic nerve sheaths and that of the brain, allowing the circulation of cerebrospinal fluid (CSF) from the perichiasmatic cistern to the ocular regions [2]. With increasing ICP, the pushing pressure drives a larger amount of CSF toward the orbital spaces. As a result, the ONSDs enlarge and optic disc elevation develops over time. However, the CSF transmission may be limited at the level of the optic canals where the composition of the subarachnoid space changes, becoming subdivided in small compartments and narrowing its lumen to a capillary size [3]. This specific architecture, made of thick pillars and trabeculae, is assumed to be responsible for the quantity and speed with which the CSF can be transferred to the optic sheaths, and its large inter-individual variability may explain the documented occurrence of asymmetric ONSD enlargement and unilateral papilledema [4, 5]. Furthermore, no data on individual interocular differences have been reported.

The ONSD may be explored with various techniques, transorbital sonography being one of the most promising due to its non-invasiveness, feasibility, and high diagnostic accuracy [6]. The application fields of this method in the clinical practice have been recently described [7]. Despite the anatomical remarks cited above, most ultrasonographic studies consider ONSD measurements as an average of binocular values, rather than the maximum value between the two eyes, leading to possible errors in estimating ICP, given the potential physiological asymmetry.

The aim of this study was to evaluate the variability, in term of symmetry, of the ONSD, by using ultrasonography in healthy subjects and patients with intracranial hypertension (IH), and to establish whether the maximum value of the ONSD could be as useful as the binocular assessment.

## METHODS

### *Subjects*

We retrospectively reviewed ONSD data from 80 subjects, collected from a dataset available from the authors [8, 9]. All participants were ≥ 18 years old; exclusion criteria were ocular trauma, glaucoma and significant orbital mass. Forty normal subjects who underwent general medical, ophthalmological, and neurological evaluation to rule out signs and symptoms of IH and ocular pathologies were included in the healthy group. Forty patients, matched for gender but not for age, composed the IH group, and included 20 consecutive subjects with idiopathic intracranial hypertension (IIH) and 20 consecutive patients with primary acute supratentorial intracerebral hemorrhage (ICH).

Patients with IIH were recruited at the "Franz Tappeiner" Hospital of Merano Hospital between March 2014 and November 2015; raised ICP was established (after ONSD evaluation) by lumbar puncture with a CSF opening pressure ≥ 25 cm $H_20$ according to the Friedmann diagnostic criteria [10]. ICH patients were admitted to the "Maggiore della Carità" Hospital of Novara from January to December 2017; elevated ICP was determined by clinical conditions and cerebral CT scan. Radiologically, we considered only medium- to large-size cerebral hemorrhages (≥ 30 ml) with at least two of the following: midline shift ≥ 3 mm, collapsed 3$^{rd}$ ventricle, hydrocephalus, compression of cisterns and effacement of sulci with evidence of substantial edema [11, 12]. Hematoma size was calculated using the ABC/2 score (if rounded or ellipsoid shape) or ABC/3 score (irregular or multinodular) [13, 14]. Contextually, at least one clinical sign of elevated ICP had to be present, including bradycardia, altered consciousness, vomit, headache, pupillary abnormalities or uncontrolled hypertension.

***Transorbital sonography***

Transorbital ONSD sonography was performed following a previously described protocol using a Toshiba Medical System Aplio 300 (Nasu, Japan; linear probe 7.5-11 MHz with lateral resolution <0.4 mm) for healthy subjects and ICH patients, and a Toshiba Aplio ultrasound system XG (Toshiba Medical Systems, Nasu, Japan; linear probe 7.2-14 MHz, lateral resolution <0.4 mm) for IIH patients [15]. Ultrasonographic evaluations were performed by two skilled neurosonologists (A.N. and P.L.); all measurements were taken off-line by a single expert operator (P.L.) to reduce interobserver variability. ONSD was calculated as the distance

between the external hyperechogenic borders surrounding the optic nerve, corresponding to the periorbital subarachnoid space.

ONSD was evaluated on the axial plane in triplicate for each eye. Binocular ONSD was obtained by averaging these values between the eyes, while maximum ONSD was obtained by first averaging the three measurements for each eye and then taking the maximum of the two values.

### *Statistical analysis*

Statistical analysis was performed using the R software, version 3.6.0 [16]. For each subject, the ONSD asymmetry was evaluated as the absolute value of the difference between the mean ONSD of the two eyes; statistical significance was assessed using Welch's *t*-test, with multiple testing correction performed with the Benjamini-Hochberg method at a false discovery rate of 5%. For group comparison, categorical variables were expressed as numbers and percentages and compared among groups with Fisher's exact test. Continuous variables, expressed as median and quartiles (Q1, Q3), were compared among more than two groups with the Kruskal-Wallis test, and between two groups with the Mann-Whitney U test.

## RESULTS

Demographic data, mean ONSD values and asymmetry are summarized in Table 1. The median age of subjects was 72.5 (range 44.75 – 79) and was significantly lower in IIH patients (37 [29 – 47.25], $p<0.001$), as expected for the pathology; gender did not differ between the three subgroups ($p=0.114$).

Forty-two out of 80 subjects (52.5%) showed a significant ONSD asymmetry between eyes at a false discovery rate of 5%, and the difference in prevalence among groups was not significant (16 for healthy subjects, 14 for ICH patients, and 12 for IIH; $p=0.28$). The median asymmetry was higher in patients with IH than in normal subjects (0.45 mm vs 0.23 mm, $p=0.007$, Figure 1a); when stratifying by pathology, the significance was confirmed for ICH patients ($p=0.012$), while the result for IIH patients was close to significance ($p=0.07$) when compared with the healthy group (Figure 1b). There was no significant difference between ICH and

IIH patients ($p$=0.58). For ICH patients, there was no significant correspondence between the hemorrhage site and the side of the larger ONSD ($p$=0.41).

Both the binocular and maximum ONSD values were significantly higher in the IH group (independently of the pathology) compared to the healthy group (both $p$<0.001, Figure 2 a-b), with no significant differences among the two pathologies ($p$=0.12 and $p$=0.15, respectively).

**Table 2**. Demographic characteristics, binocular / maximum ONSD values, and asymmetry between eyes in healthy and pathological subjects

| | Age | Gender (F) | |
|---|---|---|---|
| Healthy | 75 (61.25–78.75) | 47.5% | |
| Patients | 63 (38–79.25) | 62.5% | |
| ICH | 79.5 (76.25–86.25) | 50% | |
| IIH | 37 (29–47.25) | 66.7% | |
| | ONSD binocular (mm) | ONSD max (mm) | Asymmetry (mm) |
| Healthy | 4.72 (4.57–4.83) | 4.73 (4.65–4.87) | 0.23 (0.07–0.42) |
| Patients | 6.54 (6.22–7.03) | 6.65 (6.31–7.23) | 0.45 (0.18–0.68) |
| ICH | 6.66 (6.36–6.97) | 6.77 (6.50–7.24) | 0.53 (0.20–0.77) |
| IIH | 6.37 (6.09–7.05) | 6.48 (6.15–7.05) | 0.40 (0.10–0.67) |

All values are expressed as median (quartiles). *F*, female; *ONSD*, optic nerve sheath diameter; *ICH*, intracerebral hemorrhage; *IIH*, idiopathic intracranial hypertension

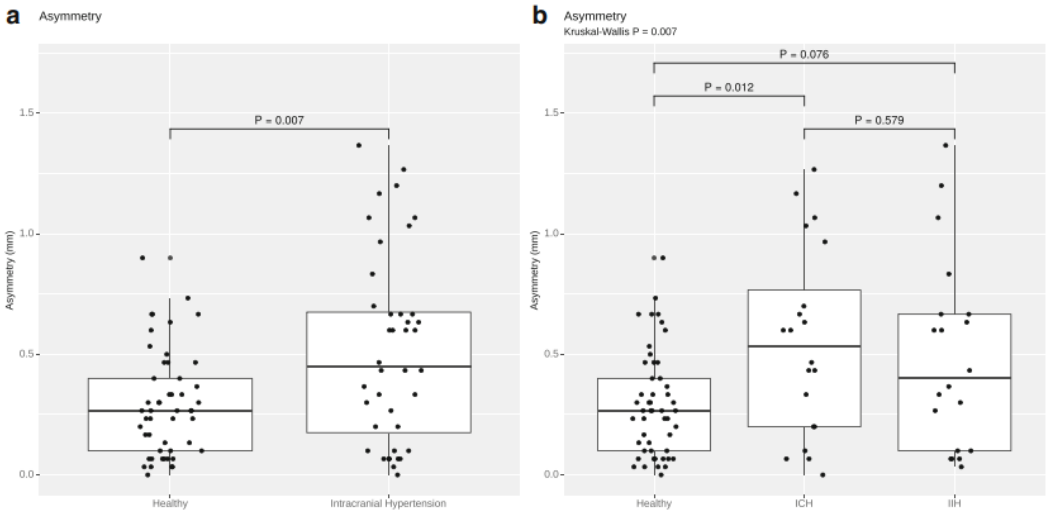


**Fig. 1** Degree of asymmetry (expressed in millimeters) in healthy subjects and patients with intracranial hypertension (**a**) and subgroup analysis dividing the cases by pathology (**b**). ICH, intracerebral hemorrhage; IIH, idiopathic intracranial hypertension

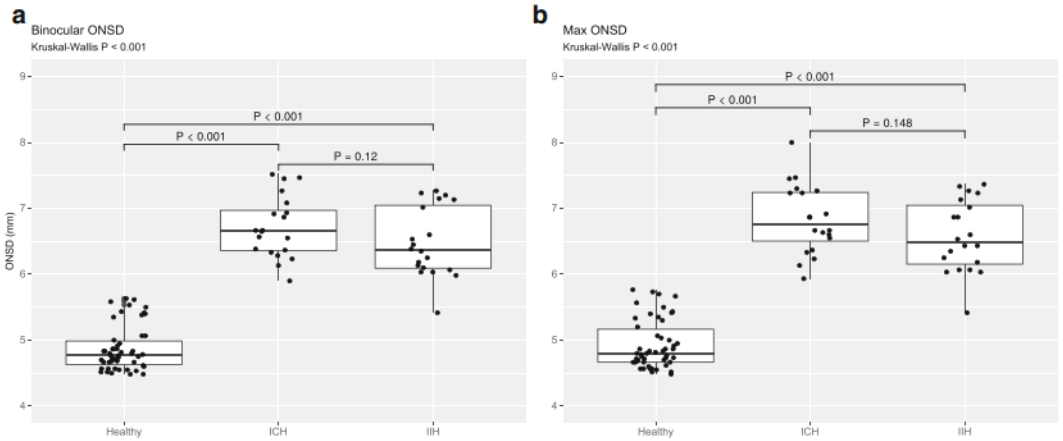


**Fig. 2** Binocular (**a**) and maximum (**b**) ONSD values in patients with intracranial hypertension and healthy subjects. ONSD, optic nerve sheath diameter; ICH, intracerebral hemorrhage; IIH, idiopathic intracranial hypertension

## DISCUSSION

This study documented for the first time in a clinical context the occurrence and degree of interocular ONSD asymmetry by using transorbital sonography in healthy and pathological subjects with IH. Ultrasonography of the ONSD has been proposed as a non-invasive technique to evaluate ICP and ONSD behavior in various conditions. The sheath diameter may increase or shrink in response to ICP changes, but above a dilation threshold the enlargement seems to be irreversible [17, 18]. However, the exact reaction of the ONSD and the optic disc upon ICP variation remains elusive, and different mechanisms may be involved in the orbital response, including optic atrophy, CSF and ocular pressure, and changes in lamina cribrosa or optic nerve structures [19]. Regarding the anatomical aspects, some authors emphasized the role of the optic canals in the transmission of the CSF toward the optic sheaths [4]. Specifically, the thick arachnoid trabeculae and pillars that compose the complex meshwork of the optic canals may limit or even prevent the flow of CSF in the course of IH, determining a disproportionate expansion of ONSDs and unilateral papilledema [20-22]. In addition, an elevated inter-individual variability of optic canal conformation among humans and animals has been described [5, 21]. However, to our knowledge, no data are available about the interocular asymmetry of the ONSD between eyes both in normal conditions and following elevated ICP, particularly in a clinical setting where only isolated descriptions of asymmetry are mentioned [22]. Nevertheless, most ultrasonographic and radiological studies related to this topic evaluated the binocular ONSD value,

without considering this anatomical variability, which may limit the enlargement of the optic sheaths, thus potentially leading to an inaccurate ICP estimation.

Our results documented an asymmetry of the ONSD of the two sides, both in healthy individuals and in patients with IH. The asymmetry increased following raised ICP, confirming the anatomical finding of a different architecture of the optic canals: if the CSF may not be adequately conveyed toward one of them because of a different composition in the trabecular network thickness, the two ONSDs may enlarge asymmetrically. No differences were observed between IIH and ICH subjects, suggesting that the asymmetry was independent on the cause and mechanism of intracranial hypertension. In fact, while in IIH increased ICP may be related to a pathological process involving the whole brain, in ICH it is a consequence of a focal event. Interestingly, there was no association between the side of cerebral hemorrhage and the maximal ONSD dilation, further suggesting that anatomical aspects may influence the ONSD behavior.

The binocular ONSD assessment is a well-known technique for assessing increased ICP; conversely, only few studies evaluated the role of maximum ONSD for this purpose [23-25]. In our series, both binocular and maximum ONSD were significantly higher in patients than in healthy subjects, thus both measures could be useful for the detection of elevated ICP. However, considering the asymmetry and the possibility of a missing or reduced enlargement of the ONSD, ideally maximum ONSD could be a more precise and quicker measurement, especially when asymmetry is present.

There are some limitations to this study, mainly related to its retrospective design and to the small sample size. In ICH patients, diagnosis of IH was based on clinical and radiological findings, without directly measuring ICP. Finally, ONSD values were recorded by using two different sonographic machines. Further studies in a larger population are needed to confirm these results.

In concusion, an interocular ONSD asymmetry exists in normal subjects and patients with elevated ICP, with a larger extent in IH. If present, the asymmetry should be considered for correct ICP estimation. Both binocular ONSD measurements and maximum ONSD may be useful for the evaluation of raised ICP.

**References study #2**


1. Khan MN, Shallwani H, Khan MU, Shamim MS. Noninvasive monitoring intracranial pressure – A review of available modalities. Surg Neurol Int. 2017 Apr 5;8:51. https://doi.org/10.4103/sni.sni_403_16.
2. Sahu S, Swain A. Optic nerve sheath diameter: A novel way to monitor the brain. J Neuroanaesthesiol Crit Care 2017;4:S13-8. https://doi.org/10.4103/jnacc.jnacc_73_16
3. Hayreh SS, Ischemic Optic Neuropathies. https://doi.org/10.1007/978-3-642-11852-4_2, © Springer-Verlag Berlin Heidelberg 2011
4. Hayreh SS. The sheath of the optic nerve. Ophthalmologica. 1984;189:54–63. https://doi.org/10.1159/000309386
5. Killer HE, Laeng HR, Flammer J, Groscurth P. Architecture of arachnoid trabeculae, pillars, and septa in the subaranchnoid space of the human optic nerve: anatomy and clinical considerations. Br J Ophthalmol 2003;87:777-781
6. Robba C, Santori G, Czosnyka M, Corradi F, Bragazzi N, Padayachy L, Taccone FS, Citerio G. Optic nerve sheath diameter measured sonographically as non-invasive estimator of intracranial pressure: a systematic review and meta-analysis. Intensive Care Med. 2018 Aug;44(8):1284-1294. https://doi.org/10.1007/s00134-018-5305-7
7. Lochner P, Czosnyka M, Naldi A, Lyros E, Pelosi P, Mathur S, Fassbender K, Robba C. Optic nerve sheath diameter: present and future perspectives for neurologists and critical care physicians. Neurol Sci. 2019 Jul 31. https://doi.org/10.007/s10072-019-04015-x [Epub ahead of print]
8. Lochner P, Fassbender K, Leismeister M, Nardone R, Orioli A, Brigo F, Stolz E. Ocular ultrasound for monitoring pseudotumor cerebri syndrome. J Neurol. 2018 Feb;265(2):356-361. https://doi.org/10.1007/s00415-017-8699-1
9. Naldi A, Pivetta E, Coppo L, Cantello R, Comi C, Stecco A, Cerrato P, Lesmeister M, Lochner P. Ultrasonography Monitoring of Optic Nerve Sheath Diameter and Retinal Vessels in Patients with Cerebral Hemorrhage. J Neuroimaging. 2019 May;29(3):394-399. https://doi.org/10.1111/jon.12604

10. Friedmann DI, Liu GT, Digre KB. Revised diagnostic criteria for the pseudotumor cerebri syndrome in adults and children. Neurology. 2013 Sep 24:81(13):1159–1165. https://doi.org/10.1212/WNL.0b013e3182a55f17
11. Lang EW, Ren Ya Z, Preul C, Hugo HH, Hempelmann RG, Buhl R, Barth H, Klinge H, Mehdorn HM. Stroke pattern interpretation: the variability of hypertensive versus amyloid angiopathy haemorrhage. Cerebrovasc Dis. 2001 Aug;12(2):121-30
12. Ohle R, McIsaac SM, Woo MY, Perry JJ. Sonography of the optic nerve sheath diameter for detection of raised intracranial pressure compared to computer tomography: a systematic review and meta-analysis. J Ultrasound Med 2015;34:1285-94. https://doi.org/10.7863/ultra.34.7.1285
13. Kothari RU, Brott T, Broderick JP, Barsan WG, Sauerbeck LR, Zuccarello M, Khoury J. The ABCs of measuring intracerebral hemorrhage volumes. Stroke 1996;27(8):1304-5
14. Huttner HB, Steiner T, Hartmann M, Köhrmann M, Juettler E, Mueller S, Wikner J, Meyding-Lamade U, Schramm P, Schwab S, Schellinger PD. Comparison of ABC/2 estimation technique to computer-assisted planimetric analysis in warfarin-related intracerebral parenchymal hemorrhage. Stroke. 2006 Feb;37(2):404-8
15. Ertl M, Barinka F, Torka E, Altmann M, Pfister K, Helbig H, Bogdahn U, Gamulescu MA, Schlachetzki F. Ocular color-coded sonography – a promising tool for neurologists and intensive care physicians. Ultraschall Med. 2014 Oct;35(5):422-31. 10.1055/s-0034-1366113
16. R Core Team (2019). R: A Language and Environment for Statistical Computing. R Foundation for Statistical Computing, Vienna, Austria. URL https://www.R-project.org
17. Hansen HC, Lagrèze W, Krueger O, Helmke K. Dependence of the optic nerve sheath diameter on acutely applied subarachnoidal pressure – an experimental ultrasound study. Acta Ophthalmol. 2011 Sep;89(6):e528-32. https://doi.org/10.1111/j.1755-3768.2011.02159.x
18. Bäuerle J, Niesen WD, Egger K, Buttler KJ, Reinhard M. Enlarged Optic Nerve Sheath in Aneurysmal Subarachnoid Hemorrhage despite Normal Intracranial Pressure. J Neuroimaging. 2016 Mar-Apr;26(2):194-6. https://doi.org/10.1111/jon.12287

19. Bidot S, Clough L, Saindane AM, Newman NJ, Biousse V, Bruce BB. The Optic Canal Size Is Associated With the Severity of Papilledema and Poor Visual Function in Idiopathic Intracranial Hypertension. J Neuroophthalmol. 2016 Jun;36(2):120–125. https://doi.org/10.1097/WNO.0000000000000318
20. Bidot S, Bruce BB, Saindane AM, Newman NJ, Biousse V. Asymmetric papilledema in idiopathic intracranial hypertension. J Neuroophthalmol. 2015 Mar;35(1):31–36. https://doi.org/10.1097/WNO.0000000000000205
21. Hayreh SS. Pathogenesis of optic disc edema in raised intracranial pressure. Prog Retin Eye Res. 2016;50:108-44. https://doi.org/10.1016/j.preteyeres.2015.10.001
22. Skoloudík D, Herzig R, Fadrná T, Bar M, Hradílek P, Roubec M, Jelínková M, Sanák D, Král M, Chmelová J, Herman M, Langová K, Kanovsky P. Distal enlargement of the optic nerve sheath in the hyperacute stage of intracerebral haemorrhage. Br J Ophthalmol. 2011 Feb;95(2):217-21. https://doi.org/10.1136/bjo.2009.172890
23. Young AM, Guilfovle MR, Donnelly J, Scoffings D, Fernandes H, Garnett M, Agrawal S, Hutchinson PJ. Correlating optic nerve sheath diameter with opening intracranial pressure in pediatric traumatic brain injury. Pediatr Res. 2017 Mar;81(3):443-447. https://doi.org/10.1038/pr.2016.165
24. Tarzamni MK, Derakhshan B, Meshkini A, Merat H, Fouladi DF, Mostafazadeh S, Rezakhah A. The diagnostic performance of ultrasonographic optic nerve sheath diameter and color Doppler indices of the ophthalmic arteries in detecting elevated intracranial pressure. Clin Neurol Neurosurg. 2016;141:82-88. https://doi.org/10.1016/j.clineuro.2015.12.007
25. Agrawal A, Cheng R, Tang J, Madhok DY. Comparison of Two Techniques to Measure Optic Nerve Sheath Diameter at Risk for Increased Intracranial Pressure. Crit Care Med. 2019 Jun;47(6):e495-e501. https://doi.org/10.1097/CCM.0000000000003742

# STUDY #3

## "AUTomatic Optic Nerve MeAsurement (AUTONoMA): a new tool to standardize the optic nerve assessment in ultrasound B-mode images"


## ABSTRACT

Transorbital sonography provides reliable information about the estimation of intracranial pressure by measuring the optic nerve sheath diameter (ONSD), while the optic nerve (ON) diameter (OND) may reveal ON atrophy in multiple sclerosis patients. Here, an AUTomatic Optic Nerve MeAsurement (AUTONoMA**)** system for OND and ONSD assessment in ultrasound B-mode images based on deformable models is presented. The automated measurements were compared to manual ones obtained by two operators, with no significant differences. AUTONoMA correctly segmented the ON and its sheath in 71 out of 75 images. The mean error compared with the expert operator was 0.06±0.52 mm and 0.06±0.35 mm for the ONSD and OND respectively. The agreement between operators and AUTONoMA was good and a positive correlation between the readers and the algorithm with errors comparable with the inter-operator variability was found. The AUTONoMA system may allow a standardization of OND and ONSD measurements, reducing manual evaluation variability.


## INTRODUCTION

Transorbital sonography (TOS) is a promising technique for the non-invasive evaluation of the optic nerve (ON) structures. This tool is particularly versatile and can be performed both in remote, prehospital setting and hospital context, either in invasive or non-invasive departments (Houzé-Cerfon et al. 2018; Lochner et al. 2015). The main use of TOS concerns the assessment of the optic nerve sheath diameter (ONSD) for the estimation and monitoring of increased intracranial pressure (ICP), particularly when the invasive referenced methods are contraindicated or unavailable (Goeres et al. 2016; Robba et al. 2015; Soliman et al. 2018). Moreover, TOS can be useful to detect ON atrophy in patients with

multiple sclerosis (Carraro et al. 2014). The current application fields of TOS in the clinical practice have been recently described (Lochner et al. 2019).

A good intra and interobserver reproducibility using high-frequency (>7.5 MHz) linear probe, which allows a lateral spatial resolution <0.4 mm, can be obtained for the ultrasonographic assessment of optic nerve diameter (OND) and ONSD (Bäuerle et al. 2012; Lochner et al. 2014; Lochner et al. 2018a). Although this, the manual evaluation of OND and ONSD can be affected by the operator's experience and artefactual images (Ballantyne et al. 2002; Copetti and Cattarossi 2009). In addition, different methods are currently described in literature for the ONSD evaluation, leading to possible misunderstanding in the results interpretation (Bloria et al. 2019).

Even if a greater experience or a continuous training have demonstrated to reduce operator variability, for a better use of the technique, a unique model of measurements and a standardization of the method are required (Zeiler et al. 2013; Zeiler et al. 2014). The development of computerized automated systems for the segmentation of structures in B-mode ultrasound images is an auspicious research field that may help reduce thereupon the operator-dependency, accelerate the acquisition time and mitigate the issue of inter-operator variability (Meiburger et al. 2018). In this context, Gerber et al. (Gerber et al. 2017) developed an algorithm to automatically estimate the ONSD from 23 ocular ultrasound images and on an eye phantom using 3D-printed optic nerves embedded under gelatin orbs. However, to the best of our knowledge, except from this work which employed a very small dataset of in-vivo images and estimated only the ONSD, there are no described methods focused on a completely automatic segmentation of the optic nerve and optic nerve sheath in ultrasound B-mode images in a large series of patients affected by neurological diseases with increased ICP and healthy subjects.

Therefore, the aim of this work is to present and validate a completely automatic system for measuring the OND and ONSD, requiring no interaction with the user.

## METHODS

The measurement of the OND and ONSD with TOS is based on the difference in echogenicity and morphology of the different retro-orbital structures. The

developed algorithm is based on the assumption that the ultrasound image presents hypoechoic structures like the vitreous, the inside of the optic nerve and the arachnoid, and hyperechoic structures like pia and dura mater and the surrounding adipose tissue. The anterior part of the optic nerve is depicted in an axial plane showing the papilla and the optic nerve in its longitudinal course. ONSD and OND are assessed 3 mm behind the papilla (Helmke and Hansen 1996) and should be calculated perpendicularly to the optic nerve centerline.

The OND is typically measured manually as the distance between the right profile of the optic nerve and the left one. To measure the ONSD, we quantified the distance between the external borders of the hyperechogenic area surrounding the optic nerve (Ertl et al. 2014), as shown in Fig. 1.

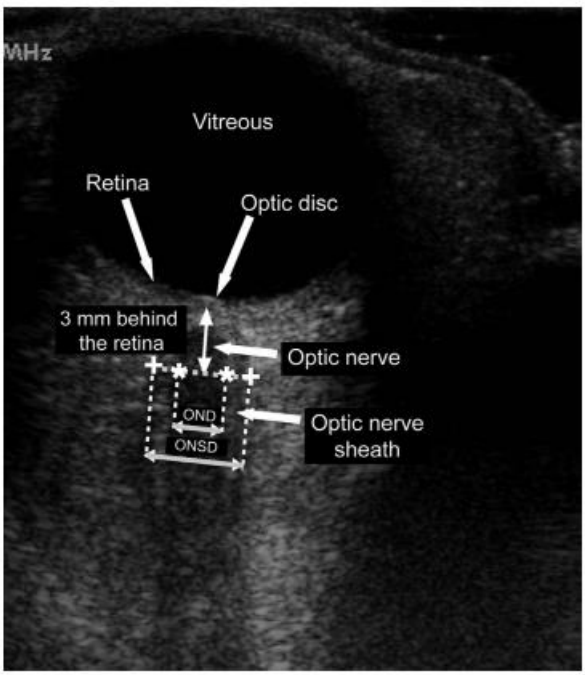


Fig. 1. Example of manual calculation of optic nerve diameter (OND) and optic nerve sheath diameter (ONSD).

***Image acquisition and database***

A total of 75 images - taken from a dataset available by the authors - were included in this study: 30 images came from 15 patients who were diagnosed either with primary or secondary intracranial hypertension (IH) according to the current diagnostic criteria (Friedman et al. 2013) and 45 images from 23 healthy controls. All images were acquired by an expert neurosonologist with more than 10 years of experience in TOS using a Vivid 7 sonography system with a 7 to 11 MHz linear

array probe with a central frequency of 10 MHz (GE Healthcare, Milwaukee, Wisconsin).

For image acquisition, a standard protocol was followed. Specifically, the patient was asked to lie in a supine position on a bed with the head reclined at a 20°-30° angle. With the patient's eyes closed, the linear array ultrasound probe was gently placed on the closed eyelids (never in direct contact with the cornea or sclera), and the image was acquired. All images were exported from the ultrasound device and transferred to a workstation for offline processing.

***AUTONoMA architecture***

An overview of our proposed AUTomatic Optic Nerve MeAsurement (AUTONoMA) system is presented in Fig. 2. It consists of a computer aided diagnosis (CAD) system that takes a B-mode image obtained from transorbital ultrasonography and gives forth an automated measurement of the optic nerve diameter and the optic nerve sheath diameter, without requiring any interaction from the user. The proposed system can be summarized in two main automatic steps:

1. Stage I: coarse localization of the ROI through the automatic recognition of the ocular bulb profile and the optic nerve centerline tracing.
2. Stage II: fine segmentation of the optic nerve and the optic nerve sheath through dual snakes and automatic measurement of OND and ONSD.

***Stage I: coarse localization of ocular bulb and optic nerve centerline***

In order to accurately locate the ocular bulb within the ultrasound image frame, a preprocessing step is first necessary to isolate the ultrasound information from the entire image frame. To do so, an automatic image cropping step was developed, using morphological operations and gradients. Fig. 3a shows the original image and Fig. 3b shows the automatically cropped image.

The automatic recognition of the ocular bulb is then done on the cropped image. First of all, the image is sharpened by summing the original image with the image obtained with the First Order Absolute Moment (FOAM), an edge operator which has been applied previously in ultrasound images (Faita et al. 2006). Subsequently, a gaussian derivative filter (sigma = 7) was applied to the image (Fig. 3c). In the obtained image, the bottom border of the optical bulb is automatically located

through a column-wise heuristic search. The beginning of the column-wise search region is found by locating the first pixel (starting from the top of the image) that is above a certain intensity and that presents a reasonably large hypoechogenic region above it (i.e., the bulb) (Fig. 3c). The point of the optical bulb boundary for the analyzed column is then automatically located by finding the first discontinuity from a hypoechoic zone to a hyperechoic zone on the B-mode cropped image. The profile obtained by analyzing each column, $AUTONoMA_{bulb}$, is then interpolated to give forth the final segmentation of the ocular bulb (Fig. 3d).

The identification of the bottom boundary of the ocular bulb makes the search for an estimation of the optic nerve centerline significantly easier by limiting the search of the optic nerve within a specific area of the image. Specifically, a gaussian derivative filter was again applied to the ultrasound image and the optic nerve centerline was located thanks to a heuristic search below the found $AUTONoMA_{bulb}$ profile similar to the one previously described but considered row-wise. The obtained centerline, $AUTONoMA_{ONc,}$ is shown in Fig. 3e.

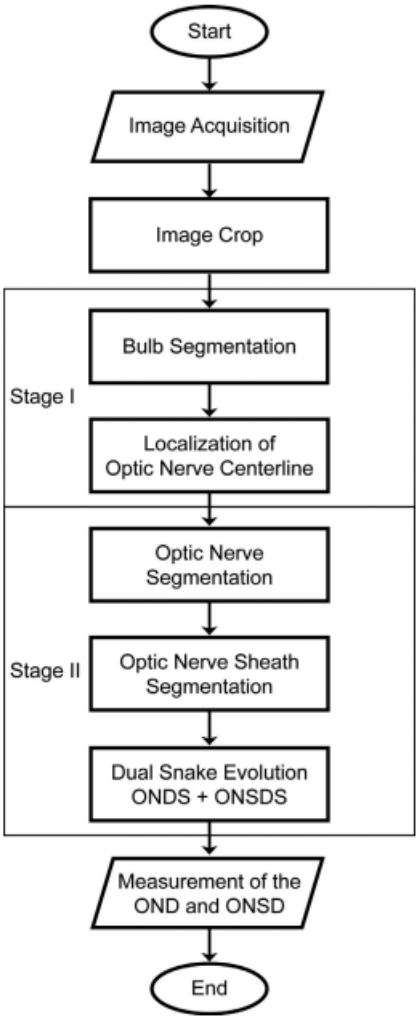


Fig. 2. Overview of steps for the AUTONoMA system. The image is first acquired, and then automatically cropped. Stage I consists of automatic recognition of the bulb and optic nerve centerline. Stage II then consists of initialization of the two dual-snake models by a rough segmentation of the optic nerve and optic nerve sheath. The dual-snake models then evolve in time until they reach the borders of the actual optic nerve and optic nerve sheath. Then the final values of optic nerve diameter (OND) and optic nerve sheath diameter (ONSD) are automatically measured from the final dual-snake boundaries.

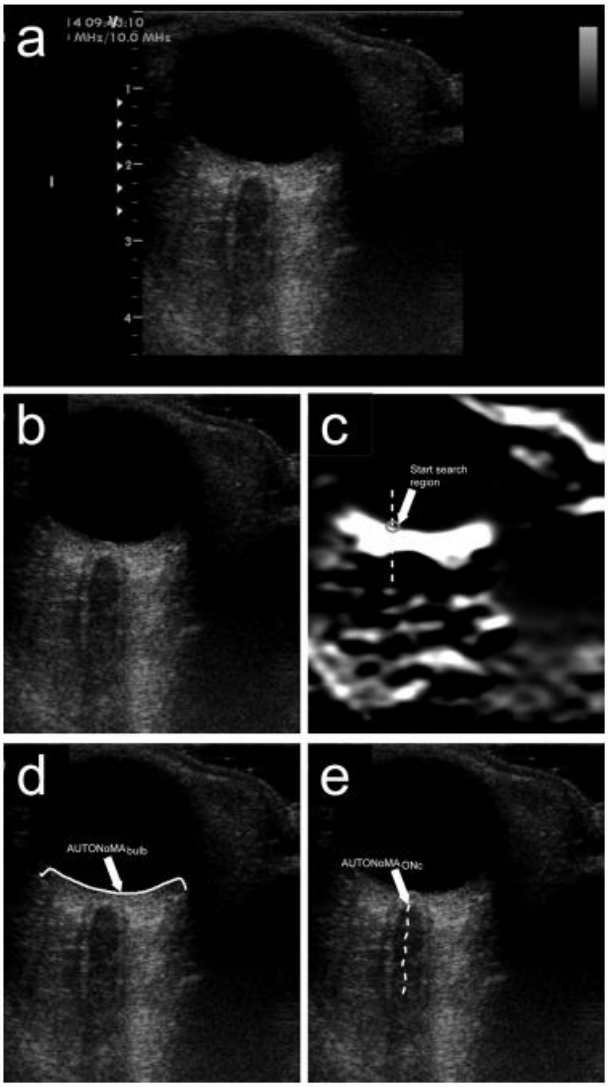


Fig. 3. Overview of the AUTONoMA stage I architecture. (a) Original image; (b) automatically cropped image; (c) first-order Gaussian derivative of (b), showing the initialization of the search region for tracing the bulb profile; (d) AUTONoMA bulb ($AUTONoMA_{bulb}$) profile segmentation results; (e) AUTONoMA optic nerve centerline ($AUTONoMA_{ONc}$) tracing.

***Stage II: fine segmentation of optic nerve and optic nerve sheath***

The fine segmentation of the optic nerve and the optic nerve sheath is done by implementing a dual snake model, similar to the one presented by Molinari et al. (Molinari et al. 2012b; Molinari et al. 2012a). Since both the optic nerve diameter and the optic nerve sheath diameter are of clinical interest, two different dual snake models were developed: one for the calculation of the optic nerve diameter, and the other for the optic nerve sheath diameter.

As all active contour models, the dual snake algorithm requires a first initialization of the snakes, which then evolve in time and adapt to the optic nerve and sheath boundaries. The snakes initialization and evolution are described in the following paragraphs.

***Snakes initialization***

The snakes initialization can be summarized as follows: 1) starting from the located optic nerve centerline, the ON dual snake (ONDS) model was initialized by locating the rough nerve boundary; 2) similarly, the optic nerve sheath dual snake (ONSDS) model was initialized by locating the rough sheath boundary starting from the rough nerve boundary located in the previous step 1.

The rough boundaries of both the optic nerve and the optic nerve sheath, hence the snakes initialization, were located thanks to a row-wise heuristic search on the original image filtered with a gaussian derivative filter in two directions. Briefly, starting from the centerline/optic nerve boundary going outwards, the first pixel in the gaussian derivative filtered image that is higher than a specific threshold is taken as the candidate point for the optic nerve/optic nerve sheath. The snake initialization then is taken as joining together all candidate points.

Fig. 4a and 4b shows the snakes initialization for the ONDS and ONSDS, respectively.

***Snakes evolution***

Once the snakes are initialized, the dual snake models *v(s)* then evolve in time thanks to three energy models: the internal, external, and mutual interaction energies.

The internal energy serves to constrain the shape of the contour and prevents the active contour from presenting an excessive curvature, which is especially necessary in this clinical application, in which the optic nerve and optic nerve sheath are represented by more or less straight lines. This energy is defined as:

$$E_{\text{int}}(v(s)) = \int_0^1 \alpha \left| v'(s) \right| ds,$$

where $s$ is the curvilinear coordinate on the image, $v^i(s)$ is the first-order derivative of the snake curve $v(s)$ and α is a parameter used to give a specific weight to the internal energy, controlling the curvature of the snake.

The external energy is what attracts the snake model toward the image discontinuities. This energy is defined as:

$$E_{ext}(v(s)) = -\int_0^1 \beta e(v(s))\, ds,$$

where β is a parameter used to give a specific weight to the external energy and the functional *e(x, y)* is a first order gaussian derivative filter, an edge operator that has been used in numerous ultrasound clinical applications (Caresio et al. 2017).

The mutual interaction energy, which can be considered as a second term of external energy, is necessary to ensure that the two models of the dual snake do not either collapse on one another or converge. So, this energy is inversely proportional to the distance between the two curves (the left and right snake, $v_L(s)$ and $v_R(s)$, respectively) and is defined as:

$$E_{mut}(v(s)) = \int_0^1 \gamma \frac{1}{|v_R(s) - v_L(s)|} ds,$$

where γ is a parameter used to give a specific weight to the mutual energy.

The values of the parameters used for each of the dual snake models are shown in Tab. 1. As can be seen, the external energy and mutual energy parameters are dependent on the conversion factor (CF), expressed in millimeters per pixel in order to make the models independent of both zooming and of the ultrasound device used to acquire the images. The value of the base conversion was 0.116mm/pixel..

The final segmentation of the optic nerve and the optic nerve sheath is shown in Fig. 4c and 4d, respectively.

Table 1. Parameter values for dual-snake models

| Model | $\alpha$ (internal energy) | $\beta$ (external energy) | $\gamma$ (mutual energy) |
|---|---|---|---|
| ONDS | 0.7 | $\frac{0.3 \cdot CF_{base}}{CF}$ | $\frac{9 \cdot CF_{base}}{CF}$ |
| ONSDS | 0.3 | $\frac{0.1 \cdot CF_{base}}{CF}$ | $\frac{6 \cdot CF_{base}}{CF}$ |

ONDS = optic nerve dual snake; ONSDS = optic nerve sheath dual snake; CF = conversion factor.

### *Calculation of the OND and ONSD*

Once the optic nerve and optic nerve sheath are correctly segmented, the diameters of the two structures (OND and ONSD) were automatically measured. This was done by using the optic nerve centerline that was found automatically and locating the point that is 3 mm behind the optic bulb. From here, the Centerline Distance

(Saba et al. 2012) between the two final snake models was calculated to give forth the final OND and ONSD values (Fig. 4e). In order to reduce the variability of the final OND and ONSD measurements, the centerline distance was calculated right at 3 mm behind the optic bulb, slightly before 3 mm, and slightly after 3 mm, and the average distance was taken to be the final diameter measurement.

The AUTONoMA system was developed in Matlab and showed an average computational time of 2 seconds for processing a single image, providing an almost real-time analysis.

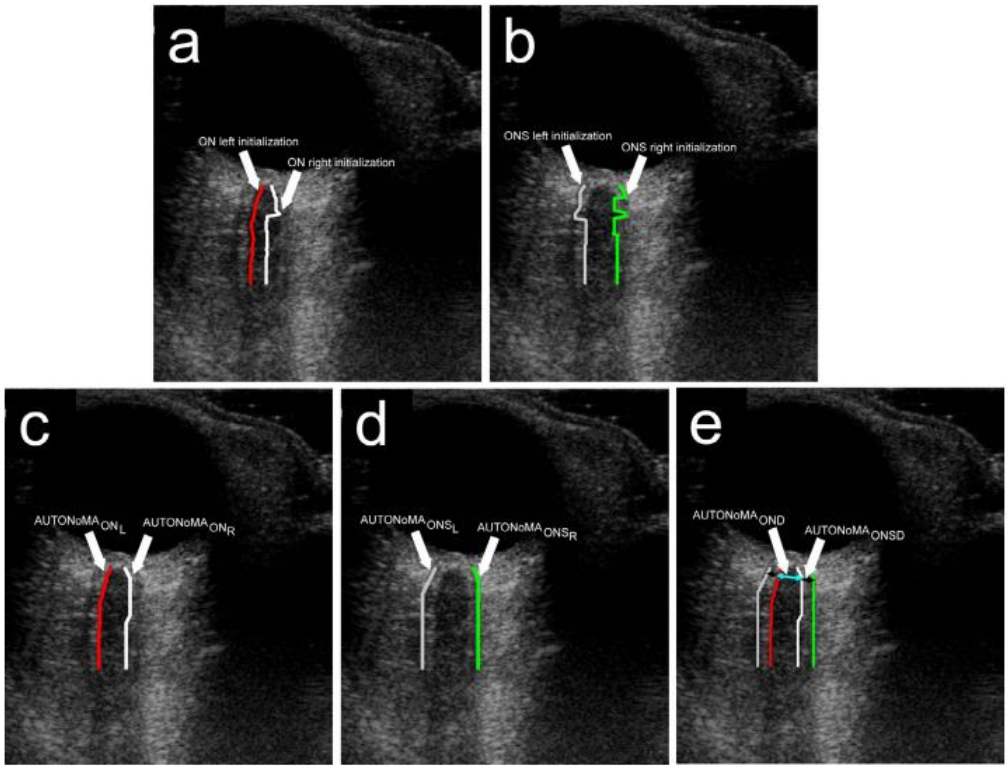


Fig. 4. Overview of the AUTONoMA stage II architecture. (a) Optic nerve (ON) dual-snake initialization; (b) optic nerve sheath (ONS) dual-snake initialization (c) final ON dual-snake segmentations ($AUTONoMA_{ON_L}$ and $AUTONoMA_{ON_R}$); (d) final ONS dual-snake segmentations ($AUTONoMA_{ONS_L}$ and $AUTONoMA_{ONS_R}$); (e) final calculation of the automatic ON diameter (OND) and ON sheath diameter (ONSD) measurements ($AUTONoMA_{OND}$ and $AUTONoMA_{ONSD}$).

***Performance evaluation***

In order to validate the results of the developed AUTONoMA algorithm, different performance evaluation metrics were used.

First of all, the OND and ONSD measurements that were obtained automatically were compared with the manual measures of an expert with more than 10 years of experience in transorbital ultrasonography and a non-expert operator (referenced as

Op1 and Op2 from here on out, respectively), considered as ground truth. To do the manual measurement, an in-house program in Matlab was developed to allow adequate zooming of the image, and the subsequent manual tracing of the optic nerve centerline. Using the calibration factor, the perpendicular line at 3mm was drawn and the operator was asked to use the mouse to measure the OND and ONSD at the correct depth. So, for each image, the error between the automatic computer-based measure and the ground truth measure was calculated. Three types of error were used to describe the overall system performance: the mean error (defined as the mean difference between the manual measure and the automatic one), the mean absolute error (MAE) and the mean squared error (MSE), along with the respective standard deviations. Another parameter, the Figure of Merit (FoM), which characterizes the overall performances of the algorithm, was calculated. This parameter is defined as:

$$\mathrm{FoM}_{\mathrm{OND}} = 100 - \left| \frac{\mathrm{mean}(\mathrm{OND}_{\mathrm{auto}}) - \mathrm{mean}(\mathrm{OND}_{\mathrm{man}})}{\mathrm{mean}(\mathrm{OND}_{\mathrm{man}})} \right| \cdot 100$$

$$\mathrm{FoM}_{\mathrm{ONSD}} = 100 - \left| \frac{\mathrm{mean}(\mathrm{ONSD}_{\mathrm{auto}}) - \mathrm{mean}(\mathrm{ONSD}_{\mathrm{man}})}{\mathrm{mean}(\mathrm{ONSD}_{\mathrm{man}})} \right| \cdot 100,$$

where $\mathrm{mean}(\mathrm{OND}_{\mathrm{auto}})$ and $\mathrm{mean}(\mathrm{ONSD}_{\mathrm{auto}})$ are respectively the average OND and ONSD values found automatically, and $\mathrm{mean}(\mathrm{OND}_{\mathrm{man}})$ and $\mathrm{mean}(\mathrm{ONSD}_{\mathrm{man}})$ are the average OND and ONSD values measured manually, respectively.

Morover, we calculated the correlation coefficient and the 95% confidence interval between the ground truth diameter values and the automated diameter values. Finally, to determine if the automatic and manual measurements present a statistically significant difference between the measurements or not, the Wilcoxon signed rank test was used.

In order to assess inter-operator variability in OND and ONSD measurements, the correlation between the manual measurements was also calculated. For each image, the manual measurements were obtained offline and independently by the two operators involved (both blinded with regard to AUTONoMA performance). The developed AUTONoMA system is completely automated and independent from the user; therefore, the system does not present any measurement variability.

## RESULTS

The proposed AUTONoMA system was able to correctly segment 71 out of 75 images, presenting a 95% success rate. Fig. 5 shows some example segmentation results obtained with the AUTONoMA system, whereas Fig. 6 shows two examples of images that were not able to be processed automatically.

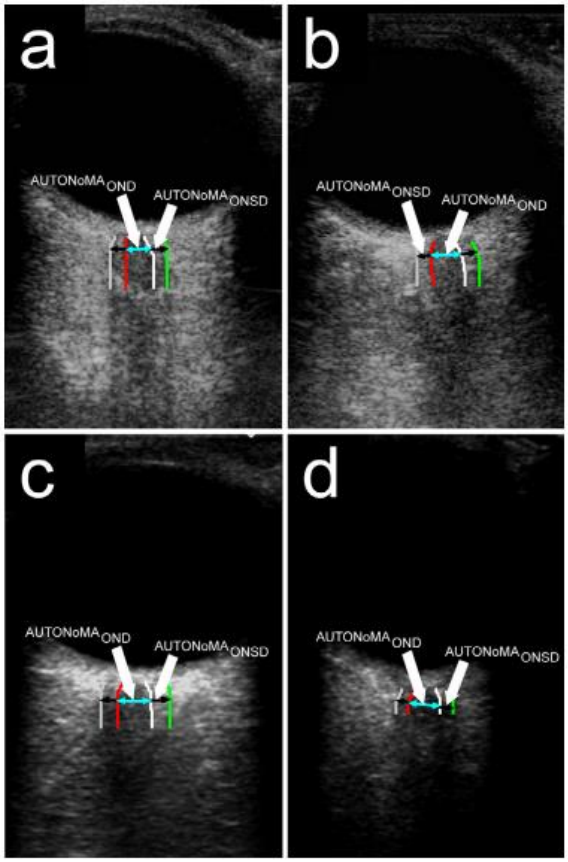


Fig. 5. Segmentation and optic nerve diameter (OND) and optic nerve sheath diameter (ONSD) measurement results of the AUTONoMA system.

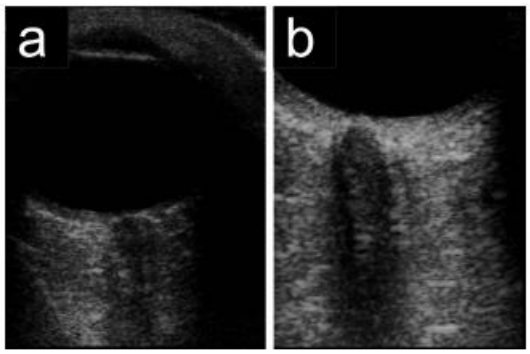


Fig. 6. Example error cases for the AUTONoMA system. (a) Insufficient intensity difference between the hypo-echogenicity of the optic nerve and the surrounding arachnoid space; (b) excessively hyper-echoic surrounding arachnoid space.

The performance values for the optic nerve and the optic nerve sheath diameter are reported in Tab. 2 and Tab. 3, respectively. No significant differences were observed between AUTONoMA and the operators for the OND values ($p > 0.05$), whereas a significant difference was found for the ONSD values between only AUTONoMA and the inexpert operator, Op2 ($p < 0.05$). Considering the OND measurements, the automatic algorithm gave mean errors of 0.06±0.35 and 0.05±0.38 mm when compared with Op1 and Op2, respectively. In both cases the algorithm underestimated the measure. The FoM was 98.2% compared with Op1 and 98.3% compared to Op2. Considering the ONSD, the mean error compared to Op1 and Op2 was 0.06±0.52 and -0.37±0.55 mm, respectively, and the FoM was 99.0% and 93.5%.

Table 2. Performance evaluation results of the AUTONoMA system compared with manual measurements for calculation of the optic nerve diameter

| OND | AUTONoMA | Operator 1 | Operator 2 |
|---|---|---|---|
| Mean value (mm) | 3.1 ± 0.3 | 3.1 ± 0.4 | 3.0 ± 0.4 |
| Mean error (mm) | | 0.06 ± 0.35 | −0.05 ± 0.38 |
| Mean absolute error (mm) | | 0.28 ± 0.22 | 0.30 ± 0.24 |
| Mean squared error ($mm^2$) | | 0.12 ± 0.17 | 0.15 ± 0.25 |
| FoM | | 98.2% | 98.3% |

OND = optic nerve diameter; FoM = figure of merit.

Table 3. Performance evaluation results of the AUTONoMA system compared with manual measurements for calculation of the optic nerve sheath diameter

| ONSD | AUTONoMA | Operator 1 | Operator 2 |
|---|---|---|---|
| Mean value (mm) | 6.2 ± 0.6 | 6.2 ± 0.6 | 5.8 ± 0.6* |
| Mean error (mm) | | 0.06 ± 0.52 | −0.37 ± 0.55 |
| Mean absolute error (mm) | | 0.41 ± 0.32 | 0.49 ± 0.45 |
| Mean squared error ($mm^2$) | | 0.27 ± 0.37 | 0.44 ± 0.66 |
| FoM | | 99.0% | 93.5% |

ONSD = optic nerve sheath diameter; FoM = figure of merit.
* Statistically significant difference ($p < 0.05$) between operator and AUTONoMA using the Wilcoxon signed rank test.

The Pearson correlation coefficient, 95% confidence interval and the p-value between the automatic measure (OND or ONSD) and the manual one performed by Op1 and Op2 are reported in Tab. 4. A statistically significant correlation was found between our AUTONoMA algorithm and the manual operators, with p values ≤ 0.05 in all cases for both OND and ONSD. The inter-operator variability also showed a statistically significant correlation (p ≤ 0.05 for both OND and ONSD).

Table 4. Correlation performance results between the AUTONoMA system and the manual operators (Op1 and Op2), and inter-operator variability

| | | | Confidence interval | | |
|---|---|---|---|---|---|
| Analysis | Measure | Correlation coefficient | Lower limit | Upper limit | *p* value |
| AUTONoMA versus Op1 | OND | 0.47 | 0.27 | 0.63 | $3.590 \times 10^{-5}$ |
| | ONSD | 0.64 | 0.48 | 0.76 | $1.541 \times 10^{-9}$ |
| AUTONoMA versus Op2 | OND | 0.35 | 0.12 | 0.54 | 0.0031 |
| | ONSD | 0.61 | 0.44 | 0.74 | $1.375 \times 10^{-8}$ |
| Op1 versus Op2 | OND | 0.69 | 0.55 | 0.80 | $2.543 \times 10^{-11}$ |
| | ONSD | 0.65 | 0.49 | 0.77 | $7.222 \times 10^{-10}$ |

OND = optical nerve diameter; ONSD = optical nerve sheath diameter.

The Bland-Altman plots of the AUTONoMA OND and ONSD compared with Op1 and Op2 are shown in Fig. 7, and those of the inter-operator analysis for OND and ONSD are shown in Fig. 8. It can be appreciated that there is an absence of any visible bias, and the automated measurements were all close to the manually measured values.

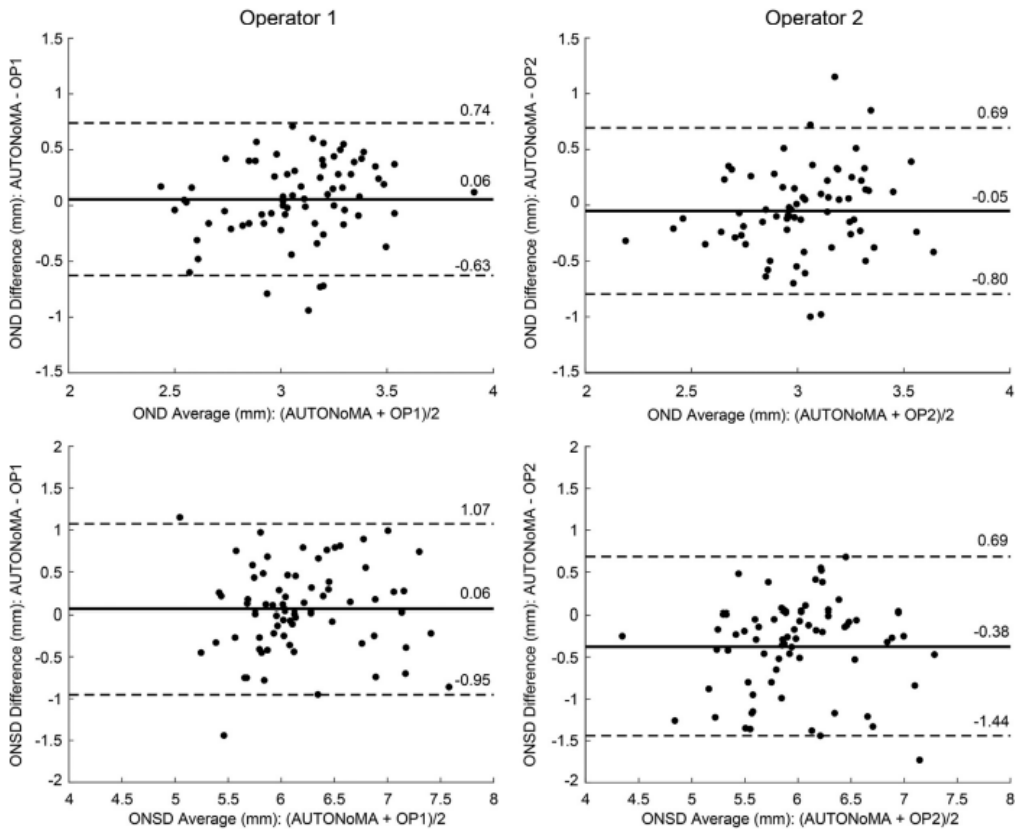


Fig. 7. Bland–Altman analysis comparing the optic nerve diameter (OND; *top row*) and optic nerve sheath diameter (ONSD; *bottom row*) with those obtained by Operator 1 (*left column*) and Operator 2 (*right column*); solid line depicts the mean of differences, dashed lines denote limits of agreement.

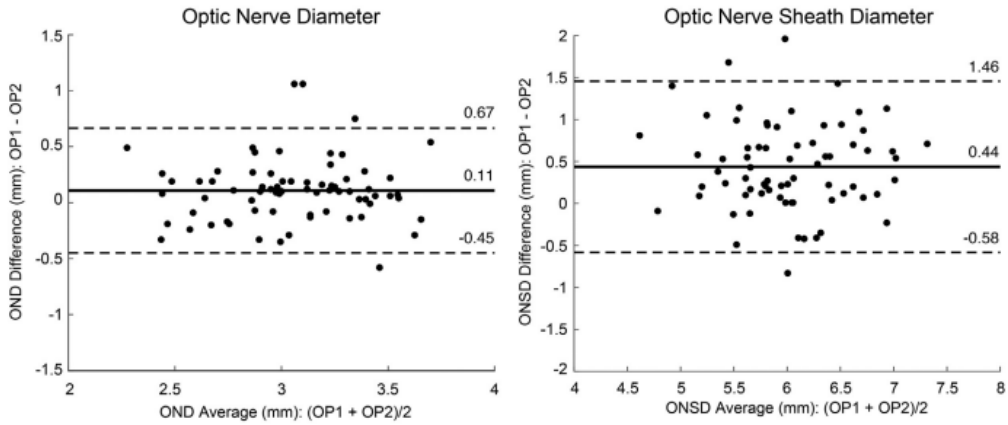


Fig. 8. Bland–Altman inter-operator analysis comparing the optic nerve diameter (OND – first column) and the optic nerve sheath diameter (ONSD – second column) with Operator 1 vs Operator 2. Continuous line depicts the mean of differences; dashed lines denote limits of agreement.

## DISCUSSION

Apart from a recent pilot study presented by Gerber et al. (Gerber et al. 2017), this is the first work that proposes an automatic optic nerve system to calculate both the

OND and the ONSD. Our set of ocular ultrasound images was three times larger, and compared the automated measurements with those of two investigators with different expertise who independently examined both parameters.

The main findings of our work are as follows.

First, the AUTONoMA algorithm is fully automated and was able to provide a correct analysis of 95% of the images present in the dataset. On further analysis, it was found that the automatic algorithm provided segmentation that the manual expert deemed acceptable in all cases except for five images (7%), where the AUTONoMA segmentation diverged from the actual ON and ONS borders.

Second, the mean value of ONSD obtained from AUTONoMA, 6.2±0.6, is very similar to the ONSD value achieved by the expert operator, 6.2±0.6 ($p=0.28$), and significantly different from that of the inexpert operator, 5.8±0.6 ($p<0.05$). Moreover, the mean absolute and mean squared errors exclude a systematic error from AUTONoMA. Similarly, the OND measurements obtained from AUTONoMA were not significantly different from those achieved by the operators ($p = 0.08$ and $p = 0.21$, respectively).

Third, regarding inter-observer reliability according to the Bland-Altman analysis, we found a good agreement between the operators. Moreover, the difference of measurements of ONSD is inferior to the intrinsic error of the machine (Ballantyne et al. 2002) and comparable with the inter-operator reproducibility reported in prior studies (Bäuerle et al. 2012; Lochner et al. 2014).

Finally, AUTONoMA calculates the OND/ONSD value simultaneously and in a very short time, approximately two seconds per image. Manual measurements take about thirty second for each image, hence the automatic algorithm provides a result 15 times faster than an expert operator. Moreover, because the system is completely automatic and independent from the user, there is no measurement variability between OND and ONSD.

Translating into clinical practice, the AUTONoMA system may represent the first step to reduce the wide variability of ONSD and OND measurements currently described in literature. These differences reflect the operator's experience, the use of different ultrasonographic machines, and a non-homogeneous and standardized method for image acquisition and measurements (Bloria et al. 2019). The presence and use of an automated system such as AUTONoMA could – at least in part –

mitigate and minimize these differences, promoting a more comparable interpretation of results among studies.

Both OND and ONSD are used to study neurological conditions that imply variations in their value. Meanwhile, the spectrum of applications for TOS in the context of neurological diseases has progressively extended (Lochner et al. 2019). This is owing to the versatility of the ultrasonographic evaluation because of its availability, inexpensiveness, repeatability and bedside use. For these reasons, the sonographic assessment of the ONSD is considered an alternative to the invasive evaluation for the estimation of increased ICP, especially in pre-hospital settings or when radiological or neurosurgical care are not available or contraindicated (Robba et al. 2018). However, a clear cut-off value to identify intracranial hypertension is not available, probably due to differences in sex, ethnicity, age, body mass index and technical limitations already cited; also, anatomical factors or previous ocular or cerebral pathologies may be implied in generating a variability of ON structures (Bäuerle et al. 2016; Naldi et al. 2020; Wang et al. 2016). Thus, the emergent concept of monitoring ONSD values from a basal level is taking root: if a growing trend is observed, it may guide the decision-making (Thotakura et al. 2017). Similar considerations may apply in the case of a progressive reduction of ONSD suggesting intracranial hypotension syndrome (Fichtner et al. 2016). In these contexts, it seems unlikely that a series of ONSD examinations to monitor ICP could be performed by the same operator; in addition, the inter/intra –observer variability is higher between expert and inexpert sonologists (Zeiler et al. 2013; Zeiler et al. 2014). Indeed, an automated system could be extremely useful for standardizing measurements.

In addition, because of the variability of measurements, most ultrasonographic studies use the averaging of at least two values (frequently three) to obtain the reference ONSD, thus extending the execution time. Instead, owing to the absence of measurement variability whit AUTONoMA, we speculate that a single (well-acquired) image could be sufficient for the ONSD measurement by using the automated system, with a reduction of calculation time in comparison with the manual evaluation (approximately 3-5 minutes). We specify that the automated system was able to correctly segment images that presented a certain amount of variability in appearance and direction of the optic nerve. In four images, the algorithm was unable to correctly segment the ON and ONS because the structures

were not sufficiently hypoechoic or hyperechoic (Fig. 6). Since the algorithm must make certain assumptions on how specific structures are represented in the ultrasound B-mode image, if the actual representation is excessively different from a typical transorbital ultrasonography image, the algorithm does not properly process the image.

From a clinical perspective, most studies documented a 1 mm difference between ONSD of healthy and pathological conditions (Lochner et al. 2017; Lochner et al. 2018b; Moretti et al. 2009). Since the measured error is inferior, it is likely that the AUTONoMA algorithm could distinguish between most pathological and healthy conditions.

An increasing number of studies examined the role of TOS for neurological disorders that may affect the OND. Candeliere Merlicco et al. (Candeliere Merlicco et al. 2018) found that patients affected by multiple sclerosis present an atrophy of ON compared to healthy subjects, and that OND values are correlated with the Kurtzke Expanded Disability Status Scale as well as with the duration of the disease. Some authors also suggested that the ultrasonographic assessment of the OND could be potentially used as a biomarker for the detection of early disability in relapsing-remitting multiple sclerosis (Koraysha et al. 2019). Because AUTONoMA was able to correctly detect also the OND, analoguous considerations of the potential role of an automated measurements system can be extended for this parameter.

This study presents some limitations. An analysis on a larger number of images is mandatory to further validate the method. To correctly process the image, AUTONoMA required a substantial difference between hyperechoic and hypoechoic structures: in case of insufficient quality, the automated system is not able to recognize the optic nerve. However, further efforts are needed to improve this algorithm in order to recognize the boundary between the hypoechogenic and hyperechogenic structure of the nerve. However, it is important to point out that images with a very low quality should also be excluded from manual evaluation. AUTONoMA was tested on images obtained from a single ultrasound machine and we have no data from different ultrasound machines. Finally, a sub-analysis of our data showed that AUTONoMA tended to underestimate the OND measurements compared with both operators, while no conclusive information can be deducted for

ONSD. We suggest that further observations are warranted in order to clarify this issue.

Despite these limits, our preliminary data are encouraging and can justify the use of AUTONoMA as a non-invasive tool for the assessment of ONSD and OND. It is important to also point out that in the present study, the true ONSD and OND values are not known and are estimated by manual measurements, which are considered as ground truth. A phantom study with known OND and ONSD values would help to confirm the algoritm accuracy and results even further; however, this is outside the scope of the present study, which aims to present a tool that can automatically measure OND and ONSD as would be done by a manual expert on a B-mode ultrasound image. In order to improve the AUTONoMA system, further investigations will be object of our future studies.

In conclusion, a novel computer-aided diagnosis system to automatically measure the OND and ONSD in ultrasound images was presented. The algorithm is based on initially locating the optic bulb and ON centerline and then implementing two dual snake models for the final nerve and sheath segmentation. The technique was validated on a database of 71 images by comparing the results with those of two manual operators (an expert and a non-expert operator). We obtained a low mean measurement error and automatic results that can be considered within the range of inter-operator variability. The system can help clinicians evaluate pathologies related to the variations of the ON morphology in a short time and mitigate the issue of inter-operator variability. In the future, we plan on testing the presented technique on a larger database to further validate the system.

**References study #3**

Ballantyne S., O'Neill G, Hamilton R, Hollman A. Observer variation in the sonographic measurement of optic nerve sheath diameter in normal adults. Eur J Ultrasound Elsevier, 2002;15:145–149.

Bäuerle J, Lochner P, Kaps M, Nedelmann M. Intra- and Interobsever Reliability of Sonographic Assessment of the Optic Nerve Sheath Diameter in Healthy Adults. J Neuroimaging 2012;22:42–45.

Bäuerle J, Niesen W-D, Egger K, Buttler K-J, Reinhard M. Enlarged Optic Nerve Sheath in Aneurysmal Subarachnoid Hemorrhage despite Normal Intracranial Pressure. J Neuroimaging John Wiley & Sons, Ltd (10.1111), 2016;26:194–196.

Bloria S, Bloria P, Luthra A. Is it the time to standardize the procedure of ultrasound guided optic nerve sheath diameter measurement? Saudi J Anaesth Medknow Publications and Media Pvt. Ltd., 2019;13:255.

Candeliere Merlicco A, Gabaldón Torres L, Villaverde González R, Fernández Romero I, Aparicio Castro E, Lastres Arias MC. Transorbital ultrasonography for measuring optic nerve atrophy in multiple sclerosis. Acta Neurol Scand John Wiley & Sons, Ltd (10.1111), 2018;138:388–393.

Caresio C, Salvi M, Molinari F, Meiburger KM, Minetto MA. Fully Automated Muscle Ultrasound Analysis (MUSA): Robust and Accurate Muscle Thickness Measurement. Ultrasound Med Biol 2017;43.

Carraro N, Servillo G, Maria Sarra V, Bignamini A, Pizzolato G, Zorzon M. Optic Nerve and its Arterial-Venous Vascularization: An Ultrasonologic Study in Multiple Sclerosis Patients and Healthy Controls. J Neuroimaging 2014;24:273–277.

Copetti R, Cattarossi L. Optic nerve ultrasound: artifacts and real images. Intensive Care Med 2009;35:1488–1489.

Cronbach LJ. Coefficient alpha and the internal structure of tests. Psychometrika Springer-Verlag, 1951;16:297–334.

Ertl M, Barinka F, Torka E, Altmann M, Pfister K, Helbig H, Bogdahn U, Gamulescu M, Schlachetzki F. Ocular Color-Coded Sonography – A Promising Tool for Neurologists and Intensive Care Physicians. Ultraschall der Medizin - Eur J Ultrasound 2014;35:422–431.

Faita F, Gemignani V, Bianchini E, Giannarelli C, Demi M. Real-time

measurement system for the evaluation of the intima media thickness with a new edge detector. 2006 Int Conf IEEE Eng Med Biol Soc IEEE, 2006. pp. 715–718.

Fichtner J, Ulrich CT, Fung C, Knüppel C, Veitweber M, Jilch A, Schucht P, Ertl M, Schömig B, Gralla J, Z'Graggen WJ, Bernasconi C, Mattle HP, Schlachetzki F, Raabe A, Beck J. Management of spontaneous intracranial hypotension – Transorbital ultrasound as discriminator. J Neurol Neurosurg & Psychiatry 2016;87:650 LP – 655.

Friedman DI, Liu GT, Digre KB. Revised diagnostic criteria for the pseudotumor cerebri syndrome in adults and children. Neurology 2013;81:1159 LP – 1165.

Gerber S, Jallais M, Greer H, McCormick M, Montgomery S, Freeman B, Kane D, Chittajallu D, Siekierski N, Aylward S. Automatic Estimation of the Optic Nerve Sheath Diameter from Ultrasound Images BT - Imaging for Patient-Customized Simulations and Systems for Point-of-Care Ultrasound. In: Cardoso MJ, Arbel T, Tavares JMRS, Aylward S, Li S, Boctor E, Fichtinger G, Cleary K, Freeman B, Kohli L, Shipley Kane D, Oetgen M, Pujol S, eds. Cham: Springer International Publishing, 2017. pp. 113–120.

Goeres P, Zeiler FA, Unger B, Karakitsos D, Gillman LM. Ultrasound assessment of optic nerve sheath diameter in healthy volunteers. J Crit Care W.B. Saunders, 2016;31:168–171.

Helmke K, Hansen HC. Fundamentals of transorbital sonographic: Evaluation of optic nerve sheath expansion under intracranial hypertension. II. Patient study. Pediatr Radiol 1996;26:706–710.

Houzé-Cerfon C-H, Bounes V, Guemon J, Le Gourrierec T, Geeraerts T. Quality And Feasibility of Sonographic Measurement of the Optic Nerve Sheath Diameter to Estimate the Risk of Raised Intracranial Pressure After Traumatic Brain Injury in Prehospital Setting. Prehospital Emerg Care Taylor & Francis, 2018;1–7.

Koraysha NA, Kishk N, Hassan A, Samy El Gendy NM, Shehata HS, Al-Azayem SA, Kamal YS. Evaluating optic nerve diameter as a possible biomarker for disability in patients with multiple sclerosis. Neuropsychiatr Dis Treat Dove Press, 2019;15:2571–2578.

Lochner P, Behnke S, Fassbender K, Andrejewski A, Knodel S, Siniscalchi A, Jenderka K-V, Lemor R. Simulation and Experimental Characterization of

Lateral Imaging Resolution of Ultrasound Systems and Assessment of System Suitability for Acoustic Optic Nerve Sheath Diameter Measurement. J Neuroimaging John Wiley & Sons, Ltd (10.1111), 2018a;0.

Lochner P, Cantello R, Fassbender K, Lesmeister M, Nardone R, Siniscalchi A, Clemente N, Naldi A, Coppo L, Brigo F, Comi C. Longitudinal Assessment of Transorbital Sonography, Visual Acuity, and Biomarkers for Inflammation and Axonal Injury in Optic Neuritis. Dis Markers Hindawi, 2017;2017:1–5.

Lochner P, Coppo L, Cantello R, Nardone R, Naldi A, Leone MA, Brigo F. Intra- and interobserver reliability of transorbital sonographic assessment of the optic nerve sheath diameter and optic nerve diameter in healthy adults. J Ultrasound 2014;19:41–45.

Lochner P, Czosnyka M, Naldi A, Lyros E, Pelosi P, Mathur S, Fassbender K, Robba C. Optic nerve sheath diameter: present and future perspectives for neurologists and critical care physicians. Neurol Sci Springer International Publishing, 2019;1–11.

Lochner P, Falla M, Brigo F, Pohl M, Strapazzon G. Ultrasonography of the Optic Nerve Sheath Diameter for Diagnosis and Monitoring of Acute Mountain Sickness: A Systematic Review. High Alt Med Biol Mary Ann Liebert, Inc., publishers, 2015;16:195–203.

Lochner P, Fassbender K, Lesmeister M, Nardone R, Orioli A, Brigo F, Stolz E. Ocular ultrasound for monitoring pseudotumor cerebri syndrome. J Neurol 2018b;265:356–361.

Meiburger KM, Acharya UR, Molinari F. Automated localization and segmentation techniques for B-mode ultrasound images: A review. Comput Biol Med 2018;92:210–235.

Molinari F, Meiburger KM, Saba L, Rajendra Acharya U, Ledda M, Nicolaides A, Suri JS. Constrained snake vs. conventional snake for carotid ultrasound automated IMT measurements on multi-center data sets. Ultrasonics Elsevier B.V., 2012a;52:949–961.

Molinari F, Meiburger KM, Saba L, Zeng G, Acharya UR, Ledda M, Nicolaides A, Suri JS. Fully automated dual-snake formulation for carotid intima-media thickness measurement: A new approach. J Ultrasound Med 2012b;31.

Moretti R, Pizzi B, Cassini F, Vivaldi N. Reliability of Optic Nerve Ultrasound for the Evaluation of Patients with Spontaneous Intracranial Hemorrhage.

Neurocrit Care 2009;11:406–410.

Naldi A, Provero P, Vercelli A, Bergui M, Mazzeo AT, Cantello R, Tondo G, Lochner P. Optic nerve sheath diameter asymmetry in healthy subjects and patients with intracranial hypertension. Neurol Sci Springer International Publishing, 2019;1–5.

Robba C, Bacigaluppi S, Cardim D, Donnelly J, Bertuccio A, Czosnyka M. Non-invasive assessment of intracranial pressure. Acta Neurol Scand Wiley/Blackwell (10.1111), 2015;134:4–21.

Robba C, Santori G, Czosnyka M, Corradi F, Bragazzi N, Padayachy L, Taccone FS, Citerio G. Optic nerve sheath diameter measured sonographically as non-invasive estimator of intracranial pressure: a systematic review and meta-analysis. Int Care Med Springer Berlin Heidelberg, 2018;44:1284–1294.

Saba L, Molinari F, Meiburger K, Piga M, Zeng G, Acharya UR, Nicolaides A, S Suri J. What is the correct distance measurement metric when measuring carotid ultrasound intimamedia thickness automatically? Int Angiol 2012;31:483–489.

Soliman I, Johnson GGRJ, Gillman LM, Zeiler FA, Faqihi F, Aletreby WT, Balhamar A, Mahmood NN, Ahmad Mumtaz S, Alharthy A, Lazaridis C, Karakitsos D. New Optic Nerve Sonography Quality Criteria in the Diagnostic Evaluation of Traumatic Brain Injury. Crit Care Res Pract Hindawi, 2018;2018:1–7.

Thotakura AK, Marabathina NR, Danaboyina AR, Mareddy RR. Role of serial ultrasonic optic nerve sheath diameter monitoring in head injury. Neurochirurgie Elsevier Masson, 2017;63:444–448.

Wang L, Feng L, Yao Y, Deng F, Wang Y, Feng J, Xing Y. Ultrasonographic Evaluation of Optic Nerve Sheath Diameter among Healthy Chinese Adults. Ultrasound Med Biol 2016;42:683–688.

Zeiler FA, Unger B, Kramer AH, Kirkpatrick AW, Gillman LM. A Unique Model for Ultrasound Assessment of Optic Nerve Sheath Diameter. Can J Neurol Sci / J Can des Sci Neurol Cambridge University Press, 2013;40:225–229.

Zeiler FA, Unger B, Zhu Q, Xiao J, Kirkpatrick AW, Kramer AH, Aleassa EM, Gillman LM. A Unique Model for ONSD Part II: Inter/Intra-operator Variability. Can J Neurol Sci / J Can des Sci Neurol Cambridge University Press, 2014;41:430–435.

# STUDY #4

**"Optic nerve sheath diameter: present and future perspectives for neurologists and critical care physicians"**

"


## ABSTRACT

**Background.** Estimation of intracranial pressure (ICP) may be helpful in the management of neurological critically ill patients. It has been shown that ultrasonography of the optic nerve sheath diameter (ONSD) is a reliable tool for non-invasive estimation of increased intracranial pressure (ICP) at hospital admission or in intensive care. Less is known about the estimation of increased ICP and usefulness of ONSD in the prehospital setting. The aim of this review was to elucidate both prevailing and novel applications of ONSD for neurologists and critical care physicians.

**Methods.** In this review, we discuss the technique and the novel approach of ONSD measurement, the clinical applications of ONSD in neurology and critical care patients.

**Results.** ONSD measurement is simple, easy to learn, and has diverse applications. ONSD has utility for ICP measurement in intracranial hemorrhage and ischemic stroke, meningitis and encephalitis, and idiopathic intracranial hypertension (IIH). It is also valuable for lesser known syndromes, where an increase of ICP is postulated, such as acute mountain sickness and posterior reversible encephalopathy syndrome. ONSD changes develop in inflammatory or ischemic optic neuropathies. Some papers demonstrate the usefulness of ONSD studies in symptomatic intracranial hypotension.

**Conclusions.** ONSD is a safe and low-cost bedside tool with the potential of screening patients who need other neuroimaging and those who may need an invasive measurement of ICP.

## INTRODUCTION

The sonographic measurement of optic nerve sheath diameter (ONSD) is a non-invasive, simple tool with a reasonable level of diagnostic accuracy for estimating intracranial hypertension (ICP) [1, 2]. Since the subarachnoid space of the optic nerve is a continuum with the intracranial cerebrospinal fluid (CSF) spaces, it can be expanded by an increase of ICP and modify the ONSD. Acute and chronic diseases with an increase in ICP (e.g., idiopathic intracranial hypertension, craniocerebral trauma, malignant middle cerebral artery stroke, intracranial hemorrhage, decompensated hydrocephalus) lead to an increase of ONSD. In cases where the increase of ICP persists, a congested papilla develops with optic disc elevation (ODE), which can be detected with ultrasonography. Furthermore, some recent papers indicate that a diminution of ICP can provoke a decrease in ONSD. Dynamic measurement including a comparison of lying and standing positions can then help further to identify symptomatic intracranial hypotension [3]. In comparison with conventional neuroimaging methods, such as computed tomography (CT) and magnetic resonance imaging (MRI), transorbital sonography (TOS) has the advantages of being low cost, with short investigation times, good reproducibility, and bedside availability, and most importantly of being non-invasive and simple [4, 5]. In the clinical decision-making, this technique, combined with clinical and neurological status and neuroimaging may help physicians (especially neurologists) to decide whether to transfer patients with severe neurological pathologies to specialized centers or to place an invasive device instead [2]. However, the modification of ONSD may take place not only alongside the variation in ICP, but may also occur due to inflammatory lesions of the optic nerve itself. In these lesions, a change in the diameter develops on an inflammatory basis due to perilesional edema which may occur in acute optic neuritis [6]. The aim of this review is to provide an update on the state of ONSD technology and potential future applications. In the first part of this review, we focus on the basic physical principles and safety in ocular sonography. In the second part, we describe clinical applications in general neurology and in critical care in the prehospital or intra-hospital setting. At the end of our review, we discuss the limitations of the technique and future perspectives.

## Optic nerve sheath diameter ultrasonography for detection of ICP

Intracranial hypertension is an emergency which can be detected using clinical symptoms, imaging data, and ophthalmologic signs. Intracranial hypertension is confirmed by invasive intracranial monitoring, which is the gold standard technique to measure ICP. Because of the risk of complications—in particular hemorrhage or infection—recently non-invasive methods such as transcranial Doppler sonography (TCD), MRI, cranial CT, and ONSD ultrasonography have been developed in order to estimate increased ICP. The optic nerve is surrounded by CSF, which is connected to the ventricular system of the brain. The sheath of the optic nerve is composed of the dura, arachnoid, and pia mater, which border a small amount of CSF in the subarachnoid space. Increased ICP is, therefore, believed to cause transmission of force through these spaces, resulting in distention of the ONSD. Notably, further support for this theory is suggested in studies showing a similar correlation in the opposite direction (i.e., a small ONSD value in the setting of decreased ICP) [7, 8]. In experimental as well as human studies, an immediate change (within minutes) of ONSD corresponding to a change of ICP has been demonstrated [9–11]. In the following sections, we describe the technique and main parameter settings of ONSD.

## Technical and safety issues of optic nerve sheath diameter ultrasonography: static and dynamic measurement

### *Technique and safety considerations*

Ultrasonography of ONSD and the optic nerve can be easily performed using most color ultrasound systems equipped with high-frequency linear probes (7.5 MHz or higher) with a lateral spatial resolution of less than 0.4 mm [12]. As a first step, the system settings should be adjusted (mechanical index = 0.23 and the thermal index (TI) = 0.0) in order to prevent the damage of sensitive structures such as the lens, retina, and vitreous body (cavitation and thermal index) [13]. Secondly, all parameters, such as time gain compensation or gray scale, depth, and gain are individually adapted in order to achieve the best image quality. Vigilant training in the examination technique is advised. Standardization of technique is of great

importance to reduce the inter- and intra-observer variation and establish the true axial plane and the exact boundaries of the sheath [14–16]. Otherwise, shadowing artifacts caused by the lens and the optic disc or by inexperienced operators may significantly alter measurement of ONSD [17]. For ONSD measurement, the examiner normally sits at the head of the examination table with the patient positioned supine with the head and upper body raised 20–30° to avoid any pressure on the eye. The patient remains in this position for at least 1 min before data are recorded. A thick layer of gel is applied to the closed upper eyelid. The transducer should be positioned on the temporal side of the eye. To help suppress eye movement and to achieve a better delineation of the major anatomical landmarks (optic nerve and lens), the patient is asked to look forward with closed eyes [15, 18, 19]. With this technique, optic nerve along with the globe and lens can be visualized. The globe appears homogenously anechoic. It is divided into anterior and posterior chambers by the hyperechoic line formed by the lens. In the axial plane, the optic nerve can be visualized posterior to the globe. Brightness and contrast should be adjusted to best define the optic nerve and surrounding sheath. The optic nerves are clearly visible because of their well-defined, longitudinal compact structure (Fig. 1). As previously described, ONSD should be measured 3 mm behind the globe, in each eye perpendicular to the optic nerve axis, using an electronic caliper and an axis perpendicular to the optic nerve (Fig. 2c) [9, 10]. Additionally, the mean of three measured values is computed, in order to reduce the intra-observer variability [15]. The correct way to measure the ONSD is between the outer hyperechogenic borders of the subarachnoid space. The sonographic aspect of the optic nerve is from the center to the periphery: hypoechogenic nerve fibers are closely surrounded by the hyperechogenic pia mater; the subarachnoid space appears hyperechogenic due to the trabecular structure and is surrounded by dura mater and periorbital fat (Fig. 1) [1]. Although the correct way of measuring ONSD is clearly described, there remain numerous studies which measure ONSD with improper, non-standard technique. In these studies, ONSD is measured incorrectly by measuring the distance between the outer hypoechogenic borders. This incorrect approach results in false and enlarged ONSD values [20, 21]. The learning curve for experienced sonologists may include as few as 10 examinations, whereas for novice sonologists the number of scans needed may be closer to 25 [22].

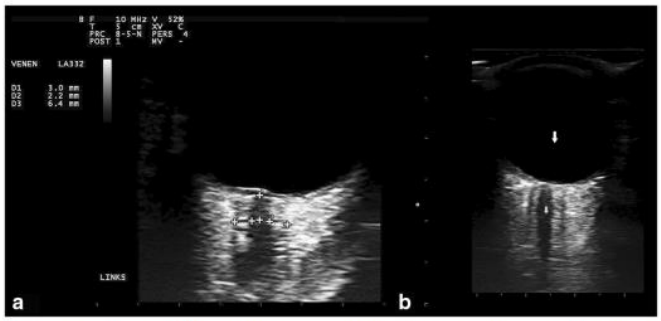


**Fig. 1** Measurement of the optic nerve diameter (OND) and optic nerve sheath diameter (ONSD) 3 mm behind the papilla (1) (**a**), using an electronic caliper and an axis perpendicular to the ON. Optic nerve diameter (OND) was measured as the distance inside the pia mater (2) and ONSD as the distance inside the dura mater on the hyperechogenic area surrounding the optic nerve (3). **b** Overview of the eyeball and the retroocular space using B mode. Ultrasonography makes an axial cut through the eye including a longitudinal section of optic nerve: hypoechogenic ocular globe (big arrow) and hypoechogenic optic nerve (small arrow)

*Dynamic measurement*

A dynamic measurement at two time points and in two different positions has proven useful in patients affected by spontaneous intracranial hypotension (SIH). The ONSD measurement should be conducted starting with the patient in supine position and then in upright position with the patient standing for 2 min (Fig. 2) [3]. Another possibility is the measurement of ONSD approximately 5 min prior to and after a lumbar puncture in order to estimate—in real time—a reduction in CSF pressure or the efficacy of postpunctural treatment in patients with idiopathic intracranial hypertension [23, 24]. Ertl et al. obtained a measurement of changes of ONSD, in supine and orthostatic position, in 31 patients with idiopathic normal pressure hydrocephalus (iNPH) before and after lumbar puncture. The mean pre-puncture ONSD-variability was significantly lower in healthy volunteers and patients with no response to CSF removal than in responsive patients. In this context, ONSD may also support selection of patients for shunt intervention [25].

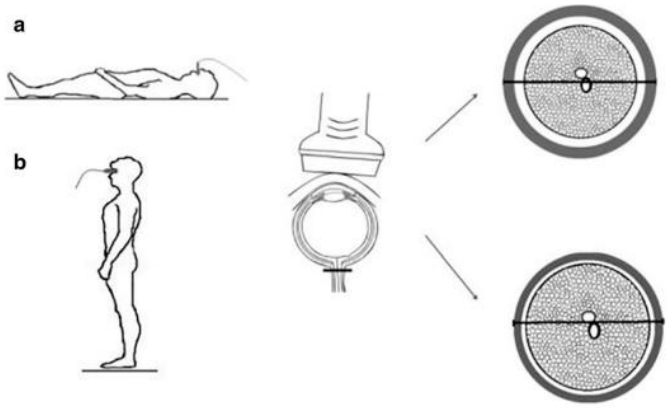


**Fig. 2** Dynamic ultrasonography measurement. Optic nerve sheath diameter (ONSD) changes in a symptomatic patient with spontaneous intracranial hypotension from supine to upright body position. **a** Supine position. **b** Orthostatic position. The upper right picture shows how the examination can be performed using transorbital ultrasound. **b** The lower right picture shows the changes of ONSD from supine to orthostatic position

## Clinical applications

### Neurological applications

A variety of potential applications have been described in different neurological settings.

*Intracranial hemorrhage and ischemic stroke*

In 25 acute intracerebral hemorrhage (ICH) patients with clinical and radiological CT signs of raised ICP, Naldi et al. report sensitivity and specificity of 100% for ONSD for the detection of increased ICP compared to the Doppler indices, with 48% sensitivity and 95% specificity for resistive index (RI) and 80% sensitivity and 62% specificity for retinal venous pulsation (RVP) [26]. Skoulodik et al. found an enlarged ONSD even in the hyperacute phases of acute ICH within 6 h of the symptom onset ($p < 0.0083$), with the best cut-off point to predict intracranial hemorrhage volume of > 2.5 $cm^3$ corresponding to an ONSD enlargement of > 0.66 cm (> 21%), with 90.3% accuracy and interrater reliability of 0.760 (95% CI 0.509 to 1.000) [27]. Yesilaras et al. measured ONSD on CT scans and found a threshold value of 6.1 mm, with sensitivity and specificity for subarachnoid hemorrhage (SAH) of 72%, to distinguish controls from SAH patients [28]. Bäuerle et al. showed an increase of ONSD in a cohort of 27 patients with subarachnoid hemorrhage (SAH) and acute hydrocephalus after aneurysm rupture, with a persistence of expansion of ONSD after normalization of ICP, postulating an impaired retraction capability of the optic nerve sheath after a massive ICP exposure [29]. Gokcen et al. found that the highest binocular ONSD was detected in patients

affected by complete anterior circulation infarction ($p < 0.001$) compared to other ischemic groups, according to the Oxfordshire Community Stroke Project. The authors showed that ONSD could identify middle cerebral artery (MCA) stroke patients at high risk of developing malignant MCA syndrome, permitting early diagnosis of a possible ICP increase using ONSD with the possible benefit of decreasing mortality and morbidity in patients with cerebrovascular diseases [30].

*Idiopathic intracranial hypertension*

Idiopathic intracranial hypertension (IIH) (also known as primary pseudotumor cerebri syndrome (PTCS)) refers to disorders in which the mechanism of increased CSF remains elusive. It is defined by an increase of ICP without neuroradiological abnormalities [31–33]. Increased ICP typically develops over a period of weeks or months. Typical signs and symptoms of IIH include headache, pulsatile tinnitus, transient visual obscurations, blurred vision, diplopia, and papilledema. Some studies addressed the role of transorbital sonography in supporting the diagnosis of primary PTCS [23, 34]. Very recently, Lochner et al. found similar results of ONSD measurements in IIH and secondary PTCS [35]. In a recent metaanalysis, Lochner et al. demonstrated that patients showed a significant thickening of ONSD, 6.2–6.76mm compared to 4.3–5.7 mm in controls. ONSD was significantly higher in IIH patients compared to controls (overall weighted mean difference of 1.3mm (95% CI 0.6–1.9mm)) [36]. ONSD could be useful for monitoring IIH. After 6 months of diet and medication, a correlation between the variation of ONSD and improvement of headache has been observed by the same author. ONSD decreased significantly from the start of the study (median, 6.51 mm (interquartile range 6.13– 7.10)) to 6 months later (6.08 mm (5.59–6.73), $p = 0.002$) [37].

*Intracranial hypotension, patch test*

Symptomatic intracranial hypotension (SIH) can be spontaneous or occur after lumbar puncture. It is characterized by orthostatic headache, associated with neck pain or stiffness, nausea, or vomiting [38]. However, a minority of SIH cases present with each classical symptom, so it may be difficult to correctly diagnose this condition. In combination with cerebral and spinal magnetic resonance imaging (MRI) or CT myelography, TOS can be useful for diagnosis and monitoring of SIH, showing a decrease in ONSD compared to normal ONSD values (Fig. 2). Another

important aspect is highlighted by the modification of ONSD by treatment of SIH using epidural patching. Indeed, Dubost et al. showed that nine out of ten patients had an increase of ONSD with successful lumbar epidural blood patching [39]. Recently, Fichtner et al. evaluated the diagnostic value of ONSD by performing two orbital ultrasound assessments, in supine and upright positions (Fig. 2), for three groups of patients (symptomatic and asymptomatic spontaneous intracranial hypotension patients and controls). The main finding was a significant decrease of ONSD when changing from the supine to upright position in symptomatic patients with SIH [3].

*Posterior reversible encephalopathy syndrome*

Posterior reversible encephalopathy syndrome (PRES) is a clinical and radiological syndrome, consisting of headache, visual changes, seizure, and imaging findings, including cerebral edema affecting the cerebral cortex and underlying white matter. It manifests as areas of hyperintensity in T2 and FLAIR imaging, most often involving the occipital and posterior parietal lobes [40]. Although rare, PRES may involve the brainstem and/or cerebellum on neuroimaging. Lee et al. showed that 22 (58%) of 38 episodes of PRES involved the brainstem and/or cerebellum on neuroimaging [41]. Another literature review reported 26 patients with brainstem involvement [42]. Although the pathogenesis of PRES is still not completely understood, it is postulated that an impairment of cerebral auto-regulation—resulting in arterial hypertension above the limit of cerebral self-regulation, breakdown of the blood– brain barrier (BBB), and subsequent brain edema—is the main underlying mechanism. This syndrome may be associated with either increased ICP or altered BBB permeability. In this context, TOS may be useful in demonstrating papilledema and an increase in the size of the ONSD. The thickening of ONSD could therefore occur as a result of increased ICP in some cases or because of an inflammatory cause due to alteration of optic nerve pathways. Very few reports are available in the literature concerning ultrasound diagnostics in patients with PRES where ONSD measurements are used to evaluate the many physiologic parameters of interest [43–45].

*Meningitis and encephalitis*

Serious bacterial meningitis or encephalitis can lead to an elevation of the ICP and

hydrocephalus. To date, there are only few reports of an increase in ICP in the context of viral or bacterial meningitis. It is also reported that ONSD can be used to detect raised ICP in patients with tuberculous meningitis or encephalitis [46, 47].

*Acute mountain sickness*

The pathophysiology of acute mountain sickness (AMS) remains under investigation. Some recent studies using neuroimaging techniques found that hypoxia may increase cerebral arterial blood flow and venous volume, leading to increased ICP [8, 48]. Further, AMS symptoms can be due to a lower ability of some subjects to cope with an increase in brain volume [49]. The development of portable ultrasound equipment has made it possible to take measurements of ONSD in remote settings, including at high altitude. In this context, some authors exploring the utility of ultrasound at high altitudes showed that ONSD rapidly increased after exposure to progressively increasing altitude [50–52]. In particular, Fagenholz et al. performed serial examinations in 10 out of 284 subjects, who traveled at high altitude through Pheriche, Nepal (4240 m). In these subjects, the change in Lake Louise score had a strong positive correlation with change in ONSD. Mean ONSD was 5.34 mm (95% CI 5.18–5.51 mm) in the 69 subjects with AMS vs. 4.46 mm (95% CI 4.39–4.54 mm) in the 218 other subjects ($p < 0.001$) [53]. In a recent systematic review, Lochner et al. concluded that the measurement of ONSD might appear to be a promising tool for diagnosis and monitoring of AMS in research on CNS changes at high altitude, but the biggest limitation of this technique are the small variations of ONSD changes after high altitude exposure in some of the reported studies [54].

*Hydrocephalus*

ONSD was measured as a predictor of increased ICP and for monitoring of hydrocephalus in several studies assessed using CT scan or ultrasound. Lee et al. evaluated ONSD in adult hydrocephalus on preoperative CT and found in eight patients with a higher ICP (> 20 mmHg) and a significant thickening of ONSD (5.8 vs. 4.9 mm, $p = 0.001$) [55]. Brzezinska et al. found a mean ONSD of 3.5 mm with a range of 2.6 to 4.1 mm in 50 patients without signs of increased ICP and a mean ONSD of 5.4 mm with a range between 3.9 and 6.9 mm in 52 patients with signs of ICP elevation [56]. Newman et al. verified the function of ventriculoperitoneal

shunt in children and reported a mean of ONSD 2.9 (SD 0.5) mm compared to those with raised ICP 5.6 (SD 0.6) [57]. Finally, Ertl et al. showed that another possible application is the measurement of ONSD changes using dynamic measurements in patients with idiopathic normal pressure hydrocephalus: mean pre-puncture ONSD-variability was significantly lower in healthy volunteers and patients with no response to CSF removal than in responsive patients. ONSD may also support selection of patients for shunt intervention [25]. Taken together, although the technique still requires wide validation, ONSD measurement presents a potentially valuable option in cases where repetitive CT measurements have to be performed to monitor obstructive hydrocephalus in an intensive care unit.

*Optic neuritis and non-arteritic ischemic optic neuropathy*

Optic neuritis (ON) is an acute multi-etiological inflammatory condition affecting the optic nerve causing retro-orbital pain and visual loss. In a high percentage of cases, it is highly associated with multiple sclerosis [58]. At an early stage of inflammation, there is an abnormal increase in permeability of the blood–brain barrier, revealed by gadolinium-DTPA enhancement in all patients examined, gradually followed by edema, which usually lasts for a few weeks and then diminishes to the point of restoring the normal permeability of the blood–brain barrier [59]. Several studies detected an increased ONSD as an expression of optic nerve inflammation due to increased perineural subarachnoid fluid. In particular, results of seven studies showed an increased ONSD in 78 to 100% of patients in the affected eye compared with its unaffected fellow eye or control subjects [60–66]. Based on the anterior location of clinical involvement, four out of seven studies demonstrated papillitis with a swollen disc in 6–43% of patients. In fact, B-mode transorbital ultrasonography provides promising support for the clinical diagnosis of acute ON (Fig. 3) [6]. Further studies are warranted in order to provide information about therapeutic monitoring in ON. The main finding of non-arteritic ischemic optic neuropathy is the papilledema. In contrast to acute optic neuritis, in non-arteritic ischemic optic neuropathy (nAION), two authors did not report any change of ONSD (Fig. 4) [60, 62].

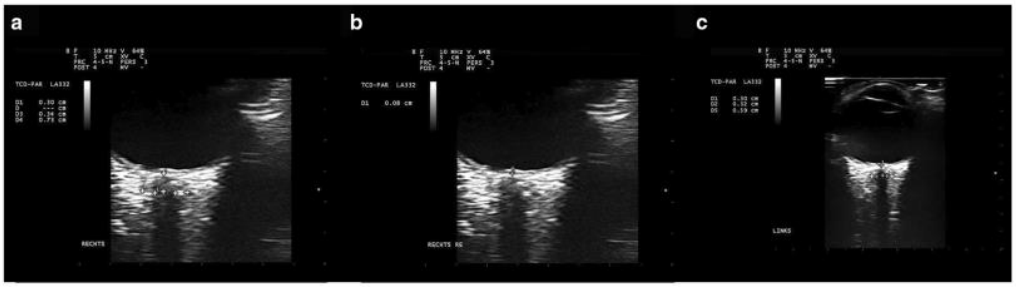


**Fig. 3** **a**–**c**. Sonographic examinations of the eye are performed in a patient affected by optic neuritis with papillitis. **a** The dotted arrow (1) denotes where the optic nerve measurement takes place, 3 mm behind the papilla in an axial plane shows the optic nerve (2) in its longitudinal course. The dotted arrow (3) denotes an increase of optic nerve sheath diameter (ONSD) in the right eye (7.3 mm). **b** Optic disc elevation of (0.8 mm) on the right side. The measurement is gauged between the fundus and the dome of the papilla. **c** (5) ONSD of 5.9 mm in the non-affected left eye

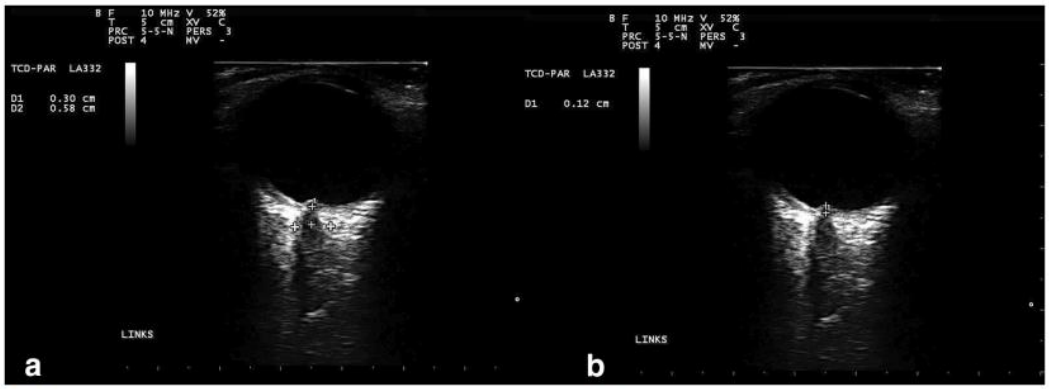


**Fig. 4** Patient affected by non-arteritic anterior ischemic optic neuropathy (nAION). In the neurological examination: reduction of visual acuity on the left side (Visus 0.2), otherwise no focal neurological deficit. The picture shows an optic nerve sheath diameter (ONSD) of 0.58 cm, associated with optic disc elevation of 0.12 cm

## Neurological complications in not neurological settings

In this section, we will describe some of the major applications in not neurological settings, where primarily systemic diseases can further cause neurological complications.

### *Pregnancy*

Pregnancy is associated with pathophysiological changes which predispose to several neurologic disorders [67]. Recent studies report that ONSD can predict the development of preeclampsia and eclampsia [68]. In a recent study, ONSD was significantly higher in preeclamptic patients compared to healthy pregnant women at delivery with 20 to 43% of preeclamptic patients having ONSD values compatible with intracranial pressure above 20 mmHg [69]. Cerebral edema and ICH are common after acute liver failure and are major causes of morbidity and

mortality [70, 71]. The role of invasive ICP monitoring remains controversial in this group of patients because of the risk of coagulopathy and intracranial hemorrhage [72–74]. ONSD can therefore play a role in this patient group. Recently, in a retrospective study of 41 patients with liver failure, ONSD and other non-invasive ICP methods were compared with invasive ICP methods [75]. ONSD had an AUC of 0.59 (95% CI 0.37–0.79, P = 0.54) with no correlation with mortality. However, in a study in a pediatric cohort with liver failure, ONSD was a good predictor of poor outcome related to increased ICP [76].

*Cardiac arrest/coma*

Few parameters are available to predict neurologic outcome of post-cardiac arrest patients. In the early stage of treatment, ONSD measurement is valuable as a prognostic indicator of hypoxic encephalopathy, both on CT or ultrasound with contrast [77]. The better prognostic value was observed when ONSD was combined with other parameters such as gray-to-white matter ratio on initial CT scan in post-cardiac arrest subjects [78]. In post-cardiac arrest patients conducted by Ueda et al., the mean ONSD at admission associated with a favorable prognosis was 5.0 mm (4.4–6.1 mm). ONSD of 6.1 mm (5.4–7.2 mm) was associated with poor prognosis. ONSD of ≤ 5.4 mm was associated with a favorable prognosis with a sensitivity of 83% (95% CI 36–100) and specificity of 73% (95% CI 39–94) [79]. In a prospective observational study of post-cardiac arrest patients, ONSD was used to predict outcomes due to brain edema caused by hypoxic-ischemic encephalopathy (HIE). For predicting mortality, an ONSD threshold value of 5.75 mm had a specificity of 100% and PPV of 100%. Non-survivors had significantly higher ONSD values ($p < 0.001$) [80]. Other studies of ONSD with serum albumin concentration or ONSD alone have demonstrated similar results [81].

*Intraoperative complications*

Intraoperative use of ONSD has gained popularity over the years and could be used in every type of surgery to monitor the occurrence of neurological complications during anesthesia for general surgery and neurosurgery. An example of an important application of ONSD in the intraoperative setting is in patients undergoing laparoscopic surgery. This technique requires adequate surgical exposure and the application of a CO2 pneumoperitoneum (PP) and often a concomitant steep head–

down position (up to 45°, Trendelenburg position), together increasing the risk for decreased venous return, variation of mean arterial pressure and systemic vascular resistance, hypercapnia, and therefore an increase of ICP [82, 83]. Some authors have reported neurological complications during laparoscopy including cerebral ischemia and cerebral edema, or minor clinical symptoms such as nausea, and headache that could be associated with increased ICP have been reported after laparoscopy [83, 84]. Because an increase of ICP above 20 mmHg has been detected in a significant number of patients without neurological disease (7.5 to 15% of cases), a non-invasive ICP measurement method would be useful [85, 86]. ONSD ultrasonography during PP and Trendelenburg positions has been studied by many authors who have demonstrated a significant increase of ONSD during PP and TP. A meta-analysis of 460 subjects showed that ONSD increases significantly in both the early period (0–30 min) and late period (30–120 min) during CO2 pneumoperitoneum [87]. In a prospective study in patients who had undergone thoracoabdominal aortic aneurysm repair surgery, Ertl et al. found a significant increase of ONSD between baseline and different intraoperative time points (right eye: $P = 0.006$; left eye: $P = 0.02$) [88]. In particular, within a group of five patients having an additional increase of ONSD during the surgery, one developed permanent paraplegia. Patients with spinal catheters had significantly lower ONSDs at nearly all time points. This technique could be useful to discover which patients need CSF drainage.

**Limitations**

The ultrasound method is limited by a lateral resolution of 0.3–0.4 mm. Ultrasonography cannot be performed in patients with ocular trauma, glaucoma, or previous optic nerve atrophy. Another limit of this technique is the marked variability of ONSD, found in studies including both healthy subjects and subjects with pathological conditions, and different cut-offs in pathological conditions. Moreover, it seems to be possible that the distensibility of ONSD is variable in individuals. After a massive increase of ICP, it is possible that the ONSD is not able to shrink. Finally, there are some concerns about the standardization of ONSD measurement.

## Future perspectives

While only two studies have been performed in the prehospital setting (in an ambulance as well as on a helicopter), both have demonstrated the feasibility of this technique treating patients with brain traumatic injuries (TBI). HouzéCerfon et al. were able to measure ONSD in 19 (82%) patients with moderate and severe TBI with 80% of ONSD measurements validated by the experts [89]. ONSD measurements were possible in 15 (79%) cases. The success rate in the helicopter was 43% compared to 80% in the ambulance. Massain et al. measured ONSD in healthy volunteers during helicopter liftoff and acceleration in the supine position or with a raised headrest. ONSD increased during helicopter acceleration (− 9° Trendelenburg, mean = 5.6 ± 0.3 mm) from baseline (0° supine position, mean = 5.0 ± 0.4 mm) [90]. Another field of research could be the development of automated, computerized systems for the segmentation of structures in B-mode ultrasound images that may help to reduce operator-dependency, accelerate the acquisition time, and mitigate the issue of inter-operator variability [91]. In this context, Gerber et al. have developed an algorithm to automatically estimate the ONSD from 23 ocular ultrasound images [92].

## Conclusion

In this review, we summarize the main indications for ONSD in neurology and intensive care. ONSD is a still underestimated imaging modality that deserves wider acceptance. Because this bedside tool allows for fast and safe realtime assessment of conditions associated with elevated intracranial pressure, we propose routine inclusion of ONSD measurement in the multimodal monitoring of patients in neurocritical care. ONSD measurement, together with invasive ICP monitoring, is valuable for neurological conditions with clinically suspected variation of ICP and in optic nerve disorders. Currently, the biggest limitation of this technique is the marked variability in ONSD reported across studies in healthy subjects and subjects with pathological conditions. For this reason, further longitudinal prospective studies with standardized technique should be encouraged to better assess the usefulness and limits of this technique.

**References study #4**


1. Ertl M et al (2014) Ocular color-coded sonography—a promising tool for neurologists and intensive care physicians. Ultraschall Med 35:422–431. https://doi.org/10.1055/s-0034-1366113

2. Robba C et al (2018) Optic nerve sheath diameter measured sonographically as non-invasive estimator of intracranial pressure: a systematic review and meta-analysis. Intensive Care Med 44: 1284–1294. https://doi.org/10.1007/s00134-018-5305-7

3. Fichtner J et al (2016) Management of spontaneous intracranial hypotension—transorbital ultrasound as discriminator. J Neurol Neurosurg Psychiatry 87:650–655. https://doi.org/10.1136/jnnp2015-31085

4. Geeraerts T, Launey Y, Martin L, Pottecher J, Vigue B, Duranteau J, Benhamou D (2007) Ultrasonography of the optic nerve sheath may be useful for detecting raised intracranial pressure after severe brain injury. Intensive Care Med 33:1704–1711. https://doi.org/10. 1007/s00134-007-0797-6

5. Geeraerts T, Merceron S, Benhamou D, Vigue B, Duranteau J (2008) Non-invasive assessment of intracranial pressure using ocular sonography in neurocritical care patients. Intensive Care Med 34:2062–2067. https://doi.org/10.1007/s00134-008-1149-x

6. Lochner P, Leone MA, Coppo L, Nardone R, Zedde ML, Cantello R, Brigo F (2016) B-mode transorbital ultrasononography for the diagnosis of acute optic neuritis. A systematic review. Clin Neurophysiol 127:803–809. https://doi.org/10.1016/j.clinph.2015. 05.005

7. Rohr A et al (2010) MR imaging of the optic nerve sheath in patients with craniospinal hypotension. AJNR Am J Neuroradiol 31: 1752–1757. https://doi.org/10.3174/ajnr.A2120

8. Wilson MH, Wright A, Imray CH (2014) Intracranial pressure at altitude. High Alt Med Biol 15:123–132. https://doi.org/10.1089/ ham.2013.1151

9. Hansen HC, Helmke K (1997) Validation of the optic nerve sheath response to changing cerebrospinal fluid pressure: ultrasound findings during intrathecal infusion tests. J Neurosurg 87:34–40. https:// doi.org/10.3171/jns.1997.87.1.0034

10. Helmke K, Hansen HC (1996) Fundamentals of transorbital sonographic evaluation of optic nerve sheath expansion under intracranial hypertension II.

Patient study. Pediatr Radiol 26:706–710

11. Liu D, Li Z, Zhang X, Zhao L, Jia J, Sun F, Wang Y, Ma D, Wei W (2017) Assessment of intracranial pressure with ultrasonographic retrobulbar optic nerve sheath diameter measurement. BMC Neurol 17:188. https://doi.org/10.1186/s12883-017-0964-5

12. Lochner P et al (2019) Simulation and experimental characterization of lateral imaging resolution of ultrasound systems and assessment of system suitability for acoustic optic nerve sheath diameter measurement. J Neuroimaging 29:34–41. https://doi.org/10.1111/ jon.12578

13. Fowlkes JB, Holland CK (2000) Mechanical bioeffects from diagnostic ultrasound: AIUM consensus statements. American Institute of Ultrasound in Medicine. J Ultrasound Med 19:69–72

14. Ballantyne SA, O'Neill G, Hamilton R, Hollman AS (2002) Observer variation in the sonographic measurement of optic nerve sheath diameter in normal adults. Eur J Ultrasound

15:145–149 15. Bauerle J, Lochner P, Kaps M, Nedelmann M (2012) Intra- and interobsever reliability of sonographic assessment of the optic nerve sheath diameter in healthy adults. J Neuroimaging 22:42–45. https://doi.org/10.1111/j.1552-6569.2010.00546.x

16. Lochner P, Coppo L, Cantello R, Nardone R, Naldi A, Leone MA, Brigo F (2016) Intra- and interobserver reliability of transorbital sonographic assessment of the optic nerve sheath diameter and optic nerve diameter in healthy adults. J Ultrasound 19:41–45. https://doi.org/10.1007/s40477-014-0144-z

17. Copetti R, Cattarossi L (2009) Optic nerve ultrasound: artifacts and real images. Intensive Care Med 35:1488–1489; author reply 1490- 1481. https://doi.org/10.1007/s00134-009-1494-4

18. Bauerle J, Schuchardt F, Schroeder L, Egger K, Weigel M, Harloff A (2013) Reproducibility and accuracy of optic nerve sheath diameter assessment using ultrasound compared to magnetic resonance imaging. BMC Neurol 13:187. https://doi.org/10.1186/1471-2377- 13-187

19. Helmke K, Hansen HC (1996) Fundamentals of transorbital sonographic evaluation of optic nerve sheath expansion under intracranial hypertension. I. Experimental study. Pediatr Radiol 26:701– 705

20. Krogias C, Ayzenberg I, Schroeder C, Gruter T, Gold R, Yoon MS (2016)

Transorbital sonography in CIDP patients: no evidence for optic nerve hypertrophy. J Neurol Sci 362:206–208. https://doi.org/ 10.1016/j.jns.2016.01.049

21. Topcuoglu MA, Arsava EM, Bas DF, Kozak HH (2015) Transorbital ultrasonographic measurement of optic nerve sheath diameter in brain death. J Neuroimaging 25:906–909. https://doi. org/10.1111/jon.12233

22. Tayal VS, Neulander M, Norton HJ, Foster T, Saunders T, Blaivas M (2007) Emergency department sonographic measurement of optic nerve sheath diameter to detect findings of increased intracranial pressure in adult head injury patients. Ann Emerg Med 49:508–514. https://doi.org/10.1016/j.annemergmed.2006.06.040

23. Bauerle J, Nedelmann M (2011) Sonographic assessment of the optic nerve sheath in idiopathic intracranial hypertension. J Neurol 258:2014–2019. https://doi.org/10.1007/s00415-011-6059- 0

24. Chen LM, Wang LJ, Hu Y, Jiang XH, Wang YZ, Xing YQ (2019) Ultrasonic measurement of optic nerve sheath diameter: a noninvasive surrogate approach for dynamic, real-time evaluation of intracranial pressure. Br J Ophthalmol 103:437–441. https://doi. org/10.1136/bjophthalmol-2018-312934

25. Ertl M, Aigner R, Krost M, Karnasova Z, Muller K, Naumann M, Schlachetzki F (2017) Measuring changes in the optic nerve sheath diameter in patients with idiopathic normal-pressure hydrocephalus: a useful diagnostic supplement to spinal tap tests. Eur J Neurol 24:461–467. https://doi.org/10.1111/ene.13225

26. Naldi A et al (2019) Ultrasonography monitoring of optic nerve sheath diameter and retinal vessels in patients with cerebral hemorrhage. J Neuroimaging. https://doi.org/10.1111/jon.12604

27. Skoloudik D et al (2011) Distal enlargement of the optic nerve sheath in the hyperacute stage of intracerebral haemorrhage. Br J Ophthalmol 95:217–221. https://doi.org/10.1136/bjo.2009.172890

28. Yesilaras M, Kilic TY, Yesilaras S, Atilla OD, Oncel D, Camlar M (2017) The diagnostic and prognostic value of the optic nerve sheath diameter on CT for diagnosis spontaneous subarachnoid hemorrhage. Am J Emerg Med 35:1408–1413. https://doi.org/10. 1016/j.ajem.2017.04.022

29. Bauerle J, Niesen WD, Egger K, Buttler KJ, Reinhard M (2016) Enlarged optic nerve sheath in aneurysmal subarachnoid hemorrhage despite normal intracranial pressure. J Neuroimaging 26: 194–196. https://doi.org/10.1111/jon.12287

30. Gokcen E, Caltekin I, Savrun A, Korkmaz H, Savrun ST, Yildirim G (2017)

Alterations in optic nerve sheath diameter according to cerebrovascular disease subgroups. Am J Emerg Med 35:1607– 1611. https://doi.org/10.1016/j.ajem.2017.04.073

31. D Amico D, Curone M, Ciasca P, Cammarata G, Melzi L, Bussone G, Bianchi Marzoli S (2013) Headache prevalence and clinical features in patients with idiopathic intracranial hypertension (IIH). Neurol Sci 34(Suppl 1):S147–S149. https://doi.org/10.1007/ s10072-013-1388-7

32. Friedman DI, Liu GT, Digre KB (2013) Revised diagnostic criteria for the pseudotumor cerebri syndrome in adults and children. Neurology 81:1159–1165. https://doi.org/10.1212/WNL. 0b013e3182a55f17

33. Raoof N, Sharrack B, Pepper IM, Hickman SJ (2011) The incidence and prevalence of idiopathic intracranial hypertension in Sheffield, UK. Eur J Neurol 18:1266–1268. https://doi.org/10.1111/j.1468- 1331.2011.03372.x

34. Lochner P, Nardone R, Tezzon F, Coppo L, Brigo F (2013) Optic nerve sonography to monitor treatment efficacy in idiopathic intracranial hypertension: a case report. J Neuroimaging 23:533–534. https://doi.org/10.1111/jon.12005

35. Lochner P, Brigo F, Zedde ML, Sanguigni S, Coppo L, Nardone R, Naldi A, Sola D, Stolz E (2016) Feasibility and usefulness of ultrasonography in idiopathic intracranial hypertension or secondary intracranial hypertension. BMC Neurol 16:85. https://doi.org/10. 1186/s12883-016-0594-3

36. Lochner P et al (2018) B-mode transorbital ultrasonography for the diagnosis of idiopathic intracranial hypertension: a systematic review and meta-analysis. Ultraschall Med. https://doi.org/10.1055/a0719-4903

37. Lochner P, Fassbender K, Lesmeister M, Nardone R, Orioli A, Brigo F, Stolz E (2018) Ocular ultrasound for monitoring pseudotumor cerebri syndrome. J Neurol 265:356–361. https:// doi.org/10.1007/s00415-017-8699-1

38. Headache Classification Committee of the International Headache Society (IHS) (2018) The international classification of headache disorders, 3rd edition. Cephalalgia 38:1–211. https://doi.org/10. 1177/0333102417738202

39. Dubost C, Le Gouez A, Zetlaoui PJ, Benhamou D, Mercier FJ, Geeraerts T (2011) Increase in optic nerve sheath diameter induced by epidural blood patch: a preliminary report. Br J Anaesth 107: 627–630. https://doi.org/10.1093/bja/aer186

40. Fugate JE, Claassen DO, Cloft HJ, Kallmes DF, Kozak OS, Rabinstein AA (2010) Posterior reversible encephalopathy syndrome: associated clinical and

radiologic findings. Mayo Clin Proc 85:427–432. https://doi.org/10.4065/mcp.2009.0590

41. Lee VH, Wijdicks EF, Manno EM, Rabinstein AA (2008) Clinical spectrum of reversible posterior leukoencephalopathy syndrome. Arch Neurol 65:205–210. https://doi.org/10.1001/archneurol. 2007.46

42. Uchino M, Haga D, Nomoto J, Mito T, Kuramitsu T (2007) Brainstem involvement in hypertensive encephalopathy: a report of two cases and literature review. Eur Neurol 57:223–226. https://doi.org/10.1159/000100015

43. Caputo ND, Fraser RM, Abdulkarim J (2012) Posterior reversible encephalopathy syndrome presenting as papilledema. Am J Emerg Med 30:835 e835-837. https://doi.org/10.1016/j.ajem.2011.03.016

44. Lochner P, Mader C, Nardone R, Cantello R, Orioli A, Brigo F (2014) Usefulness of ultrasonography in posterior reversible encephalopathy syndrome. Neurol Sci 35:475–477. https://doi.org/ 10.1007/s10072-013-1562-y

45. Lochner P, Nardone R, Brigo F, Tamber MS, Zuccoli G (2015) The diagnosis of posterior reversible encephalopathy syndrome. Lancet Neurol 14:1074–1075. https://doi.org/10.1016/S1474-4422(15) 00256-2

46. Nabeta HW et al (2014) Accuracy of noninvasive intraocular pressure or optic nerve sheath diameter measurements for predicting elevated intracranial pressure in cryptococcal meningitis. Open Forum Infect Dis 1:ofu093. https://doi.org/10.1093/ofid/ofu093

47. Sangani SV, Parikh S (2015) Can sonographic measurement of optic nerve sheath diameter be used to detect raised intracranial pressure in patients with tuberculous meningitis? A prospective observational study. Indian J Radiol Imaging 25:173–176. https:// doi.org/10.4103/0971-3026.155869

48. Lawley JS, Alperin N, Bagci AM, Lee SH, Mullins PG, Oliver SJ, Macdonald JH (2014) Normobaric hypoxia and symptoms of acute mountain sickness: elevated brain volume and intracranial hypertension. Ann Neurol 75:890–898. https://doi.org/10.1002/ana. 24171

49. Ross RT (1985) The random nature of cerebral mountain sickness. Lancet 1:990–991

50. Lawley JS, Oliver SJ, Mullins P, Morris D, Junglee NA, Jelleyman C, Macdonald JH (2012) Optic nerve sheath diameter is not related to high altitude headache: a randomized controlled trial. High Alt Med Biol 13:193–199.

https://doi.org/10.1089/ham.2012.1019

51. Strapazzon G, Brugger H, Dal Cappello T, Procter E, Hofer G, Lochner P (2014) Factors associated with optic nerve sheath diameter during exposure to hypobaric hypoxia. Neurology 82:1914– 1918. https://doi.org/10.1212/WNL.0000000000000457

52. Sutherland AI, Morris DS, Owen CG, Bron AJ, Roach RC (2008) Optic nerve sheath diameter, intracranial pressure and acute mountain sickness on Mount Everest: a longitudinal cohort study. Br J Sports Med 42:183–188. https://doi.org/10.1136/bjsm.2007. 045286

53. Fagenholz PJ, Gutman JA, Murray AF, Noble VE, Camargo CA Jr, Harris NS (2009) Optic nerve sheath diameter correlates with the presence and severity of acute mountain sickness: evidence for increased intracranial pressure. J Appl Physiol 106:1207–1211. https://doi.org/10.1152/japplphysiol.01188.2007

54. Lochner P, Falla M, Brigo F, Pohl M, Strapazzon G (2015) Ultrasonography of the optic nerve sheath diameter for diagnosis and monitoring of acute mountain sickness: a systematic review. High Alt Med Biol 16:195–203. https://doi.org/10.1089/ham.2014. 1127

55. Lee HC, Lee WJ, Dho YS, Cho WS, Kim YH, Park HP (2018) Optic nerve sheath diameter based on preoperative brain computed tomography and intracranial pressure are positively correlated in adults with hydrocephalus. Clin Neurol Neurosurg 167:31–35. https://doi.org/10.1016/j.clineuro.2018.02.012

56. Brzezinska R, Schumacher R (2002) Diagnosis of elevated intracranial pressure in children with shunt under special consideration of transglobe sonography of the optic nerve. Ultraschall Med 23: 325–332. https://doi.org/10.1055/s-2002-35050

57. Newman WD, Hollman AS, Dutton GN, Carachi R (2002) Measurement of optic nerve sheath diameter by ultrasound: a means of detecting acute raised intracranial pressure in hydrocephalus. Br J Ophthalmol 86:1109–1113

58. Foroozan R, Buono LM, Savino PJ, Sergott RC (2002) Acute demyelinating optic neuritis. Curr Opin Ophthalmol 13:375–380

59. Youl BD et al (1991) The pathophysiology of acute optic neuritis. An association of gadolinium leakage with clinical and electrophysiological deficits. Brain 114(Pt 6):2437–2450

60. Dehghani A, Giti M, Akhlaghi MR, Karami M, Salehi F (2012) Ultrasonography in distinguishing optic neuritis from nonarteritic anterior ischemic

optic neuropathy. Adv Biomed Res 1:3. https:// doi.org/10.4103/2277-9175.94425

61. Elvin A, Andersson T, Soderstrom M (1998) Optic neuritis. Doppler ultrasonography compared with MR and correlated with visual evoked potential assessments. Acta Radiol 39:243–248

62. Gerling J, Janknecht P, Hansen LL, Kommerell G (1997) Diameter of the optic nerve in idiopathic optic neuritis and in anterior ischemic optic neuropathy. Int Ophthalmol 21:131–135

63. Karami M, Janghorbani M, Dehghani A, Riahinejad M (2012) Orbital Doppler evaluation of blood flow velocities in optic neuritis. Korean J Ophthalmol 26:116–122. https://doi.org/10.3341/kjo. 2012.26.2.116

64. Lochner P et al (2014) Transorbital sonography in acute optic neuritis: a case-control study. AJNR Am J Neuroradiol 35:2371–2375. https://doi.org/10.3174/ajnr.A4051

65. Neroev VV, Karlova IZ, Zaitseva OV, Kruzhkova GV, Boiko AN (2001) Role of ultrasonic B-scanning in differential diagnosis and prognosis of the course of optic neuritis. Vestn oftalmol 117:25–29

66. Stefanovic IB, Jovanovic M, Krnjaja BD, Veselinovic D, Jovanovic P (2010) Influence of retrobulbar neuritis and papillitis on echographically measured optic nerve diameter. Vojnosanit Pregl 67:32–35

67. Block HS, Biller J (2014) Neurology of pregnancy. Handb Clin Neurol 121:1595–1622. https://doi.org/10.1016/B978-0-7020- 4088-7.00105-X

68. Dubost C, Le Gouez A, Jouffroy V, Roger-Christoph S, Benhamou D, Mercier FJ, Geeraerts T (2012) Optic nerve sheath diameter used as ultrasonographic assessment of the incidence of raised intracranial pressure in preeclampsia: a pilot study. Anesthesiology 116: 1066–1071. https://doi.org/10.1097/ALN.0b013e318246ea1a

69. Brzan Simenc G, Ambrozic J, Prokselj K, Tul N, Cvijic M, Mirkovic T, Lucovnik M (2018) Ocular ultrasonography for diagnosing increased intracranial pressure in patients with severe preeclampsia. Int J Obstet Anesth 36:49–55. https://doi.org/10.1016/j. ijoa.2018.06.005

70. Bernal W, Wendon J (1999) Acute liver failure; clinical features and management. Eur J Gastroenterol Hepatol 11:977–984

71. Ware AJ, D'Agostino AN, Combes B (1971) Cerebral edema: a major complication of massive hepatic necrosis. Gastroenterology 61:877–884

72. Karvellas CJ, Fix OK, Battenhouse H, Durkalski V, Sanders C, Lee WM, Group USALFS (2014) Outcomes and complications of intracranial pressure monitoring in acute liver failure: a retrospective cohort study. Crit Care Med 42:1157–1167. https://doi.org/10. 1097/CCM.0000000000000144

73. Peck M, Wendon J, Sizer E, Auzinger G, Bernal W (2010) Intracranial pressure monitoring in acute liver failure: a review of 10 years experience. Crit Care 14:P542

74. Vaquero J et al (2005) Complications and use of intracranial pressure monitoring in patients with acute liver failure and severe encephalopathy. Liver Transpl 11:1581–1589. https://doi.org/10. 1002/lt.20625

75. Rajajee V, Williamson CA, Fontana RJ, Courey AJ, Patil PG (2018) Noninvasive intracranial pressure assessment in acute liver failure. Neurocrit Care 29:280–290. https://doi.org/10.1007/s12028-018- 0540-x

76. Ganschow R, Nolkemper D, Helmke K, Harps E, Commentz JC, Broering DC, Pothmann W, Rogiers X, Hellwege HH, Burdelski M (2000) Intensive care management after pediatric liver transplantation: a single-center experience. Pediatr Transplant 4:273–279

77. Chelly J et al (2016) The optic nerve sheath diameter as a useful tool for early prediction of outcome after cardiac arrest: a prospective pilot study. Resuscitation 103:7–13. https://doi.org/10.1016/j. resuscitation.2016.03.006

78. Chae MK et al (2016) Better prognostic value with combined optic nerve sheath diameter and grey-to-white matter ratio on initial brain computed tomography in post-cardiac arrest patients. Resuscitation 104:40–45. https://doi.org/10.1016/j.resuscitation.2016.04.001

79. Ueda T, Ishida E, Kojima Y, Yoshikawa S, Yonemoto H (2015) Sonographic optic nerve sheath diameter: a simple and rapid tool to assess the neurologic prognosis after cardiac arrest. J Neuroimaging 25:927–930. https://doi.org/10.1111/jon.12246

80. Ertl M, Weber S, Hammel G, Schroeder C, Krogias C (2018) Transorbital sonography for early prognostication of hypoxicischemic encephalopathy after cardiac arrest. J Neuroimaging 28: 542–548. https://doi.org/10.1111/jon.12528

81. You Y et al (2018) Relationship between time related serum albumin concentration, optic nerve sheath diameter, cerebrospinal fluid pressure, and neurological prognosis in cardiac arrest survivors. Resuscitation 131:42–47. https://doi.org/10.1016/j.resuscitation. 2018.08.003

82. Citerio G, Vascotto E, Villa F, Celotti S, Pesenti A (2001) Induced abdominal compartment syndrome increases intracranial pressure in neurotrauma patients: a prospective study. Crit Care Med 29: 1466–1471

83. Cooke SJ, Paterson-Brown S (2001) Association between laparoscopic abdominal surgery and postoperative symptoms of raised intracranial pressure. Surg Endosc 15:723–725

84. Ficarra V et al (2009) Retropubic, laparoscopic, and robot-assisted radical prostatectomy: a systematic review and cumulative analysis of comparative studies. Eur Urol 55:1037–1063. https://doi.org/10. 1016/j.eururo.2009.01.036

85. Kim MS, Bai SJ, Lee JR, Choi YD, Kim YJ, Choi SH (2014) Increase in intracranial pressure during carbon dioxide pneumoperitoneum with steep trendelenburg positioning proven by ultrasonographic measurement of optic nerve sheath diameter. J Endourol 28: 801–806. https://doi.org/10.1089/end.2014.0019

86. Robba C et al (2016) Effects of pneumoperitoneum and Trendelenburg position on intracranial pressure assessed using different non-invasive methods. Br J Anaesth 117:783–791. https:// doi.org/10.1093/bja/aew356

87. Kim EJ, Koo BN, Choi SH, Park K, Kim MS (2018) Ultrasonographic optic nerve sheath diameter for predicting elevated intracranial pressure during laparoscopic surgery: a systematic review and meta-analysis. Surg Endosc 32:175–182. https://doi. org/10.1007/s00464-017-5653-3

88. Ertl M, Schierling W, Kasprzak P, Schomig B, Bruckl C, Schlachetzki F, Pfister K (2015) Optic nerve sheath diameter measurement to identify high-risk patients for spinal ischemia after endovascular thoracoabdominal aortic aneurysm repair. J Neuroimaging 25:910–915. https://doi.org/10.1111/jon.12234

89. Houze-Cerfon CH, Bounes V, Guemon J, Le Gourrierec T, Geeraerts T (2019) Quality and feasibility of sonographic measurement of the optic nerve sheath diameter to estimate the risk of raised intracranial pressure after traumatic brain injury in prehospital setting. Prehosp Emerg Care 23:277–283. https://doi.org/10.1080/ 10903127.2018.1501444

90. Maissan IM, Verbaan LA, van den Berg M, Houmes RJ, Stolker RJ, den Hartog D (2018) Helicopter transportation increases intracranial pressure: a proof-of-principle study. Air Med J 37:249–252. https://doi.org/10.1016/j.amj.2018.02.010

91. Meiburger KM, Acharya UR, Molinari F (2018) Automated localization and segmentation techniques for B-mode ultrasound images: a review. Comput Biol

Med 92:210–235. https://doi.org/10. 1016/j.compbiomed.2017.11.018
92. Gerber S et al (2017) Automatic estimation of the optic nerve sheath diameter from ultrasound images imaging for patient-customized simulations and systems for point-of-care ultrasound : International Workshops, BIVPCS 2017 and POCUS 2017, held in conjunction with MICCAI 2017, Quebec City, QC 10549:113– 120 https://doi.org/10.1007/978-3-319-67552-7_14

## GENERAL DISCUSSION AND CONCLUSIONS

The results presented in this thesis increase the knowledge of the applicability of TOS in clinical practice and try to propose solutions to some unsolved questions in this issue.

Whether there are no doubts regarding the usefulness of this approach for the assessment of IH, improvements are still required for reducing the variability of measurements, standardizing the execution technique, and identifying the best setting for its application.

In the first study, we applied the technique to ICH, a severe neurological condition associated with elevated mortality or disability [Kuramatsu, 2013]. ICH is determined by the rupture of a cerebral artery, with extravasation of blood into the brain. ICH is a dynamic process [Van Stavern, 2005]. Following the rupture – the hyper-acute phase – in absence of a spontaneous arrest of the bleeding, the hematoma growth may rapidly induce IH. After 24-72 hours – the subacute phase – the cell death consequent to vascular damage may determine the development of cerebral edema, which further increases the ICP [Mayer, 2002]. The edema may persist for days – subacute/chronic phase – maintaining the IH. In clinical practice, these dynamic changes are monitored both clinically (possible deterioration of the neurological performances) and by repeated CT scans to establish adequate treatments and evaluate the indication for neurosurgical craniectomy or evacuation of the hematoma [Cook, 2020].

TOS appears particularly suitable in this dynamic process, being of aid both in the hyper-acute phase and later by diagnosing and confirming the persistence of IH. However, until the publication of our work, only a few studies evaluated the role of TOS in ICH. In 2009, Moretti et al. demonstrated the reliability of ONSD to detect raised ICP in patients with cerebral hemorrhage, including both primary cerebral and subarachnoid hemorrhages [Moretti, 2009]. They also found that the best cut-off point of ONSD to predict IH was 5.2 mm. In 2011, Skoloudic et al. showed that an enlargement of ONSD could be detected in the hyper-acute phase of cerebral hemorrhage within 6 hours from onset. A good correlation between ONSD values and hemorrhage volume and midline shift was documented [Skoloudic, 2011]. However, in both studies, the findings were confined to the acute phase of cerebral

hemorrhage and no information regarding the persistence of elevated ICP over time were available. In 2014, Lochner et al. first provided data on a very small case series of four patients in which the persistence of IH in ICH patients was confirmed by TOS also beyond the early phase of the disease [Lochner, 2014].

The results of our study are relevant because they confirmed the feasibility of TOS in detecting IH, with higher accuracy compared to doppler indexes of retinal vessels. Previous works in this field suggested the role of orbital vessels as a marker of ICP, with the advantages to be evaluated through the orbital acoustic windows rather than the temporal one, which may be insufficient or even absent in some patients [Marinoni, 1997; Ragauskas, 2012; Siaudvityte, 2015; Tarzamni, 2016]. Our optimal cut-off point to detect IH was 5.60 mm, in line with previous descriptions. This study showed for the first time the utility of the second assessment of ONSD which was able to detect the persistency of elevated ICP beyond the acute phase of ICH. We also found a high correlation between ONSD and hemorrhage volume in the acute phase of the disease. This finding is particularly relevant because the hemorrhage volume has been associated with neurological outcomes, potentially giving a prognostic role to the ONSD assessment, as demonstrated for other critical conditions [Broderick, 1993; Zhang, 2020; Xu, 2022]. Recently, Bender et al. confirmed the usefulness of serial assessment of the ONSD in patients with ICH. Specifically, they observed that relevant oscillations of ONSD from basal values over time were associated with the worst neurological outcome, emphasizing the role of TOS in monitoring the evolution of the disease [Bender, 2020].

In the second study, we tried to propose a different approach to ONSD assessment. We focused on the possibility that the maximum ONSD values could be as accurate as the binocular ONSD assessment in detecting IH. For this purpose, we looked for an asymmetry of the ONSD between the eyes. As previously described in this thesis' introduction, in presence of an interocular asymmetry the use of the binocular assessment of ONSD could lead to false-negative results. This is due to the averaging of measurements between the eyes, which may reduce the final ONSD value if a significant ONSD asymmetry is detected. In this context, there were no previous studies in the literature that specifically explore this issue.

Anatomical studies and clinical reports have demonstrated that the ONSD may enlarge differently between the eyes, and cases of unilateral papilledema have been

extensively described [Hayreh, 1984; Van Stavern, 2007]. Several hypotheses have been proposed and they mainly focused on the transmission of CSF through the optic canals, which may differ on the two sides [Bidot, 2016]. This is due to the variability of the optic canal conformation in animals and humans, which is responsible for the velocity and amount of CSF transmission towards the orbital regions from the intracranial ones [Killer, 2003; Hayreh, 2016]. As a result, the expansion of the ONSD can be disproportionated.

Our findings confirmed the existence of a significant asymmetry of ONSD between the eyes in more than half of the examined subjects, both healthy and those with IH. The study quantified the degree of asymmetry which was higher for patients with IH (0.45 mm) compared to healthy subjects (0.23 mm), which indicates that the error of measurements determined by the binocular evaluation is higher in patients with raised ICP.

Furthermore, by comparing the diagnostic accuracy of the maximum ONSD values between the eyes to the binocular assessment, both methods were adequate for detecting IH. These findings may have relevant implications in clinical practice because – when present – the asymmetry should be considered, and, consequently, which method should be used for the ONSD assessment (binocular vs maximum value). Based on the anatomical concepts and our findings, theoretically, the use of the maximum value appears more precise. We probably were not able to demonstrate a superiority of the maximum ONSD evaluation compared to the binocular one because of the sample size. Despite this consideration, our findings are consistent and show that the maximum value should be used for the ONSD assessment, particularly in patients with IH.

In the third work, we focused on the absence of standardization for the ONSD assessment. As discussed in this thesis' introduction, there is heterogeneity among the studies regarding how to measure the ONSD. These methodological discrepancies produce uncertainty in the interpretation of results. To reduce this variability, we proposed an automated system able to ensure adequate measurements of OND and ONSD. The development of AUTONoMA allowed measuring in completely automatic way the optic nerve structures, with no interaction with the user. The results of the automatic assessment are excellent compared to the manual ones, particularly for the expert operator, both for the OND

and ONSD. The AUTONoMA system may mitigate and minimize the differences derived from manual evaluations; in addition, we estimated that the automatic measurement was 15 times faster than the manual assessment, being able to calculate simultaneously the ONSD and OND. Thus, the advantages of the automatic assessment appear multiple and consistent.

A standardization of the execution technique for the ONSD assessment by TOS is mandatory and recommendations or guidelines are expected in the next years. However, automatic measurements may ensure another step forward in this field because they may limit the errors of measurements and favoring the homogeneity of results among studies. Before our work, only two studies (which employed a small sample size and different algorithms) tried to establish the role of a computerized system for the ONSD evaluation [Gerber; 2017; Soroushmehr, 2019]. To date, two recent studies confirmed the benefit of automatic measurements [Rajajee, 2021; Stevens, 2021]. Nevertheless, the sampling of our study is still the larger available. Based on the relevance of the issue, we are currently working on a new automated system of ONSD measurement (deep learning approach), which will include a broad number of patients, both healthy and pathological with IH.

In conclusion, the findings of our studies may help to clarify some uncertainties regarding the ONSD assessment by TOS, proposing solutions to unsolved questions in this topic. The application fields of TOS for the identification and monitoring of ICP are various. As described in our review, TOS may be applied as a diagnostic or monitoring instrument in many clinical conditions including traumatic brain injury, intracranial hemorrhage and ischemic stroke, idiopathic intracranial hypertension, intracranial hypotension, posterior reversible encephalopathy syndrome, meningitis and encephalitis, hydrocephalus, acute mountain sickness, multiple sclerosis, optic neuritis, non-arteritic ischemic optic neuropathy, surgery and its intraoperative complications, cardiac arrest and coma, pregnancy [Lochner, 2019].

We hope that our works will be the object of debate in the next years, contributing to the development of a unique consensus and recommendations for the ONSD assessment. Approaches that include an automatic system for the optic nerve structures assessment might represent the future in this field.

## REFERENCES (INTRODUCTION AND DISCUSSION)


- Agrawal A, Cheng R, Tang J, Madhok DY. Comparison of Two Techniques to Measure Optic Nerve Sheath Diameter in Patients at Risk for Increased Intracranial Pressure. Crit Care Med. 2019 Jun;47(6):e495-e501. doi: 10.1097/CCM.0000000000003742. PMID: 30882482.
- Albert AF, Kirkman MA. Clinical and Radiological Predictors of Malignant Middle Cerebral Artery Infarction Development and Outcomes. J Stroke Cerebrovasc Dis. 2017 Nov;26(11):2671-2679. doi: 10.1016/j.jstrokecerebrovasdis.2017.06.041. PMID: 28736129.
- Aletreby W, Alharthy A, Brindley PG, Kutsogiannis DJ, Faqihi F, Alzayer W, Balhahmar A, Soliman I, Hamido H, Alqahtani SA, Karakitsos D, Blaivas M. Optic Nerve Sheath Diameter Ultrasound for Raised Intracranial Pressure: A Literature Review and Meta-analysis of its Diagnostic Accuracy. J Ultrasound Med. 2022 Mar;41(3):585-595. doi: 10.1002/jum.15732. PMID: 33893746.
- Amini R, Stolz LA, Patanwala AE, Adhikari S. Coronal Axis Measurement of the Optic Nerve Sheath Diameter Using a Linear Transducer. J Ultrasound Med. 2015 Sep;34(9):1607-12. doi: 10.7863/ultra.15.14.09039. PMID: 26254151.
- Aspide R, Bertolini G, Albini Riccioli L, Mazzatenta D, Palandri G, Biasucci DG. A Proposal for a New Protocol for Sonographic Assessment of the Optic Nerve Sheath Diameter: The CLOSED Protocol. Neurocrit Care. 2020 Feb;32(1):327-332. doi: 10.1007/s12028-019-00853-x. PMID: 31583527.
- Ballantyne SA, O'Neill G, Hamilton R, Hollman AS. Observer variation in the sonographic measurement of optic nerve sheath diameter in normal adults. Eur J Ultrasound. 2002 Oct;15(3):145-9. doi: 10.1016/s0929-8266(02)00036-8. PMID: 12423741.
- Bäuerle J, Lochner P, Kaps M, Nedelmann M. Intra- and interobsever reliability of sonographic assessment of the optic nerve sheath diameter in healthy adults. J Neuroimaging. 2012 Jan;22(1):42-5. doi: 10.1111/j.1552-6569.2010.00546.x. PMID: 21121998.

- Bäuerle J, Niesen WD, Egger K, Buttler KJ, Reinhard M. Enlarged Optic Nerve Sheath in Aneurysmal Subarachnoid Hemorrhage despite Normal Intracranial Pressure. J Neuroimaging. 2016 Mar-Apr;26(2):194-6. doi: 10.1111/jon.12287. PMID: 26278326.
- Bäuerle J, Schuchardt F, Schroeder L, Egger K, Weigel M, Harloff A. Reproducibility and accuracy of optic nerve sheath diameter assessment using ultrasound compared to magnetic resonance imaging. BMC Neurol. 2013 Dec 1;13:187. doi: 10.1186/1471-2377-13-187. PMID: 24289136; PMCID: PMC4219451.
- Bender M, Lakicevic S, Pravdic N, Schreiber S, Malojcic B. Optic nerve sheath diameter sonography during the acute stage of intracerebral hemorrhage: a potential role in monitoring neurocritical patients. Ultrasound J. 2020 Nov 25;12(1):47. doi: 10.1186/s13089-020-00196-1. PMID: 33237373.
- Bidot S, Bruce BB, Saindane AM, Newman NJ, Biousse V. Asymmetric papilledema in idiopathic intracranial hypertension. J Neuroophthalmol. 2015 Mar;35(1):31-6. doi: 10.1097/WNO.0000000000000205. PMID: 25494197.
- Bidot S, Clough L, Saindane AM, Newman NJ, Biousse V, Bruce BB. The Optic Canal Size Is Associated With the Severity of Papilledema and Poor Visual Function in Idiopathic Intracranial Hypertension. J Neuroophthalmol. 2016 Jun;36(2):120-5. doi: 10.1097/WNO.0000000000000318. PMID: 26580295.
- Blehar DJ, Gaspari RJ, Montoya A, Calderon R. Correlation of visual axis and coronal axis measurements of the optic nerve sheath diameter. J Ultrasound Med. 2008 Mar;27(3):407-11. doi: 10.7863/jum.2008.27.3.407. PMID: 18314519.
- Bloria SD, Bloria P, Luthra A. Is it the time to standardize the procedure of ultrasound guided optic nerve sheath diameter measurement? Saudi J Anaesth. 2019 Jul-Sep;13(3):255-256. doi: 10.4103/sja.SJA_752_18. PMID: 31333376.
- Broderick JP, Brott TG, Duldner JE, Tomsick T, Huster G. Volume of intracerebral hemorrhage. A powerful and easy-to-use predictor of 30-day

mortality. Stroke. 1993 Jul;24(7):987-93. doi: 10.1161/01.str.24.7.987. PMID: 8322400.

- Cardim D, Czosnyka M, Chandrapatham K, Badenes R, Bertuccio A, Noto AD, Donnelly J, Pelosi P, Ball L, Hutchinson PJ, Robba C. Effects of Age and Sex on Optic Nerve Sheath Diameter in Healthy Volunteers and Patients With Traumatic Brain Injury. Front Neurol. 2020 Aug 7;11:764. doi: 10.3389/fneur.2020.00764. PMID: 32849220; PMCID: PMC7426488.
- Cardim D, Robba C, Bohdanowicz M, Donnelly J, Cabella B, Liu X, Cabeleira M, Smielewski P, Schmidt B, Czosnyka M. Non-invasive Monitoring of Intracranial Pressure Using Transcranial Doppler Ultrasonography: Is It Possible? Neurocrit Care. 2016 Dec;25(3):473-491. doi: 10.1007/s12028-016-0258-6. PMID: 26940914; PMCID: PMC5138275.
- Chen LM, Wang LJ, Hu Y, Jiang XH, Wang YZ, Xing YQ. Ultrasonic measurement of optic nerve sheath diameter: a non-invasive surrogate approach for dynamic, real-time evaluation of intracranial pressure. Br J Ophthalmol. 2019 Apr;103(4):437-441. doi: 10.1136/bjophthalmol-2018-312934. Epub 2018 Oct 25. PMID: 30361274; PMCID: PMC6691934.
- Cook AM, Morgan Jones G, Hawryluk GWJ, Mailloux P, McLaughlin D, Papangelou A, Samuel S, Tokumaru S, Venkatasubramanian C, Zacko C, Zimmermann LL, Hirsch K, Shutter L. Guidelines for the Acute Treatment of Cerebral Edema in Neurocritical Care Patients. Neurocrit Care. 2020 Jun;32(3):647-666. doi: 10.1007/s12028-020-00959-7. PMID: 32227294.
- Copetti R, Cattarossi L. Optic nerve ultrasound: artifacts and real images. Intensive Care Med. 2009 Aug;35(8):1488-9; author reply 1490-1. doi: 10.1007/s00134-009-1494-4. PMID: 19367390.
- Dubourg J, Javouhey E, Geeraerts T, Messerer M, Kassai B. Ultrasonography of optic nerve sheath diameter for detection of raised intracranial pressure: a systematic review and meta-analysis. Intensive Care Med. 2011 Jul;37(7):1059-68. doi: 10.1007/s00134-011-2224-2. PMID: 21505900.
- Eisenberg HM, Gary HE Jr, Aldrich EF, et al. Initial CT findings in 753 patients with severe head injury. A report from the NIH Traumatic coma data bank. J Neurosurg 1990;73:688-98.

- Ertl M, Barinka F, Torka E, Altmann M, Pfister K, Helbig H, Bogdahn U, Gamulescu MA, Schlachetzki F. Ocular color-coded sonography - a promising tool for neurologists and intensive care physicians. Ultraschall Med. 2014 Oct;35(5):422-31. English, German. doi: 10.1055/s-0034-1366113. PMID: 24647767.
- Ertl M, Knüppel C, Veitweber M, Wagner A, Pfister K, Wendl C, Baldaranov D, Beck J, Linker RA, Schlachetzki F. Normal Age- and Sex-Related Values of the Optic Nerve Sheath Diameter and Its Dependency on Position and Positive End-Expiratory Pressure. Ultrasound Med Biol. 2020 Dec;46(12):3279-3285. doi: 10.1016/j.ultrasmedbio.2020.08.025. PMID: 32962893.
- Evensen K.B., Eide P.K. Measuring intracranial pressure by invasive, less invasive or non-invasive means: limitations and avenues for improvement. Fluids Barriers CNS 17, 34 (2020). https://doi.org/10.1186/s12987-020-00195-3
- Geeraerts T, Merceron S, Benhamou D, Vigué B, Duranteau J. Non-invasive assessment of intracranial pressure using ocular sonography in neurocritical care patients. Intensive Care Med. 2008 Nov;34(11):2062-7. doi: 10.1007/s00134-008-1149-x. PMID: 18509619.
- Gerber S, Jallais M, Greer H, McCormick M, Montgomery S, Freeman B, Kane D, Chittajallu D, Siekierski N, Aylward S. Automatic Estimation of the Optic Nerve Sheath Diameter from Ultrasound Images. Imaging Patient Cust Simul Syst Point Care Ultrasound (2017). 2017 Sep;10549:113-120. doi: 10.1007/978-3-319-67552-7_14. PMID: 29984363.
- Hansen G, Vallance JK, Beer DL, Clark I, Sellers EAC. Serial optic nerve sheath diameter ultrasonography during pediatric diabetic ketoacidosis management: A pilot study. J Diabetes Complications. 2016 Nov-Dec;30(8):1600-1602. doi: 10.1016/j.jdiacomp.2016.07.010. PMID: 27476639.
- Hansen HC, Helmke K. Validation of the optic nerve sheath response to changing cerebrospinal fluid pressure: ultrasound findings during intrathecal infusion tests. J Neurosurg. 1997 Jul;87(1):34-40. doi: 10.3171/jns.1997.87.1.0034. PMID: 9202262.

- Hansen HC, Lagrèze W, Krueger O, Helmke K. Dependence of the optic nerve sheath diameter on acutely applied subarachnoidal pressure - an experimental ultrasound study. Acta Ophthalmol. 2011 Sep;89(6):e528-32. doi: 10.1111/j.1755-3768.2011.02159.x. PMID: 21518306.
- Hayreh SS. Pathogenesis of optic disc edema in raised intracranial pressure. Prog Retin Eye Res. 2016 Jan;50:108-44. doi: 10.1016/j.preteyeres.2015.10.001. PMID: 26453995.
- Hayreh SS. The sheath of the optic nerve. Ophthalmologica. 1984;189(1-2):54-63. doi: 10.1159/000309386. PMID: 6472807.
- Helmke K, Hansen HC. Fundamentals of transorbital sonographic evaluation of optic nerve sheath expansion under intracranial hypertension II. Patient study. Pediatr Radiol. 1996 Oct;26(10):706-10. doi: 10.1007/BF01383384. PMID: 8805600.
- Killer HE, Laeng HR, Flammer J, Groscurth P. Architecture of arachnoid trabeculae, pillars, and septa in the subarachnoid space of the human optic nerve: anatomy and clinical considerations. Br J Ophthalmol. 2003 Jun;87(6):777-81. doi: 10.1136/bjo.87.6.777. PMID: 12770980; PMCID: PMC1771732.
- Kim DY, Kim SY, Hong DY, Sung BY, Lee S, Paik JH, Jung HM. Comparison of ultrasonography and computed tomography for measuring optic nerve sheath diameter for the detection of elevated intracranial pressure. Clin Neurol Neurosurg. 2021 May;204:106609. doi: 10.1016/j.clineuro.2021.106609. PMID: 33813371.
- Kimberly HH, Shah S, Marill K, Noble V. Correlation of optic nerve sheath diameter with direct measurement of intracranial pressure. Acad Emerg Med. 2008 Feb;15(2):201-4. doi: 10.1111/j.1553-2712.2007.00031.x. PMID: 18275454.
- Kuramatsu JB, Huttner HB, Schwab S. Advances in the management of intracerebral hemorrhage. J Neural Transm (Vienna). 2013 Sep;120 Suppl 1:S35-41. doi: 10.1007/s00702-013-1040-y. PMID: 23720189.
- Lin JJ, Chen AE, Lin EE, Hsia SH, Chiang MC, Lin KL. Point-of-care ultrasound of optic nerve sheath diameter to detect intracranial pressure in neurocritically ill children - A narrative review. Biomed J. 2020

Jun;43(3):231-239. doi: 10.1016/j.bj.2020.04.006. PMID: 32335329; PMCID: PMC7424084.

- Lochner P, Coppo L, Cantello R, Nardone R, Naldi A, Leone MA, Brigo F. Intra- and interobserver reliability of transorbital sonographic assessment of the optic nerve sheath diameter and optic nerve diameter in healthy adults. J Ultrasound. 2014 Nov 20;19(1):41-5. doi: 10.1007/s40477-014-0144-z. PMID: 26941872; PMCID: PMC4762843.
- Lochner P, Czosnyka M, Naldi A, Lyros E, Pelosi P, Mathur S, Fassbender K, Robba C. Optic nerve sheath diameter: present and future perspectives for neurologists and critical care physicians. Neurol Sci. 2019 Dec;40(12):2447-2457. doi: 10.1007/s10072-019-04015-x. PMID: 31367861.
- Lochner P, Fassbender K, Andrejewski A, Behnke S, Wagenpfeil G, Fousse M, Helwig SA, Lesmeister M, Stolz E, Reith W, Brigo F, Yilmaz U. Sonography of optic nerve sheath diameter identifies patients with middle cerebral artery infarction at risk of a malignant course: a pilot prospective observational study. J Neurol. 2020 Sep;267(9):2713-2720. doi: 10.1007/s00415-020-09906-0. PMID: 32440922.
- Lochner P, Mader C, Nardone R, Tezzon F, Zedde ML, Malferrari G, Brigo F. Sonography of the optic nerve sheath beyond the hyperacute stage of intracerebral hemorrhage. J Ultrasound. 2014 Jan 31;17(3):225-8. doi: 10.1007/s40477-014-0069-6. PMID: 25177397.
- Marinoni M, Ginanneschi A, Forleo P, Amaducci L. Technical limits in transcranial Doppler recording: inadequate acoustic windows. Ultrasound Med Biol. 1997;23(8):1275-7. doi: 10.1016/s0301-5629(97)00077-x. PMID: 9372576.
- Mayer SA. Intracerebral hemorrhage: natural history and rationale of ultra-early hemostatic therapy. Intensive Care Med. 2002 Oct;28 Suppl 2:S235-40. doi: 10.1007/s00134-002-1470-8. PMID: 12404092.
- Meiburger KM, Naldi A, Michielli N, Coppo L, Fassbender K, Molinari F, Lochner P. Automatic Optic Nerve Measurement: A New Tool to Standardize Optic Nerve Assessment in Ultrasound B-Mode Images. Ultrasound Med Biol. 2020 Jun;46(6):1533-1544. doi: 10.1016/j.ultrasmedbio.2020.01.034. PMID: 32147099.

- Mitchell C, Mathew S, Harris A, Lang M, Mackay D, Kovoor J. Etiology, pathogenesis and management of idiopathic intracranial hypertension, and role of optic canal size in asymmetric papilledema: A review. Eur J Ophthalmol. 2021 May;31(3):892-903. doi: 10.1177/11206721211005709. PMID: 33779328.
- Montorfano L, Yu Q, Bordes SJ, Sivanushanthan S, Rosenthal RJ, Montorfano M. Mean value of B-mode optic nerve sheath diameter as an indicator of increased intracranial pressure: a systematic review and meta-analysis. Ultrasound J. 2021 Jul 2;13(1):35. doi: 10.1186/s13089-021-00235-5. PMID: 34215966; PMCID: PMC8253877.
- Moraes FM, Silva GS. Noninvasive intracranial pressure monitoring methods: a critical review. Arq Neuropsiquiatr. 2021 May;79(5):437-446. doi: 10.1590/0004-282X-ANP-2020-0300. PMID: 34161530.
- Moretti R, Pizzi B, Cassini F, Vivaldi N. Reliability of optic nerve ultrasound for the evaluation of patients with spontaneous intracranial hemorrhage. Neurocrit Care. 2009 Dec;11(3):406-10. doi: 10.1007/s12028-009-9250-8. PMID: 19636971.
- Moretti R, Pizzi B. Ultrasonography of the optic nerve in neurocritically ill patients. Acta Anaesthesiol Scand. 2011 Jul;55(6):644-52. doi: 10.1111/j.1399-6576.2011.02432.x. PMID: 21463263.
- Ragauskas A, Matijosaitis V, Zakelis R, Petrikonis K, Rastenyte D, Piper I, Daubaris G. Clinical assessment of noninvasive intracranial pressure absolute value measurement method. Neurology. 2012 May 22;78(21):1684-91. doi: 10.1212/WNL.0b013e3182574f50. PMID: 22573638.
- Rajajee V, Soroushmehr R, Williamson CA, Najarian K, Gryak J, Awad A, Ward KR, Tiba MH. Novel Algorithm for Automated Optic Nerve Sheath Diameter Measurement Using a Clustering Approach. Mil Med. 2021 Jan 25;186(Suppl 1):496-501. doi: 10.1093/milmed/usaa231. PMID: 32830251.
- Rajajee V, Vanaman M, Fletcher JJ, Jacobs TL. Optic nerve ultrasound for the detection of raised intracranial pressure. Neurocrit Care. 2011 Dec;15(3):506-15. doi: 10.1007/s12028-011-9606-8. PMID: 21769456.
- Rangel-Castilla L, Gopinath S, Robertson CS. Management of intracranial hypertension. Neurol Clin. 2008 May;26(2):521-41, x. doi:

10.1016/j.ncl.2008.02.003. Erratum in: Neurol Clin. 2008 Aug;26(3):xvii. Rangel-Castillo, Leonardo [corrected to Rangel-Castilla, Leonardo]. PMID: 18514825; PMCID: PMC2452989.

- Robba C, Bacigaluppi S, Cardim D, Donnelly J, Bertuccio A, Czosnyka M. Non-invasive assessment of intracranial pressure. Acta Neurol Scand. 2016 Jul;134(1):4-21. doi: 10.1111/ane.12527. PMID: 26515159.
- Robba C, Santori G, Czosnyka M, Corradi F, Bragazzi N, Padayachy L, Taccone FS, Citerio G. Optic nerve sheath diameter measured sonographically as non-invasive estimator of intracranial pressure: a systematic review and meta-analysis. Intensive Care Med. 2018 Aug;44(8):1284-1294. doi: 10.1007/s00134-018-5305-7. PMID: 30019201.
- Robba, C, Goffi, A, Geeraerts, T. et al. Brain ultrasonography: methodology, basic and advanced principles and clinical applications. A narrative review. Intensive Care Med 45, 913–927 (2019).
- Schroeder C, Katsanos AH, Richter D, Tsivgoulis G, Gold R, Krogias C. Quantification of Optic Nerve and Sheath Diameter by Transorbital Sonography: A Systematic Review and Metanalysis. J Neuroimaging. 2020 Mar;30(2):165-174. doi: 10.1111/jon.12691. PMID: 32022367.
- Shah S, Kimberly H, Marill K, Noble VE. Ultrasound techniques to measure the optic nerve sheath: is a specialized probe necessary? Med Sci Monit. 2009 May;15(5):MT63-8. PMID: 19396044.
- Shankar H, Pagel PS. Potential adverse ultrasound-related biological effects: a critical review. Anesthesiology. 2011 Nov;115(5):1109-24. doi: 10.1097/ALN.0b013e31822fd1f1. PMID: 21866043.
- Siaudvytyte L, Januleviciene I, Ragauskas A, Bartusis L, Siesky B, Harris A. Update in intracranial pressure evaluation methods and translaminar pressure gradient role in glaucoma. Acta Ophthalmol. 2015 Feb;93(1):9-15. doi: 10.1111/aos.12502. PMID: 25043873.
- Skoloudík D, Herzig R, Fadrná T, Bar M, Hradílek P, Roubec M, Jelínková M, Sanák D, Král M, Chmelová J, Herman M, Langová K, Kanovsky P. Distal enlargement of the optic nerve sheath in the hyperacute stage of intracerebral haemorrhage. Br J Ophthalmol. 2011 Feb;95(2):217-21. doi: 10.1136/bjo.2009.172890. PMID: 20679081.

- Soroushmehr R, Rajajee K, Williamson C, Gryak J, Najarian K, Ward K, Tiba MH. Automated Optic Nerve Sheath Diameter Measurement Using Super-pixel Analysis. Annu Int Conf IEEE Eng Med Biol Soc. 2019 Jul;2019:2793-2796. doi: 10.1109/EMBC.2019.8856449. PMID: 31946473.
- Stevens RRF, Gommer ED, Aries MJH, Ertl M, Mess WH, Huberts W, Delhaas T. Optic nerve sheath diameter assessment by neurosonology: A review of methodologic discrepancies. J Neuroimaging. 2021 Sep;31(5):814-825. doi: 10.1111/jon.12906. PMID: 34270144.
- Stevens RRF, Huberts W, Gommer ED, Ertl M, Aries M, Mess WH, Delhaas T. An Automated Algorithm for Optic Nerve Sheath Diameter Assessment from B-mode Ultrasound Images. J Neuroimaging. 2021 Jul;31(4):724-732. doi: 10.1111/jon.12851. PMID: 33783910.
- Swinkin E, Jabehdar Maralani P, Sundaram AN. Unilateral Papilledema in Idiopathic Intracranial Hypertension: A Case Series. Can J Neurol Sci. 2022 Mar;49(2):278-281. doi: 10.1017/cjn.2021.79. PMID: 33888167.
- Tarzamni MK, Derakhshan B, Meshkini A, Merat H, Fouladi DF, Mostafazadeh S, Rezakhah A. The diagnostic performance of ultrasonographic optic nerve sheath diameter and color Doppler indices of the ophthalmic arteries in detecting elevated intracranial pressure. Clin Neurol Neurosurg. 2016 Feb;141:82-8. doi: 10.1016/j.clineuro.2015.12.007. PMID: 26771156.
- Tayal VS, Neulander M, Norton HJ, Foster T, Saunders T, Blaivas M. Emergency department sonographic measurement of optic nerve sheath diameter to detect findings of increased intracranial pressure in adult head injury patients. Ann Emerg Med. 2007 Apr;49(4):508-14. doi: 10.1016/j.annemergmed.2006.06.040. PMID: 16997419.
- Thotakura AK, Marabathina NR, Danaboyina AR, Mareddy RR. Role of serial ultrasonic optic nerve sheath diameter monitoring in head injury. Neurochirurgie. 2017 Dec;63(6):444-448. doi: 10.1016/j.neuchi.2017.06.001. PMID: 29122307.
- Toms DA. The mechanical index, ultrasound practices, and the ALARA principle. J Ultrasound Med. 2006 Apr;25(4):560-1; author reply 561-2. doi: 10.7863/jum.2006.25.4.560. PMID: 16567451.

- Toscano M, Spadetta G, Pulitano P, Rocco M, Di Piero V, Mecarelli O, Vicenzini E. Optic Nerve Sheath Diameter Ultrasound Evaluation in Intensive Care Unit: Possible Role and Clinical Aspects in Neurological Critical Patients' Daily Monitoring. Biomed Res Int. 2017;2017:1621428. doi: 10.1155/2017/1621428. PMID: 28421189.
- Van Stavern GP. Optic disc edema. Semin Neurol. 2007 Jul;27(3):233-43. doi: 10.1055/s-2007-979684. PMID: 17577865.
- Van Stavern RB, Primary Intracerebral Hemorrhage: Natural History, Prognosis, and Outcomes, Seminars in Cerebrovascular Diseases and Stroke, Volume 5, Issue 3, 2005, Pages 163-167.
- Wang LJ, Chen LM, Chen Y, Bao LY, Zheng NN, Wang YZ, Xing YQ. Ultrasonography Assessments of Optic Nerve Sheath Diameter as a Noninvasive and Dynamic Method of Detecting Changes in Intracranial Pressure. JAMA Ophthalmol. 2018 Mar 1;136(3):250-256. doi: 10.1001/jamaophthalmol.2017.6560. PMID: 29392301; PMCID: PMC5885896.
- Xu H, Li Y, Liu J, Chen Z, Chen Q, Xiang Y, Zhang M, He W, Zhuang Y, Yang Y, Chen W, Chen Y. Dilated Optic Nerve Sheath Diameter Predicts Poor Outcome in Acute Spontaneous Intracerebral Hemorrhage. Cerebrovasc Dis. 2022;51(2):199-206. doi: 10.1159/000518724. PMID: 34569518.
- Zeiler FA, Unger B, Zhu Q, Xiao J, Kirkpatrick AW, Kramer AH, Aleassa EM, Gillman LM. A Unique Model for ONSD Part II: Inter/Intra-operator Variability. Can J Neurol Sci. 2014 Jul;41(4):430-5. doi: 10.1017/s0317167100018448. PMID: 24878465.
- Zhang YW, Zhang S, Gao H, Li C, Zhang MX. Prognostic Role of Optic Nerve Sheath Diameter for Neurological Outcomes in Post-Cardiac Arrest Patients: A Systematic Review and Meta-Analysis. Biomed Res Int. 2020 Dec 23;2020:5219367. doi: 10.1155/2020/5219367. PMID: 33426054; PMCID: PMC7775140.

## ACNOWLEDGMENTS

I would like to thank all the participants in the described studies and their families.
I wish to thank my tutors, Prof. Bergui and Prof. Vercelli, for their trust and for the possibility to complete this Ph.D. I thank them for their supervision and scientific support, and for allowing me to improve my professional background.
A special thanks to Piergiorgio Lochner, my first scientific mentor, for his countless hours of reflecting, reading, encouraging, and for being a very good friend. I'm sure that our relationship will fruitfully continue, with many other satisfying moments.
Thanks to Prof. Meiburger and the PolitoBioMedLab team for their work, their teaching, and their help in collecting and analyzing data.
I would like to acknowledge all my colleagues of the Neurology of San Giovanni Bosco Hospital for their support and for sharing with me this experience.

## DEDICATION

I dedicate this thesis to my family and myself.
Thanks to my wife Silvia, for being unique as you are. Thanks for your unconditional support, your help, and for encouraging me constantly. You were close to me also in my most difficult times, and I am deeply grateful to you for that.
Thanks to my wonderful children, Lorenzo and Eleonora. Thanks for being as special as you are, and for loving me as I love you.
A special thanks to my aunt Raffaella: it wouldn't be the same without you, your love, and your empathy.
Thanks to my friends and to all those who have been close to me over these four years.